UCTEA Turkish Chamber of Civil Engineers
TMMOB İnşaat Mühendisleri Odası

Turkish Journal of Civil Engineering

formerly
Teknik Dergi

Volume 34
Issue 5
September 2023

Turkish Journal of Civil Engineering (formerly Teknik Dergi) Publication Principles

Turkish Journal of Civil Engineering (TJCE), a non-profit, open access scientific and technical periodical of UCTEA Chamber of Civil Engineers, publishes papers reporting original research work and major projects of interest in the area of civil engineering. TJCE annually publishes six issues and is open to papers in English and Turkish. It should be noted that TJCE (formerly, Teknik Dergi/ Technical Journal of Turkish Chamber of Civil Engineers) is being published regularly for more than 30 years since 1990. Main publication principles of TJCE are summarized below:

1. Articles reporting original scientific research and those reflecting interesting engineering applications are accepted for publication. To be classified as original, the work should either produce new scientific knowledge or add a genuinely new dimension to the existing knowledge or develop a totally new method or substantially improve an existing method.
2. Articles reporting preliminary results of scientific studies and those which do not qualify as full articles but provide useful information for the reader can be considered for publication as technical notes.
3. Discussions received from the readers of the published articles within three months from publication are reviewed by the Editorial Board and then published together with the closing remarks of the author.
4. Manuscripts submitted for publication are evaluated by two or three reviewers unknown to the authors. In the light of their reports, final decision to accept or decline is taken by the Editorial Board. General policy of the Board is to get the insufficient manuscripts improved in line with the reviewers' proposals. Articles that fail to reach the desired level are declined. Reasons behind decisions are not declared.
5. A signed statement is taken from the authors, declaring that the article has not been published as a "journal article or book chapter". In case the Editorial Board is in the opinion that the article has already been published elsewhere with minor changes or suspects plagiarism or a similar violation of ethics, then not only that article, but none of the articles of the same authors are published.
6. Papers reporting works presented as conference papers and developed further may be considered for publication. The conference it was presented to is given as a footnote in the first page.
7. Additionally, a document signed by all authors, transferring the copyright to UCTEA Chamber of Civil Engineers is submitted together with the manuscript.

UCTEA Turkish Chamber of Civil Engineers
TMMOB İnşaat Mühendisleri Odası

Turkish Journal of Civil Engineering

(formerly Teknik Dergi)

Volume 34 Issue 5 September 2023

UCTEA Turkish Chamber of Civil Engineers
TMMOB İnşaat Mühendisleri Odası
Necatibey St. No: 57, Kızılay 06440 Ankara, Turkey
Tel: +90.312.294 30 00 - Faks: +90.312.294 30 88
E-mail: imo@imo.org.tr - www.imo.org.tr

Publisher *(Sahibi)*:
Taner YÜZGEÇ
On behalf of UCTEA Turkish Chamber of Civil Engineers

Administrative Officer *(Yazı İşleri Müdürü)*:
Özer AKKUŞ

Volume 34 - Issue 5 - September 2023 *(Cilt 34 - Sayı 5 - Eylül 2023)*
Published bi-monthly. Local periodical. *(İki ayda bir yayınlanır, yerel süreli yayın)*
Date of Print: September 1, 2023 *(Baskı Tarihi: 1 Eylül 2023)*
Number of copies: 800 *(800 adet basılmıştır)*

ISSN: 2822-6836

Turkish Journal of Civil Engineering (formerly Teknik Dergi) is indexed by
- Science Citation Index Expanded
- Scopus
- Journal Citation Reports / Science Edition
- Engineering Index
- Concrete Abstracts (American Concrete Institute)
- National Technical Information Service (US NTIS)
- CITIS
- Ulrich's International Periodical's Directory
- Google Scholar
- TR Index

Turkish Journal of Civil Engineering (formerly Teknik Dergi) is a peer reviewed open access periodical publishing papers of original research and interesting practice cases. It addresses both the research community and the practicing engineers.

Printed by *(Baskı)*:
Ziraat Gurup Matbaacılık Ambalaj San. Tic. A.Ş.
Bahçekapı Mah. 2534 Sok. No: 18 Şaşmaz, Etimesgut / Ankara
Tel: 0.312.384 73 44 - Faks: 0.312.384 73 46

Reviewers:

This list is renewed each year and includes reviewers who served in the last two years of publication.

Şükran AÇIKEL
Merve AÇIKGENÇ ULAŞ
Perviz AHMEDZADE
Bülent AKBAŞ
Şeref Doğuşcan AKBAŞ
Rıfat AKBIYIKLI
Özge AKBOĞA KALE
Sarven AKCELYAN
Burcu AKÇAY ALDANMAZ
Cihan Taylan AKDAĞ
Cem AKGÜNER
Çağlar AKKAYA
Fevziye AKÖZ
Erkan AKPINAR
Muhammet Vefa AKPINAR
Atakan AKSOY
Hafzullah AKSOY
Tülay AKSU ÖZKUL
Uğurhan AKYÜZ
Sadık ALASHAN
Cenk ALHAN
Ayşe Burcu ALTAN SAKARYA
Sinan ALTIN
Adlen ALTUNBAŞ
Ahmet Can ALTUNIŞIK
Yalçın ALVER
Bahadır ALYAVUZ
Özgür ANIL
Necati ARAS
Davit ARDİTİ
Yalın ARICI
Deniz ARTAN İLTER
Ali Osman ATAHAN
Hakan Nuri ATAHAN
Ali Osman ATEŞ
Bekir Özer AY
Gökçe AYDIN
Metin AYDOĞDU
Hakan AYGÖREN
Mustafa Tamer AYVAZ
Ülker Güner BACANLI
İhsan Engin BAL
Selim BARADAN
Eray BARAN
Özgür Uğraş BARAN
Türkay BARAN
Bekir Oğuz BARTIN
Mustafa Gökçe BAYDOĞAN
Cüneyt BAYKAL
Niyazi Özgür BEZGİN
Senem BİLİR MAHÇİÇEK
Gökçen BOMBAR
Burak BOYACI
İlknur BOZBEY
Ali BOZER
Zafer BOZKUŞ
Erdem CANBAY
Zekai CELEP
Cihan CENGİZ
Halim CEYLAN
Hüseyin CEYLAN
Ömer CİVALEK
Joao Ramoa CORREIA
Ayşe COŞKUN BEYAN
Ali Fırat ÇABALAR
Barlas Özden ÇAĞLAYAN
Melih ÇALAMAK
Gülben ÇALIŞ
Umut ÇALIŞKAN
Süheyla Pelin ÇALIŞKANELLİ
Mehmet Alper ÇANKAYA
Dilay ÇELEBİ
Tevfik Kutay ÇELEBİOĞLU
Ahmet Ozan ÇELİK
Oğuz Cem ÇELİK
Semet ÇELİK
Hilmi Berk ÇELİKOĞLU
Kemal Önder ÇETİN
Mahmut ÇETİN
Mecit ÇETİN
Erdal ÇOKÇA
Semra ÇOMU
İsmail DABANLI
Ömer DABANLI
Atilla DAMCI
Yakup DARAMA
Osama M.F. DAWOUD
Tayfun DEDE
Abdullah DEMİR
Cem DEMİR
Emre DEMİR
Uğur DEMİR (İTÜ)
Uğur DEMİR (İYTE)
Munise Didem DEMİRBAŞ
Ender DEMİREL
Mehmet Cüneyd DEMİREL
Seyyit Ümit DİKMEN
Ali Ersin DİNÇER
İsmail DURANYILDIZ
Selim DÜNDAR
Nurhan ECEMİŞ ZEREN
Volkan Ş. EDİGER
Özgür EKİNCİOĞLU
Murat Altuğ ERBERİK
Ali ERCAN
Sinan Turhan ERDOĞAN
Şakir ERDOĞDU
Ramazan Cüneyt ERENOĞLU
Esin ERGEN PEHLEVAN
Gökmen ERGÜN
Bülent ERKMEN
Barış ERKUŞ
Yusuf Çağtay ERŞAN
Kağan ERYÜRÜK
Tuğba ESKİŞAR TEFÇİ
Burak FELEKOĞLU
Mahmut FIRAT
Okan FISTIKOĞLU
Onur GEDİK
Abdullah GEDİKLİ
Ahmet Talha GEZGİN
Sadık Can GİRGİN
Zehra Canan GİRGİN
Ilgın GÖKAŞAR
Serdar GÖKTEPE
Rahmi GÜÇLÜ
Ali GÜL
Fazlı Erol GÜLER
Ilgın GÜLER
Hamza GÜLLÜ
Gürkan GÜNAY
Taylan GÜNAY
Murat GÜNAYDIN
Samet GÜNER
Oğuz GÜNEŞ
Mehmet Şükrü GÜNEY
Tuba GÜRBÜZ BÜYÜKKAYIKÇI
Aslı Pelin GÜRGÜN
Soner HALDENBİLEN
Murat HAMDERİ
Ingo A. HANSEN
Umut HASGÜL
Bo-Tao HUANG
Zeynep IŞIK
Sabriye Banu İKİZLER
Erol İSKENDER
Medine İSPİR ARSLAN
Recep İYİSAN
Nihat KABAY
Mehmet Sedat KABDAŞLI
Mehmet Rifat KAHYAOĞLU
Özkan KALE
Volkan KALPAKÇI
Elif Çağda KANDEMİR
Tanay KARADEMİR
Hüseyin Faruk KARADOĞAN
Ümit KARADOĞAN
Mustafa Erkan KARAGÜLER
Halil KARAHAN
Zülküf KAYA
Oğuz KAYABAŞI
Hasan Ahmed KAZMEE
Mustafa Kubilay KELEŞOĞLU
Elçin KENTEL
Hadi KHANBABAZADEH
Havvanur KILIÇ
Ufuk KIRBAŞ
Veysel Şadan Özgür KIRCA
Cem KIRLANGIÇOĞLU
Güven KIYMAZ
Gökhan KİRKİL
Esat Selim KOCAMAN
Kasım KOÇAK
Salih KOÇAK
Niyazi Uğur KOÇKAL
Baha Vural KÖK
Mete KÖKEN
Hasan KURTARAN
Murat KURUOĞLU
Akif KUTLU
Abdullah KÜRKÇÜ
Hilmi LUŞ
Kasım MERMERTAŞ
Mahmoud MIARI
Yetiş Şazi MURAT
Öcal NECMİOĞLU
Fuad OKAY
Umut OKKAN
Derviş Volkan OKUR
Mehmet Hakkı OMURTAG
Sezan ORAK
Engin ORAKDÖĞEN
Akın ÖNALP
Bihrat ÖNÖZ
Ali Hakan ÖREN
Ceyhun ÖZÇELİK
Yiğit ÖZÇELİK
Gökhan ÖZDEMİR
Murat ÖZEN
Pelin ÖZENER
Hasan ÖZER
Hakkı Oral ÖZHAN
Mehmet Fatih ÖZKAL
Zeynep Huri ÖZKUL BİRGÖREN
Ahmet ÖZTOPAL
Sadık ÖZTOPRAK
Turan ÖZTURAN
Mustafa ÖZUYSAL
Tolga Yılmaz ÖZÜDOĞRU
Atilla ÖZÜTOK
Nilüfer ÖZYURT ZİHNİOĞLU
Ahmet Onur PEHLİVAN
Seval PINARBAŞI ÇUHADAROĞLU
Elişan Filiz PİROĞLU
Selman SAĞLAM
Mehmet SALTAN
Metin SARIGÖL
Altuğ SAYGILI
Serdar SELAMET
Osman SİVRİKAYA
Behzad SOLTANBEIGI
Serdar SOYÖZ
Rifat SÖNMEZ
Tayfun Altuğ SÖYLEV
Erol ŞADOĞLU
Olcay ŞAHİN
Yuşa ŞAHİN
Zekai ŞEN
Burak ŞENGÖZ
Karin ŞEŞETYAN
Ali Ünal ŞORMAN
Gülüm TANIRCAN
Serhan TANYEL
Kerem TAŞTAN
Gökmen TAYFUR
Rasim TEMÜR
Serdal TERZİ
Berrak TEYMUR
Hüseyin Onur TEZCAN
Mesut TIĞDEMİR
Salih TİLEYLİOĞLU
Vedat TOĞAN
Onur Behzat TOKDEMİR
İrem Dikmen Toker TOKER
Ali TOPAL
Cem TOPKAYA
Kamile TOSUN FELEKOĞLU
Erkan TÖRE
Ülgen Mert TUĞSAL
Gürsoy TURAN
Ö. Tuğrul TURAN
Cüneyt TÜZÜN
Eren UÇKAN
Latif Onur UĞUR
Ergin ULUTAŞ
Dilay UNCU
Tayfun UYGUNOĞLU
Volkan Emre UZ
İbrahim Mert UZUN
Deniz ÜLGEN
Mehmet Barış Can ÜLKER
Yurdanur ÜNAL
Cüneyt VATANSEVER
Syed Tanvir WASTI
Ahmet YAKUT
Erkut YALÇIN
Mehmet Cem YALÇIN
Aslı YALÇIN DAYIOĞLU
Mustafa Sinan YARDIM
Mert Yücel YARDIMCI
Anıl YAZICI
Gökhan YAZICI
Halit YAZICI
Mehmet YETMEZ
Tahsin Alper YIKICI
İrem Zeynep YILDIRIM
Mehmet YILDIRIMOĞLU
Abdülazim YILDIZ
Mustafa Tolga YILMAZ
Berivan YILMAZER POLAT
İsmail YÜCEL
Yeliz YÜKSELEN AKSOY
Shaban Isamel Albrka Ali ZANGENA
Abdullah Can ZÜLFİKAR

Turkish Journal of Civil Engineering (formerly Teknik Dergi)

Volume 34 Issue 5 September 2023

CONTENTS

RESEARCH ARTICLE

Turkish Journal of Civil Engineering, 2023 1-29, Paper 744, ***Research Article***

Simulation Models for Hydro-Electric Energy by Steady-Rate and Night-Shift-Pumped-Storage Operations

Tefaruk HAKTANIR[1]
Alper AYDEMİR[2]

ABSTRACT

New operation simulation models for hydroelectric energy and its financial benefit over an N-year period in daily time steps by the steady-rate and the open-loop night-shift-pumped-storage rules are developed. These models are applied on 11 existing dams in Türkiye, which reflect a wide range of hydrologic and hydraulic peculiarities, for regulations between 90% through 40% and the outputs are compared. Regulation is the ratio of (outflow for energy generation, hm^3/day) / (average inflow, hm^3/day). The present worth of energy benefits and of that of pumping costs computed with a discount rate of 9.5% over a 35-year period yield that the night-shift pumped-storage operations are more profitable than the steady-rate rule. Finally, generalized regression equations for average annual produced energy and for present worth of net benefits by both operation rules against statistically significant explanatory variables are developed using the results of these 11 dams, which are all meaningful by relevant statistical criteria.

Keywords: Reservoir operation, hydro-electric production by daily time steps, pumped-storage hydropower plants, renewable energy, water resources.

1. INTRODUCTION

According to a relevant report by the International Hydropower Association (IHA), the pumped-storage hydropower is the world's water battery because it provides flexible power services to grids since the beginning of the 20th century [1]. Zhang et al (2015) mention the advantages of the pumped-storage hydropower systems as balancing the peaking and dipping energy demands, providing reserve capacity, controlling frequency, and regulating phase fluctuations [2]. The pumped-storage hydropower is said to be the least-cost and hence the

Note:
- This paper was received on October 26, 2022 and accepted for publication by the Editorial Board on May 26, 2023.
- Discussions on this paper will be accepted by November 30, 2023.
- https://doi.org/10.18400/tjce.1310667

1 Nuh Naci Yazgan University, Department of Civil Engineering, Kayseri, Türkiye
thaktanir@nny.edu.tr - https://orcid.org/0000-0002-8111-4557

2 Nuh Naci Yazgan University, Department of Civil Engineering, Kayseri, Türkiye
aydemir@nny.edu.tr - https://orcid.org/0000-0003-3143-6758

preferred means for storing energy for durations between 4 and 16 hours in the Highlights section of *U.S. Hydropower Market Report* [3].

In a fairly recent paper, having done detailed research by GIS and DEM analyses, considering the existing reservoirs having at most 20 km distance from each other, it is concluded that the realizable potential of pumped-storage hydropower of all of Europe including Türkiye is 28.7 TWh/year and of Türkiye alone is 19.63 TWh/year [4]. This means the pumped-storage hydropower potential of Türkiye accounts for 68% of the European total. In spite of this fact, unfortunately, there is not a single pumped storage system operating in Türkiye.

In the 'Proposed Measures to be Taken in The Near Future' Section of the *General Activities Report of the Year 2021* published by the General Directorate of State Hydraulic Works of Türkiye, recommendations are made about implementing pumped-storage hydropower systems by dams in cascade positions to serve for the same objectives as those expressed in the first paragraph above [5] (www.dsi.gov.tr).

The Official Gazette of Republic of Türkiye dated 12.2.2020 presents the list of projects of agreed upon and endorsed investments by then (https://www.resmigazete.gov.tr). One of these projects is a closed-loop system of pumped-storage to be formed by constructing an upper reservoir along with a hydropower plant (HPP) having a capacity of 1400 MW to be jointly operated with the present Gökçaya Dam and HPP. This project, which will be the first pumped-storage system in Türkiye, is to be carried out by the Joint Venture formed by two Japanese companies and one Turkish company. Aside from this tangible action for realization of a first pumped-storage hydropower system, there have been quite a few academic theses, technical reports, and papers about pumped-storage hydropower in Türkiye [6, 7, 8, 9, 10, 11, 12, 13, 14, 15, 16].

Ak et al (2019) using 19-year long gauged monthly stream flows data, formed an objective function expressing the revenues gained by marketing the generated electricity minus the costs spent for pumping at night hours by the hydropower plants of three dams of Arkun, Yusufeli and Artvin, which are serially located in a cascading form on Coruh River [6]. Having solved the objective function using the package CONPOT, they determined that the net annual benefit of these three dams were greater when they were operated as if they had pumped storage hydropower plants than their present conventional hydropower operation. According to Ak et al (2019), in spite of suffering an energy loss about 15 ~ 25%, the pumped-storage systems provide technical benefits by regulating the fluctuations in electricity flow in the grid, and by taking advantage of the variations in electricity prices in parallel with demand patterns they also provide gains in financial revenues [6].

The main constraint of converting a dam into a pump storage facility is the excessive power needed to pump the same amount of water back up to the main reservoir. This fact includes two sub features. The first one is that the total head loss between the pump and the reservoir through the penstock must be added to the gross head. The second one is that the overall pump efficiency coefficient is in the denominator of the equation defining the power needed to run the pump. These two disadvantages analytically show up as: the power generated by the turbine is about 8*Q*(Hgross − Total head loss), whereas the power needed for the pump is about 12*Q*(Hgross + Total head loss) for the same gross head (Hgross) and the same discharge (Q) on the assumption that the overall turbine and pump efficiencies are tantamount at the value of 0.8155. Yet, the costs of either a reversible turbine-pump system or of a

separate turbine-generator and motor-pump system are greater than that of a conventional turbine-generator unit.

Therefore, it is obvious that in order for a pumped-storage hydropower project to be feasible, the market unit price of the hydroelectric energy generated during the peak-demand period should be considerably higher than that of the low-demand time, the so-called energy arbitrage as pointed out by both Zhang et al [2] and Firis et al [13]. The price differences in parallel with the grid demands may also affect the overall financial benefit of even the conventional HPPs. A typical example for this case exists in the feasibility report of Karakurt Dam in Türkiye [17], in which the benefit/cost ratio of the overall project is computed by taking 0.10 $/kWh during the peak-demand period in a day and 0.06 $/kWh during rest of the day.

IHA classifies the pumped hydropower systems as ‘closed-loop’ and ‘open-loop’ [1] . The closed-loop systems consist of two reservoirs, not necessarily on a running stream, having a fairly high elevation difference from each other, and they circulate the same volume of water between the upper and the lower reservoirs, pumping when there is a low demand and ample extra energy in the grid, and generating during peak-demand periods. The cases mentioned by DSI (2022), Ak et al (2019), and Gimeno-Gutierrez and Lacal-Arantegui (2015) are about the open-loop systems [5, 6, 4] . There is a final disadvantage of the open-loop pumped-storage hydropower systems, which is the necessity for a sufficient volume capacity just downstream of the hydropower station to store water to be pumped back during the low-demand night period. If there is another dam downstream in cascade position and if the backwater extension of its reservoir stores a sufficient amount of water for pumping, this will be an ideal case. Otherwise, there should be a small dam downstream to store the extra volume of water to be pumped back. This problem can be solved at a minimal cost by placing the downstream cofferdam a little further downstream from the construction site before the beginning of the construction of the dam and its appurtenant structures.

The theme of this study is also about the open-loop systems. Here, the summary of comparing the outcomes of the operation rules of the steady-rate and of the night-shift-pumped-storage by applying them on 11 existing dams in Türkiye, which are selected within criteria based on low-high dam body height, small-large reservoir volume, low-high hydropower energy production capacity, is presented. The steady-rate rule aims to generate power at a constant pace on a 7/24 basis. The night-shift-pumped-storage rule splits a day’s period in three segments called DAYTIME shift (11-hours-long between 06 and 17 hours), PEAK shift (5-hours-long between 17 and 22 hours), NIGHT shift (8-hours-long between 22 and 06 hours) as done by the Energy Market Regulatory Authority of Türkiye (known by the acronym EPDK in Türkiye) (www.epdk.gov.tr/Home/En). By the night-shift-pumped-storage rule energy is generated at full power capacity during the PEAK shift, and it is generated at a percentage between about 50% and 100% of full capacity during the DAYTIME shift. The extra volume of discharged water beyond the targeted release further downstream is pumped back up to the main reservoir during the NIGHT shift. We have developed models for operation simulations in daily time steps by these two rules and coded them as computer programs. Our models are of “sequential streamflow routing” type as called in *Engineering and Design HYDROPOWER* by USACE (1985) [18]. According to this relevant technical report, the sequential streamflow routing is the most detailed approach for determining the hydro-electric energy potential and the resultant financial benefits of hydropower dams, and

yet analytically it is the most complex method [18]. A study of similar theme by the steady-rate rule was done by Sever and Yurtal using the package program HEC-ResSim on three dams sequentially positioned on Ceyhan River in Türkiye [19].

Each one of our models is concisely explained in the 'Method' section. As will be noticed having perused the 'Method' and the 'Results' sections, they have original details peculiar to themselves. For example, each package repeats the operations for 11 regulations of 90%, 85%, 70%, …, 45%, 40%, all executed in a single run. Regulation is the ratio of (outflow for energy generation, hm^3/day)/(average inflow, hm^3/day). The objectives of this study are (1) to summarize the formulations and the steps of these newly developed models, (2) to apply the coded programs executing these models to 11 dams serving for hydropower generation in Türkiye, and (3) to determine generalized relationships for the average annual energy and the net financial benefit relating them to effective explanatory variables by these two different operation rules.

2. CASE STUDIES

Table 1 gives the names of 11 existing dams having hydropower plants in Türkiye along with characteristic information about them.

Table 1 - Descriptive data of dams used in this study

Name of dam	Name of stream	Active storage capacity (hm^3)	Average annual inflow (hm^3/yr)	Maximum gross head (m)	Type and number of turbines	Turbine design head (m)	Turbine design discharge (m^3/s)
Ağaçhisar	Orhaneli	77.8	526	75	Francis (2)	70	16.5
Altınkaya	Kızılırmak	2893	5755	133	Francis (4)	126	172
Bahçelik	Zamantı	185	333	29	Kaplan (3)	25	11.3
Berdan	Berdan	156	1632	39	Francis (2)	33	50
Ermenek	Ermenek	1747	1459	360	Francis (2)	327	53
Hasan Uğurlu	Yeşilırmak	662	5417	126	Francis (4)	121	128
Karakurt	Aras	447	1329	134	Francis (3)	130	2×46, 1×10
Kılıçkaya	Kelkit	831	2212	98	Francis (2)	91	83
Susurluk	Simav	165	1095	32	Kaplan (2)	30	60
Yamula	Kızılırmak	2020	2123	105	Francis (2)	97	55
Yedigöze	Seyhan	300	4425	95	Francis (2)	91	190

The stream-gauging stations 1501-Yamula, 1533-İnözü, 1818-Üçtepe, 1823-Emegil are almost at the same cross-sections where Yamula, Altınkaya, Yedigöze, and Bahçelik dams are located. The construction of Yamula dam was completed in 2004. The gauging record of

1501-Yamula began in 1939, and there are no missing records since then. The unregulated 35-year-long daily flows series between the years 1969 and 2003 are taken as the inflows to Yamula dam. The construction of Yedigöze dam was completed in 2011. The gauging at this station began in 1966 and continued until 2010 incessantly. The 35-year-long daily flows between the years 1976 and 2010 measured at station 1818-Üçtepe are considered to be the inflows to Yedigöze dam. The construction of Bahçelik dam was completed in the year 2012; but the station was closed in 2000. The gauging at 1823-Emegil began in 1974. In order to complete the record length to 35 years, the missing 8-year-long part between 2001 and 2008 was approximately computed by the drainage-area-ratio formula using the daily flows gauged at the close-by gauging station 1834-Kılıçmehmet.

There are not any gauging stations close enough to the embankments of the other seven dams. By investigating the beginning and ending record lengths of the nearest-by gauging stations around those seven dams and by choosing the most suitable stations, the 35-year-long gauged daily flows are approximately computed for them again by the drainage-area-ratio formula, by the procedure proposed in a relevant study [20].

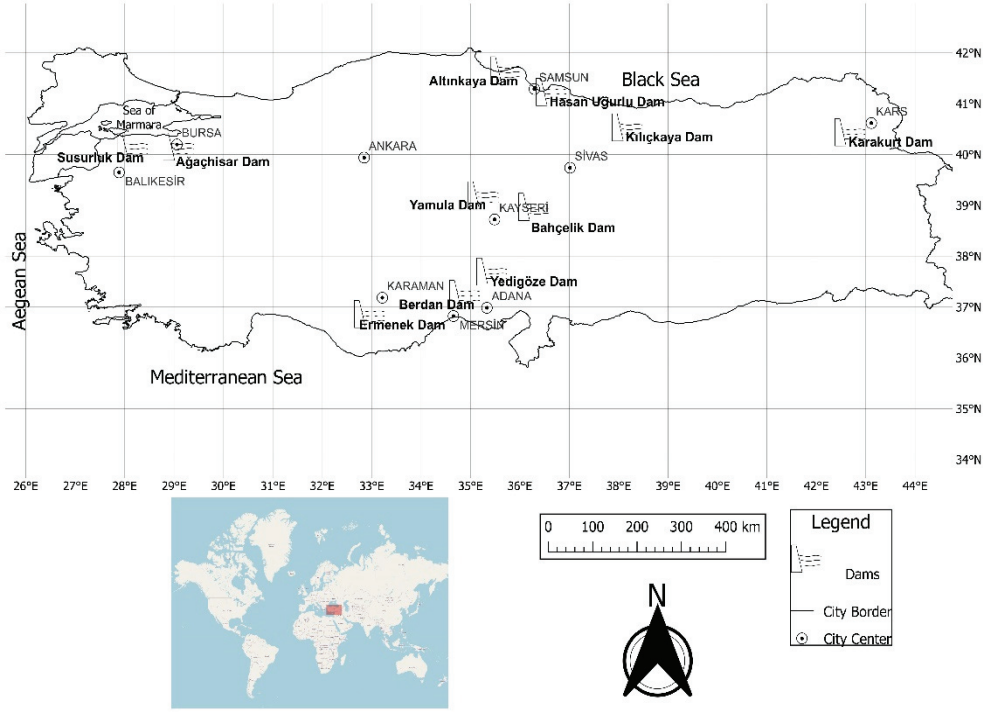

Figure 1 - Map of case study dams

All of the necessary technical data of the pipes constituting the penstocks such as the lengths, diameters, materials, and other peculiarities like bends, contractions, and valves were taken from the final project drawings of these 11 dams. Similarly, the storage volume (hm^3) and the lake surface area (km^2) against the lake water surface elevation (m) relationships were

also obtained from their final project drawings. The pan evaporation data in mm/day units at meteorological stations close-by to the reservoirs were obtained from the Turkish State Meteorological Service. A map of the case study dams created using the Free and Open Source QGIS software is given in Figure 1 [21, 22].

3. METHOD

3.1. Common Parts of the Two Simulation Models

The reservoir is top full at the beginning of an operation period of N years; namely, S_0 = Smax and WSE_0 = WSEmax, where S_0 is the volume of water in the reservoir and WSE_0 is the lake water surface elevation at the beginning of the first day of operations, WSEmax is the maximum operation elevation which is the top of active pool, and Smax is the volume of reservoir under WSEmax. The operation in a day is simulated by

$$S_{i,j,k} = S_{i-1,j,k} + I_{i,j,k} - EL_{i,j,k} - \sum_{s=1}^{NS} Os_{i,j,k} \quad (1)$$

Here, $S_{i-1,j,k}$ and $S_{i,j,k}$ are the volumes of water in the reservoir at the beginning and at the end of the i'th day of the j'th month of the k'th year (hm^3), $I_{i,j,k}$ is the inflow (hm^3/day), $EL_{i,j,k}$ is the loss of evaporation from the lake surface (hm^3/day), $Os_{i,j,k}$ is the flow released through the s'th spillway (hm^3/day) during the i'th day, and NS is the number of spillways. i varies from 1 through 30 for November, April, June, September, 1 through 31 for October, December, January, March, May, July, August, 1 through 28 for February and 1 through 29 for February every other four years. j varies from 1 through 12 and k varies from 1 through N. j=1 is October and j=12 is September. There are at least two spillways in a dam having a hydropower plant (HPP): the penstock and the flood spillway. There may be more spillways for other releases like irrigation and municipal waters.

We compute the evaporation loss by multiplying the lake surface area in km^2 at the beginning of the i'th day by 80% of daily pan evaporation value in m/day measured at a nearby meteorological station.

The water surface elevations of the tail-water pond in m is given against the total released discharges in m^3/s in form of two numerical columns at small enough increments of discharge in the input data file. The gross head of the penstock at the end of the i'th day is computed by

$$Hgr_{i,j,k} = WSE_{i,j,k} - TWS_{i,j,k} \quad (2)$$

The average gross head during the i'th day is computed as the average of the gross heads at the beginning and at the end of the i'th day by

$$\overline{Hgr}_{i,j,k} = (Hgr_{i-1,j,k} + Hgr_{i,j,k})/2 \quad (3)$$

In some dams, there is one shaft spillway which branches in the powerhouse into as many pipes as the number of turbines by means of a manifold (e.g. Yamula dam). In some other dams, there are as many pipes as the number of turbines in parallel layouts from the intake

down to the powerhouse (e.g. Yedigöze dam). Our models simulate both cases properly. We denote the number of pressure conduits culminating in the powerhouse by NP. The total head loss in m throughout the p'th pipe during the i'th day is computed by

$$\mathrm{THLp}_{i,j,k} = \mathrm{Cp} * \mathrm{Qp}_{i,j,k}^2 \quad (4)$$

Here, Cp is the overall loss coefficient for the p'th pipe accounting for all the friction and local losses from the trash rack down to the exit of the draft tube, $Qp_{i,j,k}$ is the discharge in m^3/s through the p'th pipe during the i'th day. With the help of another computer program, the numerical value of the Cp coefficient is obtained beforehand taking into account all geometrical and hydraulic peculiarities pertaining to that pipe covering a wide range of discharges up to the maximum capacity [23].

The average net head on the turbine at the end of the p'th pipe during the i'th day is computed by

$$\overline{\mathrm{Hnetp}}_{i,j,k} = \overline{\mathrm{Hgr}}_{i,j,k} - \mathrm{THLp}_{i,j,k} \quad (5)$$

3.2. Steady-Rate Operation Simulation

The relation between the target discharge to be released through the energy spillway in hm^3/day ($Qes_{i,j,k}$) and the same discharge in m^3/s ($Qest_{i,j,k}$) is

$$\mathrm{Qest}_{i,j,k}\ (m^3/s) = \mathrm{Qes}_{i,j,k}\ (hm^3/day) * (10^6/86400) \quad (6)$$

The maximum capacity discharge in m^3/s of a single turbine unit, denoted by Qt_{max}, is determined beforehand by the designers considering all the relevant geometric and hydraulic peculiarities pertaining to the head race, tail race conditions and the chosen turbine properties. If NP = 1, then $Qest_{i,j,k} \leq Qt_{max}$. If NP > 1, then as many pipes as the integer part of the division of ($Qest_{i,j,k}$ / Qt_{max}), denoted by NFP, will flow with full capacity while one pipe will convey as much a discharge as ($Qest_{i,j,k} - NFP*Qt_{max}$). Let NT denote the number of turbines. And, the net power generated by a turbine-generator-transformer unit is determined by

$$\mathrm{Pp}_{i,j,k} = \eta * \gamma * \mathrm{Qtp}_{i,j,k} * \overline{\mathrm{Hnetp}}_{i,j,k} \quad (7)$$

Here, η is the overall efficiency which equals multiplication of individual efficiencies of the turbine, the generator, and the transformer, γ is the unit weight of water in kN/m^3, $Pp_{i,j,k}$ is the net power to generate electric energy by that turbine in kW. In Section 7 of *Standard Handbook of Power Plant Engineering* it is suggested that 0.815 is a reasonable value for η [24]. In *Engineering and Design HYDROPOWER* by USACE (1985), it is written: "A value of 80 to 85 percent can be used prior to turbine selection, but once a turbine design has been chosen, an average efficiency based on the characteristics of that unit should be used." [18]. In a technical report about the hydropower potential of Sır Dam in Türkiye, 0.866 is taken for η [25] The efficiency of the transformer is the highest and about 0.98. Next comes the efficiency of the generator, which according to USACE (1985), is between 0.95 and 0.98

[18]. The turbine efficiency depends on the specific velocity and hence on both the discharge through and the net head on the turbine and also on the type and brand name of the turbine. When both are operated at their optimum heads and discharges, the efficiency of the Pelton turbines is said to be a little higher than that of the Francis turbines (e.g. [26]). Generally, the efficiency of Francis turbines varies between 0.70 and 0.92, and for close to optimum ranges, their efficiency is in the range: 0.80 and 0.92 [18, 26]. Our models use an average value for $\eta*\gamma$ in the range: $8.0 - 8.5$ given by the user.

There are operable ranges of net head and turbine discharge depending on type of the turbine (e.g. [18, 24, 26]). The efficiency at heads and discharges higher than the design values will be close to the design conditions. The lower bounds are problematic. Much lower discharges and heads than the design values may cause cavitation damage on the runner blades, vibration of the unit and will result in too low an efficiency. Table 5-1 in *Engineering and Design HYDROPOWER* by USACE (1985) and Table 4.2 in *Hydropower Engineering Handbook* (Gulliver and Arndt 1991) offer operable ranges of heads, discharges, and powers for various types of turbines [18, 26]. In our models, we specify a lower bound for the power accounting for the effects of head and discharge jointly, and we suggest this to be 25% of the rating capacity. In any day, the turbine is shut off when the net power by that turbine turns out to be smaller than this lower-bound value and power is not generated. That discharge is not released downstream and the unreleased amount is recorded as the shortage of that day from the target release.

The total power generated by the HPP of the dam in the i'th day is computed by

$$\mathrm{Ptotal}_{i,j,k} = \sum_{p=1}^{NT} \mathrm{Pp}_{i,j,k} \tag{8}$$

Here, $\mathrm{Pp}_{i,j,k}$ is the net power by the p'th turbine in the i'th day in kW. If the energy shaft spillway is of a single pipe, then the total power is computed by equation (7), which is distributed to NT number of turbines in the powerhouse in proportion to their capacities.

The energy produced in a normal day is computed by

$$\mathrm{HEE}_{i,j,k} = \mathrm{Ptotal}_{i,j,k} * 24 \tag{9}$$

Here, $\mathrm{HEE}_{i,j,k}$ is the energy generated in the i'th day in kWh/day. Next, the monthly energy produced is computed by

$$\mathrm{MHEE}_{j,k} = \sum_{i=1}^{\text{iend-j}} \mathrm{HEE}_{i,j,k} \tag{10}$$

Here, iend-j equals one of 30, 31, 28, 29 depending on the j'th month, $\mathrm{MHEE}_{j,k}$ is the generated energy in the j'th month of the k'th year in kWh/month. Next, the annual energy produced in the k'th year in kWh/year is computed by

$$\mathrm{AHEE}_{k} = \sum_{j=1}^{12} \mathrm{MHEE}_{j,k} \tag{11}$$

The minimum of 365.25*N $\mathrm{HEE}_{i,j,k}$'s is known as the 'firm energy' (FE) [18]. In any day, the difference of the energy of that day from the firm energy is called the 'secondary energy'.

Because the firm energy is available in any day over the entire N year period, it is treated as an assured energy and that is why its unit price is a little greater than the secondary energy. The annual financial benefit due to marketing of the produced energy in the k'th year is computed by

$$FB_k = 365 * FE * UP\text{-}FE + \sum_{j=1}^{12} \sum_{i=1}^{iend\text{-}j} (HEE_{i,j,k} - FE) * UP\text{-}SE \quad (12)$$

Until 2015, in Türkiye the unit prices of the firm and the secondary energies were taken as: UP-FE = 0.06 $/kWh and UP-SE = 0.033 $/kWh. By a circular issued in 2015 by the General Directorate of State Hydraulic Works [27], the concepts of firm and secondary energies are abolished and a steady unit price for hydroelectric energy is adopted. Our model by the steady-rate rule still determines the firm energy and computes the financial accounts of the firm and the secondary energies separately. However, in the current study we have given the same numerical value for both, which is 0.04 $/kWh.

The overall financial benefit is computed by

$$PWFB = \sum_{k=1}^{N} FB_k * (1 + dr)^{-k} \quad (13)$$

Here, dr is the discount ratio, which is being taken as 0.095 over the last few decades in Türkiye (e.g. [27]) and PWFB is the present worth of the financial benefits by the produced energy at the beginning of the N-year operation period in Dollars.

Our models generate extra energy by releasing greater discharges than the target discharge through the energy spillway during a day in which the lake water surface elevation is equal to or very close to the maximum operation elevation (top of active pool) when a high inflow comes such that the lake water surface elevation at the end of the day will exceed the top of active pool. During such a day all of the turbines will run at or close to their maximum capacity discharges and extra energy is produced by surplus waters which would otherwise be discarded over the flood spillway. For a mild flood the excessive waters may be small enough to be taken up by the turbines. As an example, while the average inflow to Altınkaya Dam is 182 m^3/s, the total discharge of its four turbines when all run at full capacity is 688 m^3/s, about 3.8 times the average inflow. For a massive flood however, the excessive amount of flows left over from fully operating turbines will still be conveyed over the flood spillway. The surplus amount of water in such a day is given by

$$Surplus_{i,j,k} = S_{i-1,j,k} + I_{i,j,k} - EL_{i,j,k} - \sum_{s=1}^{NS-2} Os_{i,j,k} - S_{max} \quad (14)$$

Here, NS−2 is the number of spillways other than the flood spillway and the energy spillway (penstock) and $Surplus_{i,j,k}$ is the surplus amount of water in the i'th day in hm^3/day that can be diverted through the penstock. If $Surplus_{i,j,k}$ is greater than the sum of capacity discharges of NP pipes of the energy spillway, then all of the turbines will run with their maximum discharges, and as much water as ($Surplus_{i,j,k} - NP*Qt_{max}*86400/10^6$) in hm^3/day will flow over the flood spillway. If $Surplus_{i,j,k} < NP*Qt_{max}*86400/10^6$, then that means a mild flood is effective while the lake is top full whose excess waters will all be taken up by the energy spillway. In such a day, the integer part of the division: [($Surplus_{i,j,k}*10^6/86400$) / Qt_{max}] gives the number of turbines running at full capacity, denoted by NTF and one turbine will run

with a discharge: $[(\text{Surplus}_{i,j,k}*10^6/86400) - \text{NTF}*\text{Qt}_{max}]$. The total head losses, the generated powers and energies are computed by the equations given above.

Throughout the simulation, those discharges for purposes other than the energy generation depending on their priorities in a day are either reduced or completely shut off when the lake water surface elevation equals the minimum operation elevation (bottom of active pool) or very close to that when little amount of inflow comes such that the lake water surface elevation at the end of the day will become less than or equal to the bottom of active pool. In that day a shortage from the targeted energy discharge also may occur and hence small power and small energy is generated. In such a day, the power that could be generated may fall below the lower-limit value peculiar to the used turbine, and hence, no flow is discharged through any turbine, zero power is generated, and the target energy spillway flow of that day in hm^3/day is recorded as a shortage in release further downstream of the dam. In such a critical day, the amount of water left for possible but little amount of power is given by

$$\text{Left}_{i,j,k} = S_{i-1,j,k} + I_{i,j,k} - EL_{i,j,k} - \sum_{s=1}^{NS-2} Os_{i,j,k} - S_{min} \quad (15)$$

The discharge that can be released through a turbine in m^3/s equals $(\text{Left}_{i,j,k}*10^6/86400)$.

3.3. Night-Shift-Pumped-Storage Operation Simulation

All of the turbines run at their maximum capacities during the PEAK shift. The turbines run with a discharge in proportion to their maximum capacities during the DAYTIME shift. The ratio of DAYTIME discharge to the maximum penstock discharge, which is within the range: 0.5 - 1.0, is initially assigned by the user. The difference of the volume of water released during the DAYTIME and PEAK shifts from the target release further downstream is pumped back up to the main reservoir during the NIGHT shift. The durations of these within-day shifts are determined by the Energy Market Regulatory Authority (EPDK). The user of the program can give durations different from the ones adopted by EPDK.

3.3.1. Energy Produced During the PEAK Shift and its Financial Worth

If the energy spillway is a single pipe branching into as many small pipes as the number of turbines, then the total head loss, the average net head on each one of the turbines, and the generated power during the PEAK shift of the i'th day are computed as follows.

$$\text{THL}_{\text{peak}_{i,j,k}} = C * (NT * \text{Qt}_{max})^2 \quad (16)$$

$$\overline{\text{Hnet}}_{\text{peak}_{i,j,k}} = \overline{\text{Hgr}}_{i,j,k} - \text{THL}_{\text{peak}_{i,j,k}} \quad (17)$$

$$\text{Ppeaktotal}_{i,j,k} = \eta * \gamma * NT * \text{Qt}_{max} * \overline{\text{Hnet}}\text{peak}_{i,j,k} \quad (18)$$

In these equations, C is the total head loss coefficient of the energy spillway including the branching-pipe local loss and the exit velocity head of the draft tube of a turbine.

If the energy spillway consists of as many pipes as the number of turbines from the intake at the forebay down to the tailrace, then the total head loss, the average net head, and the generated power during the PEAK shift of the i'th day are computed as follows.

$$\mathrm{THL}_{\mathrm{peak}}\mathrm{p}_{\mathrm{i,j,k}} = \mathrm{Cp} * \mathrm{Qt}_{\mathrm{max}}{}^{2} \tag{19}$$

$$\overline{\mathrm{Hnet}}_{\mathrm{peak}}\mathrm{p}_{\mathrm{i,j,k}} = \mathrm{Hgr}_{\mathrm{i,j,k}} - \mathrm{THL}_{\mathrm{peak}}\mathrm{p}_{\mathrm{i,j,k}} \tag{20}$$

$$\mathrm{P}_{\mathrm{peak}}\mathrm{p}_{\mathrm{i,j,k}} = \eta * \gamma * \mathrm{Qtmax} * \overline{\mathrm{Hnet}}_{\mathrm{peak}}\mathrm{p}_{\mathrm{i,j,k}} \tag{21}$$

$$\mathrm{P}_{\mathrm{peak}}\mathrm{total}_{\mathrm{i,j,k}} = \sum_{\mathrm{p=1}}^{\mathrm{NT}} \mathrm{P}_{\mathrm{peak}}\mathrm{p}_{\mathrm{i,j,k}} \tag{22}$$

Here, Cp is the total head loss coefficient of the p'th pipe.

In either case, the produced energy and its financial benefit during the PEAK shift of the i'th day are computed by

$$\mathrm{HEE}_{\mathrm{peak}_{\mathrm{i,j,k}}} = \mathrm{P}_{\mathrm{peak}}\mathrm{total}_{\mathrm{i,j,k}} * \mathrm{D}_{\mathrm{peak}} \tag{23}$$

$$\mathrm{FB}_{\mathrm{peak}_{\mathrm{i,j,k}}} = \mathrm{HEE}_{\mathrm{peak}_{\mathrm{i,j,k}}} * \mathrm{UP}_{\mathrm{peak}} \tag{24}$$

Here, D_{peak} is the duration of the PEAK shift in hours, UP_{peak} is the unit marketing price of energy produced during the PEAK shift.

The volume of water released through the energy spillway in hm^3/day during the PEAK shift of the i'th day while all of the turbines are running with their maximum capacity discharges, $Qes_{peaki,j,k}$, is

$$\mathrm{Qes}_{\mathrm{peak}_{\mathrm{i,j,k}}} = \mathrm{NT} * \mathrm{Qt}_{\mathrm{max}} * \mathrm{D}_{\mathrm{peak}} * 3600/10^{6} \tag{25}$$

3.3.2. Energy Produced During the DAYTIME Shift and its Financial Worth

The upper limit for volume of water that can be released through the energy spillway during the DAYTIME shift is equal to the sum of the maximum capacity discharges of all of the turbines running throughout the DAYTIME shift. And, the lower limit equals the daily target release minus the volume of water discharged during the PEAK shift. The below inequalities depict these verbally expressed bounds.

$$(\mathrm{Qes}_{\mathrm{i,j,k}} - \mathrm{Qes}_{\mathrm{peak}_{\mathrm{i,j,k}}}) < \mathrm{Qesdaytime}_{\mathrm{i,j,k}} < (\mathrm{NT} * \mathrm{Qt}_{\mathrm{max}} * \mathrm{Ddaytime} * 3600/10^{6}) \tag{26}$$

Here, $Qes_{i,j,k}$ is the daily target release for energy production in hm^3/day, also called target penstock release, $Qesdaytime_{i,j,k}$ is the volume of water released through the energy spillway in hm^3/day during the DAYTIME shift of the i'th day, Ddaytime is the duration of the DAYTIME shift in hours, and obviously this expression is valid for a daily target energy spillway release greater than the amount discharged during the PEAK shift. In that case, if

$Qesdaytime_{i,j,k}$ equals the lower bound of this inequality, then there is no amount of water to be pumped back up to the main reservoir.

Labeling a ratio as: "ratio of daytime penstock target release" (symbolized by RDPR) which equals (actual DAYTIME penstock discharge in m^3/s)/(maximum possible penstock discharge in m^3/s), taking Ddaytime as 11 hours and Dpeak as 5 hours, the algebraic manipulations lead to the following boundaries for RDPR.

$$\{Qes_{i,j,k} \div [0.0396 * NT * Qt_{max}]\} - 0.4545455 \ < RDPR < 1.0 \quad (27)$$

Here, Qt_{max} is the maximum capacity discharge of one of NP number of pipes constituting the penstock. Having chosen a magnitude for RPDR within these bounds, the discharge of energy spillway during the DAYTIME shift in m^3/s units is computed by

$$Qesdaytimet_{i,j,k} = RDPR * NT * Qt_{max} \quad (28)$$

The number of turbines running at their maximum capacities during the DAYTIME shift equals the integer part of the division ($Qesdaytime\text{-}t_{i,j,k}$ / Qt_{max}). Denoting this number by NTD, one turbine other than NTD turbines runs with a discharge: $Qesdaytimet_{i,j,k}$ − NTD*Qt_{max}.

If the energy spillway is a single pipe branching into as many small pipes as the number of turbines, then the total head loss, the average net head on each one of the turbines, and the generated power during the DAYTIME shift of the i'th day are computed as follows.

$$THL\text{-}daytime_{i,j,k} = C * Qesdaytimet_{i,j,k}{}^2 \quad (29)$$

$$\overline{Hnet}daytime_{i,j,k} = \overline{Hgr}_{i,j,k} - THLdaytime_{i,j,k} \quad (30)$$

$$Pdaytimetotal_{i,j,k} = \eta * \gamma * Qesdaytimet_{i,j,k} * \overline{Hnet}daytime_{i,j,k} \quad (31)$$

If the energy spillway consists of as many pipes as the number of turbines, then the total head loss and the average net head in NTD number of pipes, and the generated power at NTD turbines during the DAYTIME shift are the same as those of the PEAK shift. The total head loss and the average net head in the pipe carrying a smaller-than-maximum discharge and the power generated by the turbine at the end of that pipe are computed by equations (19), (20), (21) by substituting ($Qesdaytimet_{i,j,k}$ − NTD*Qt_{max}) for Qt_{max}. Next, the generated power during the DAYTIME shift of the i'th day is computed by

$$Pdaytimetotal_{i,j,k} = \sum_{p=1}^{NDT+1} Pdaytimep_{i,j,k} \quad (32)$$

In either case, the produced energy and its financial benefit during the DAYTIME shift of the i'th day are computed by

$$HEEdaytime_{i,j,k} = Pdaytimetotal_{i,j,k} * Ddaytime \quad (33)$$

$$\mathrm{FBdaytime_{i,j,k}} = \mathrm{HEEdaytime_{i,j,k}} * \mathrm{UPdaytime} \quad (34)$$

Here, UPdaytime is the unit marketing price of energy produced during the DAYTIME shift.

3.3.3. Energy Produced During the NIGHT Shift and its Financial Worth

At the beginning of an i'th day, if the reservoir water surface elevation is equal to or very close to the top of active pool and the inflow in that day is too much so as to cause the lake water level at the end of the day to exceed the top of active pool, then, all of the turbines are run at their full capacities during the DAYTIME shift also. Namely, regardless of the target energy release, the actual DAYTIME release is increased to the value of the upper bound of inequality (26). If the maximum operation elevation is still exceeded with all of the turbines operating at full capacities during both the DAYTIME and the PEAK shifts, then pumping during the NIGHT shift is not done since there is not available storage volume in the reservoir. Instead, energy is generated during the NIGHT shift as well using some of these surplus waters which would otherwise be discharged by the flood spillway. The volume of water in hm^3/day which will be used for power generation during the NIGHT shift of such a day equals the smaller one of those computed by the two equations below.

$$\mathrm{Qesnight_{i,j,k}} = \mathrm{Surplus_{i,j,k}} - [(\mathrm{NT} * \mathrm{Qt_{max}} * \mathrm{Ddaytime_{peak}} * 3600)/10^6] \quad (35a)$$

$$\mathrm{Qesnight_{i,j,k}} = (\mathrm{NT} * \mathrm{Qt_{max}} * \mathrm{Dnight} * 3600)/10^6 \quad (35b)$$

Here, $\mathrm{Ddaytime_{peak}}$ equals the sum of Ddaytime plus $\mathrm{D_{peak}}$, Dnight is the duration of the HIGHT shift in hours, and $\mathrm{Surplus_{i,j,k}}$ is the surplus amount of water given by equation (14). Conversion of $\mathrm{Qesnight_{i,j,k}}$ from hm^3/day to m^3/s units is done by

$$\mathrm{Qesnightt_{i,j,k}} = (\mathrm{Qesnight_{i,j,k}} * 10^6)/(\mathrm{Dnight} * 3600) \quad (36)$$

The number of turbines running with their maximum capacity discharges equals the integer part of the division of ($\mathrm{Qesnightt_{i,j,k}}$ / $\mathrm{Qt_{max}}$), which could be zero if $\mathrm{Qesnightt_{i,j,k}} < \mathrm{Qt_{max}}$. Denoting this number by NTN, one turbine other than NTN turbines runs with a discharge: $\mathrm{Qesnightt_{i,j,k}} - \mathrm{NTN}*\mathrm{Qt_{max}}$.

If the energy spillway is a single pipe branching into as many small pipes as the number of turbines, then the total head loss, the average net head on each one of the turbines, and the generated power during the NIGHT shift of the i'th day are computed as follows.

$$\mathrm{THLnight_{i,j,k}} = \mathrm{C} * \mathrm{Qesnightt_{i,j,k}}^2 \quad (37)$$

$$\overline{\mathrm{Hnet}}\mathrm{night_{i,j,k}} = \overline{\mathrm{Hgr}}_{\mathrm{i,j,k}} - \mathrm{THLnight_{i,j,k}} \quad (38)$$

$$\mathrm{Pnighttotal_{i,j,k}} = \eta * \gamma * \mathrm{Qesnightt_{i,j,k}} * \overline{\mathrm{Hnet}}\mathrm{night_{i,j,k}} \quad (39)$$

If the energy spillway consists of as many pipes as the number of turbines, then the total head loss and the average net head in NTN number of pipes, and the generated power at NTN

turbines during the NIGHT shift are the same as those of the PEAK shift. The total head loss and the average net head in the pipe carrying a smaller-than-maximum discharge and the power generated by the turbine at the end of that pipe are computed by equations (19), (20), (21) by substituting ($Qesnight_{i,j,k} - NTN*Qt_{max}$) for Qt_{max}. Next, the generated power during the NIGHT shift of the i'th day is computed by

$$\text{Pnighttotal}_{i,j,k} = \sum_{p=1}^{NTN+1} \text{Pnight-p}_{i,j,k} \tag{40}$$

In either case, the produced energy and its financial benefit during the NIGHT shift of the i'th day are computed by

$$\text{HEEnight}_{i,j,k} = \text{Pnighttotal}_{i,j,k} * \text{Dnight} \tag{41}$$

$$\text{FBnight}_{i,j,k} = \text{HEEnight}_{i,j,k} * \text{UPnight} \tag{42}$$

Here, UPnight is the unit marketing price of energy produced during the NIGHT shift.

3.3.4. Energy Consumed for Pumping During the NIGHT Shift and its Financial Cost

At the end of a normal day of operations, the volume of water in the reservoir will be between the dead storage and (dead storage + active storage capacity) ($Smin < S_{i,j,k} < Smax$). In such a day, all turbines run at their full capacities during the PEAK shift and the total volume of energy flows during the DAYTIME shift, $Qesdaytime_{i,j,k}$, will be between the lower and upper bounds of inequality (26), which is decided on by the operators of the dam. Then, the flowrate of water in m^3/s to be pumped back up to the main reservoir during the NIGHT shift, $Qpumpt_{i,j,k}$, is computed by

$$\text{Qpumpt}_{i,j,k} = \left(\text{Qes}_{\text{peak}_{i,j,k}} + \text{Qesdaytime}_{i,j,k} - \text{Qes}_{i,j,k}\right) * 10^6/(3600 * \text{Dnight}) \tag{43}$$

In this study, we assume that the turbo-machinery units are either reversible turbine-pump types or ternary systems having a common shaft.

We use the term Qpumpmax denoting the maximum capacity discharge of a pump, which will be a close value to that of a turbine, Qt_{max}. Both Qt_{max} and $Qpump_{max}$ are predetermined values computed by the project designers of the dam and the hydropower plant. Then, the number of pumps running at their maximum capacities during the NIGHT shift equals the integer part of the division ($Qpumpt_{i,j,k}$ / $Qpump_{max}$). Denoting this number by NPN, one pump other than NPN pumps runs with a discharge: $Qpumpt_{i,j,k} - NPN*Qpump_{max}$.

If the energy spillway is a single pipe branching into as many small pipes as the number of turbines, then the total head loss, the average net head on each one of the pumps, and the power consumed by all of the pumps during the NIGHT shift of the i'th day are computed as follows.

$$\text{THLpump}_{i,j,k} = \text{Cpump} * \text{Qpumpt}_{i,j,k}{}^2 \tag{44}$$

$$\overline{\text{Hnet}}\text{pump}_{i,j,k} = \overline{\text{Hgr}}_{i,j,k} + \text{THLpump}_{i,j,k} \quad (45)$$

$$\text{Ppumptotal}_{i,j,k} = \gamma * \text{Qpumpt}_{i,j,k} * \overline{\text{Hnet}}\text{pump}_{i,j,k} / \eta\text{pump} \quad (46)$$

In these equations, Cpump is the total head loss coefficient of the pipe used for pumping when the flow is in reverse direction, ηpump is the overall pumping efficiency. Equations (44) and (45) are valid for any system, whether it is the same pipe of a reversible turbine-pump unit or of a ternary unit or even if the pumping is done through a separate pipe.

If the energy spillway consists of as many pipes as the number of turbines, then the total head loss and the average net head in each one of NPN number of pipes, and the power needed for each pump during the NIGHT shift are computed as follows.

$$\text{THLpumpp}_{i,j,k} = \text{Cpumpp} * \text{Qpump}_{max}{}^2 \quad (47)$$

$$\overline{\text{Hnet}}\text{pumpp}_{i,j,k} = \overline{\text{Hgr}}_{i,j,k} + \text{THLpumpp}_{i,j,k} \quad (48)$$

$$\text{Ppumpp}_{i,j,k} = \gamma * \text{Qpumpmax} * \overline{\text{Hnet}}\text{pumpp}_{i,j,k} / \eta\text{pumpp} \quad (49)$$

The total head loss and the average net head in the pipe in which a smaller-than-maximum discharge is pumped, and the power needed for that pump during the NIGHT shift are computed by equations (47) − (49) by inserting ($\text{Qpumpt}_{i,j,k}$ − NPN*Qpump_{max}) for Qpump_{max}. The total power needed for all of the running pumps are computed by

$$\text{Ppumptotal}_{i,j,k} = \sum_{p=1}^{NPN+1} \text{Ppumpp}_{i,j,k} \quad (50)$$

In either case, the energy needed for pumping during the NIGHT shift of the i'th day and its financial cost are computed by

$$\text{EEpump}_{i,j,k} = \text{Ppumptotal}_{i,j,k} * \text{Dnight} \quad (51)$$

$$\text{FCpump}_{i,j,k} = \text{HEEpump}_{i,j,k} * \text{UCpump} \quad (52)$$

Here, UCpump is the unit cost of energy consumed for pumping during the NIGHT shift.

3.3.5. Daily, Monthly, and Yearly Produced Energies and Their Financial Benefits

The generated energy and its financial benefit in an i'th day are computed as follows.

$$\text{HEE}_{i,j,k} = \text{HEEdaytime}_{i,j,k} + \text{HEE}_{\text{peak}_{i,j,k}} + \text{HEEnight}_{i,j,k} \quad (53)$$

$$\text{FB}_{i,j,k} = \text{FBdaytime}_{i,j,k} + \text{FB}_{\text{peak}_{i,j,k}} + \text{FBnight}_{i,j,k} \quad (54)$$

The monthly and yearly generated energies are computed by equations (10) and (11), and their financial benefits are computed as follows.

$$\text{MFB}_{j,k} = \sum_{i=1}^{\text{iend-j}} \text{FB}_{i,j,k} \quad (55)$$

$$\mathrm{YFB_k} = \sum_{j=1}^{12} \mathrm{MFB_{j,k}} \tag{56}$$

The monthly and yearly energies spent for pumping and their financial costs are computed as follows.

$$\mathrm{EEpump_{j,k}} = \sum_{i=1}^{\mathrm{iend\text{-}j}} \mathrm{EEpump_{i,j,k}} \tag{57}$$

$$\mathrm{FCpump_{j,k}} = \sum_{i=1}^{\mathrm{iend\text{-}j}} \mathrm{FCpump_{i,j,k}} \tag{58}$$

$$\mathrm{YEEpump_k} = \sum_{j=1}^{12} \mathrm{EEpump_{j,k}} \tag{59}$$

$$\mathrm{YFCpump_k} = \sum_{j=1}^{12} \mathrm{FCpump_{j,k}} \tag{60}$$

The net difference of yearly financial benefit on account of marketing the generated energies from the yearly cost accrued due to the electrical energy charged to the pump motors is computed by

$$\mathrm{NFB_k} = \mathrm{YFB_k} - \mathrm{YFCpump_k} \tag{61}$$

3.4. Present worth Values at the Beginning of an N-Year Operation Period and Overall Optimization

The present worth at the beginning of an N-year operation period of either the benefits by marketing the produced energy or the costs of energy consumed by pumping taking into account the time value of money in proportion to the adopted discount ratio (dr) is computed by the known formula as follows.

$$\mathrm{PWFB} = \sum_{k=1}^{N} \mathrm{YFB_k} * (1 + \mathrm{dr})^{-k} \tag{62}$$

$$\mathrm{PWFCpump} = \sum_{k=1}^{N} \mathrm{YFCpump_k} * (1 + \mathrm{dr})^{-k} \tag{63}$$

And, the present worth of the net income by the night-shift-pumped-storage rule is computed by

$$\mathrm{PWFBnet} = \mathrm{PWFB} - \mathrm{PWFCpump} \tag{64}$$

The operation simulation models in daily time steps by a definite regulation summarized heretofore determine that average energy spillway release providing for the highest present worth of the net benefits over an N-year period as the outcome of 11 large loops for regulations of 90% through 40% at 5% decrements. The execution of such a run for a 12,784-day operation period (N=35) takes about five seconds in common PCs.

Although operations with regulations as low as 40% of the average inflow are executed, our models automatically release more than the target flows in any day when the active pool is top full. The assumption here is that the extra energy produced in any day will be used

somehow. For example, according to a report funded by the European Union's Horizon 2020 Research and Innovation Programme, the extra electric energy can be used up for desalinization of sea water which in turn will be diverted to a nearby urban center [28]. Other plausible usages of extra energy are: extraction of oxygen and hydrogen gases by electrolysis of water, recharging of large-capacity battery fields developed in recent years to instantly counter peak demands of towns for periods of a few hours or even a couple of days. In a recent summit initiated by the European Union, a commitment for investment of large-scale electrolysis facilities for production of hydrogen has been signed by many relevant organizations including private commercial companies [29].

Our models take into account daily releases for all purposes next to energy, and they account for all of them quantitatively and detect that regulation providing for the highest present worth of financial benefits due to energy production. In short, our models realistically quantify the potential capacity of optimum energy production and the net financial gains thereof by simulating the actual hydrologic, hydraulic, and electric happenings in conjunction with the active storage capacity and its rate of change with elevation, with the rating curve of the tailwater pool, and with all the relevant peculiarities of the hydropower plant affecting the production of energy such that over an operation period of 35 or 50 years, the optimum potential is obtained as the outcome.

Concise flowcharts depicting all these phases and succinct details of our models are given in Figure 2a and Figure 2b.

3.5. Regressions for the Average Energy Production and the Optimum Financial Benefit

We have applied the steady-rate and the night-shift-pumped-storage operation simulation models to 11 dams in various regions in Türkiye. By experience (e.g. [14, 23]) we hypothesize that both the average annual produced energy and the present worth of financial benefits by marketed energy over an N-year operation period may be related to some relevant explanatory variables. In the following we are listing these variables along with the reasons for choosing them.

1) Average inflow in hm^3/year (symbolized by x_1 in the regression analyses).

Obviously, there must exist a positive relationship between the average hydroelectric energy and the average inflow coming to the reservoir.

2) Ratio of (target outflow for energy generation in hm^3/day)/(average inflow in hm^3/day), which is the regulation for a hydropower dam (symbolized by x_2 in the regression analyses).

If the total storage capacity of a dam is very large, then it can keep all of the hydrograph of an extreme incoming flood. If such a case were real, then the maximum value of the average outflow for generation of hydropower would equal the long-term average inflow. This is impossible, and even those dams having considerably large storage capacities will have to discard some portions of extreme floods over the flood spillway. Therefore, a regulation of 1.0 is impossible and it must be smaller than 1.0. Yet, it is a known fact that higher the active storage capacity higher the regulation without causing depletion of water in the active storage.

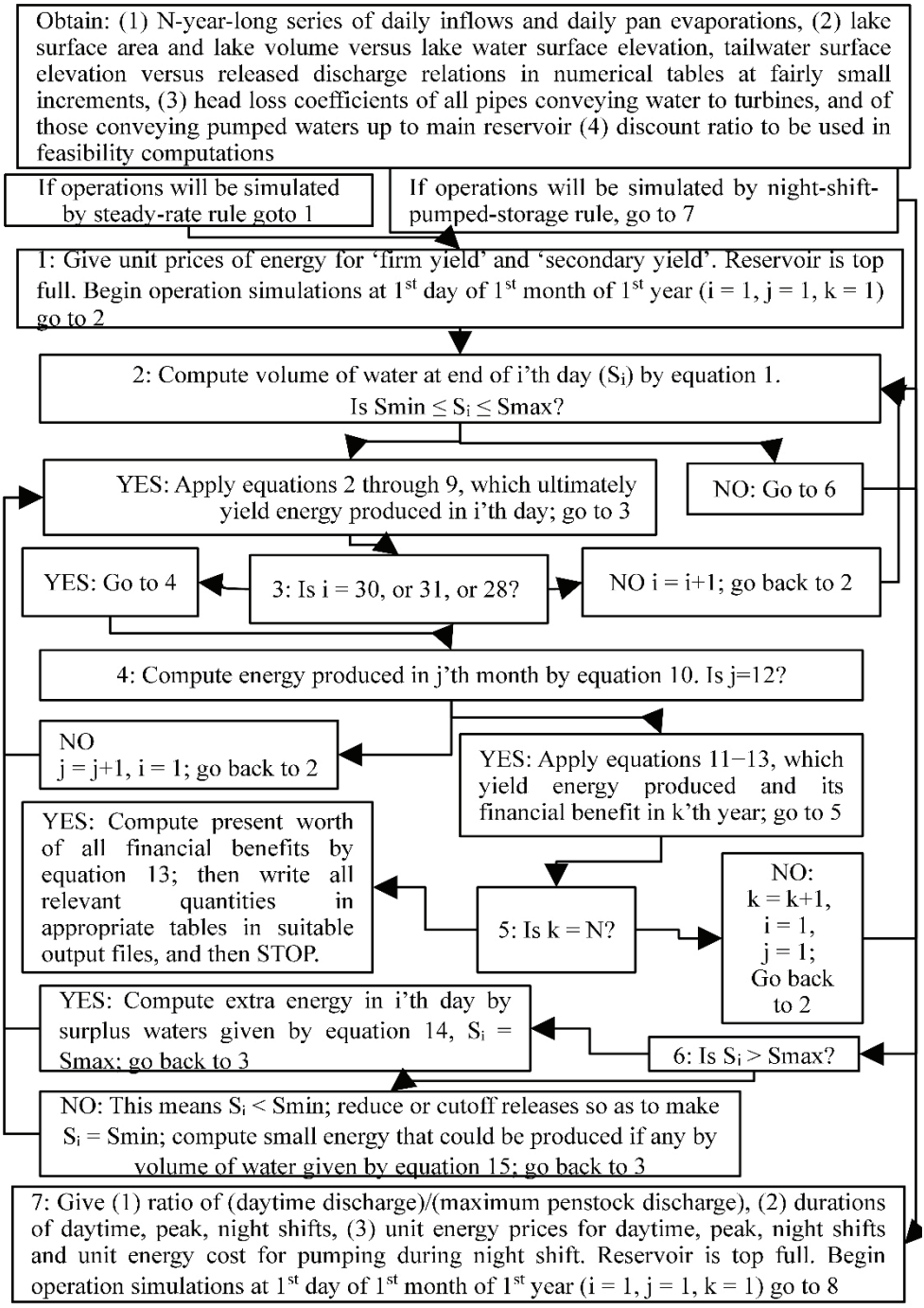

Figure 2a - Flowchart of the onset and flowchart of the model for the steady-rate rule

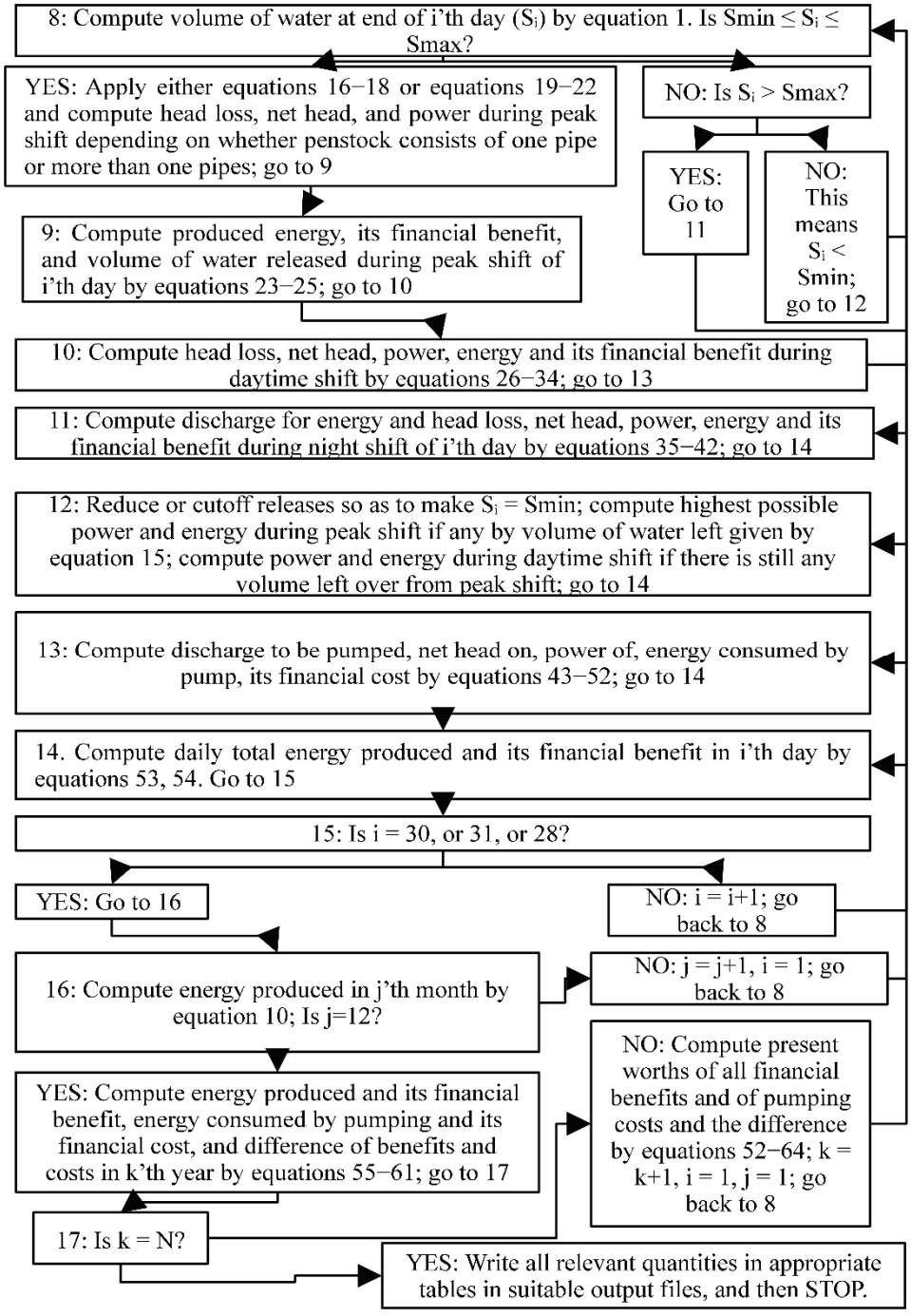

Figure 2b - Flowchart of the model for the night-shift-pumped-storage rule

3) Average net head on a turbine in m with the average target outflow for energy generation when the volume of water in the active storage is as much as half of the active storage capacity (symbolized by x_3 in the regression analyses).

Because of existence of sub-periods of droughts and of excessive flows over the total N-year operation, the water surface level fluctuates between the maximum and the minimum operation elevations. Hence, the net head on turbines when the reservoir is half full should be a realistic explanatory variable affecting the generated power and the resultant energy.

4) Ratio of (active storage capacity in hm^3)/(average inflow in hm^3/year) (symbolized by x_4 in the regression analyses).

This ratio reflects the maximum amount of storable water to be used during periods of low flow and it quantitatively describes the relative size of the active storage capacity in proportion to the average inflow. Higher this ratio higher the possible target outflow for energy generation and higher the energy production capacity should be.

5) Ratio of (maximum penstock discharge in m^3/s)/(average inflow in m^3/s) (symbolized by x_5 in the regression analyses).

Higher this ratio higher the energy production potential should be simply because a large portion of high flows will be diverted to the energy spillway instead of being discarded over the flood spillway.

6) Variation coefficient of the long series of N*365.25 daily inflows (symbolized by x_6 in the regression analyses).

This single variation coefficient of the long series of daily flows will reflect the fluctuations both in annual inflows and in seasonal flows. If the fluctuations are mild, a high average target energy outflow can be released from even small active storage capacities without going dry. Therefore, a small-magnitude variation coefficient should positively affect the average energy production.

7) Ratio of (average annual evaporation loss in hm^3/year)/(active storage capacity in hm^3).

Higher this ratio smaller the energy production potential should be because more volume of stored water will be lost without being used for power.

4. RESULTS AND DISCUSSION

One of the results is that for a dam whose active storage capacity is fairly small as compared to the average annual inflow, both the average annual produced energy and the present worth of financial benefits tend to increase towards the lowest regulation of 40%. This is because as the target release for energy gets small as compared to the average inflow, the active storage becomes top full many times during the operation period and more than the targeted discharge is released through the penstock in order to produce surplus energy using extra waters which otherwise would be discarded over the flood spillway. Yedigöze dam is a typical example for this case. On the other hand, for dams whose active storage capacity is considerably large as compared to the average annual inflow, like Yamula and Ermenek, 90% regulation or close to it yields the highest average annual produced energy. As examples to these cases, the results for Yedigöze and Yamula dams are presented in Tables 2 and 3 below. Some relevant input data of Yedigöze and Yamula dams are: Average annual inflows =

4424.7, 2123.2 hm^3/year; ratios of (active storage capacity, hm^3)/(average annual inflow, hm^3/year) = 0.068, 0.95; ratios of (maximum penstock discharge, m^3/s)/(average long-term inflow, m^3/s) = 2.71, 1.78; variation coefficients of observed daily flows over 35-year period of record = 0.797, 1.30, respectively.

Table 2 - Final parts of the output files of the runs for the operations by (a) the steady-rate and (b) the night-shift-pumped-storage rules for Yedigöze Dam

Regulation(*) (%)	**Average annual energy by steady-rate rule (GWh/year)**	**Average annual energy by night-shift-pumped-storage rule (GWh/year)**	**Average annual energy spent for pumping during NIGHT shift (GWh/year)**	**Average net head when active storage is half full (m)**
90	804.83	1014.09	390.49	82.20
85	814.93	1059.60	452.95	82.44
80	822.05	1106.64	519.76	82.67
75	830.24	1160.42	595.25	82.88
70	838.87	1211.39	655.50	83.08
65	846.86	1262.16	712.22	83.27
60	854.80	1319.38	777.46	83.44
55	863.42	1363.34	796.38	83.60
50	869.18	1344.35	740.10	83.74
45	872.01	1316.76	645.51	83.87
40	872.79	1281.71	591.42	83.99

(*): Regulation = (outflow for energy generation, hm^3/day)/(average inflow, hm^3/day)

The computer programs coded by the authors are executed to operation simulation models used the unit prices of marketed energy as: 0.04 $/kWh by the steady-rate rule, 0.04 $/kWh during the 11-hour-long DAYTIME shift, 0.06 $/kWh during the 5-hour-long PEAK shift, and 0.02 $/kWh during the 8-hour-long NIGHT shift in those days when the reservoir is overflowing by the night-shift-pumped-storage rule. In order for pumped-storage projects to be feasible, it is obvious that the unit cost of energy spent for pumping must be as low as possible as suggested by some relevant publications cited above. Therefore, the unit cost of energy used for pumping during the 8-hour-long NIGHT shift is taken as 0.02 $/kWh, the same price for the energy we use as that we sell. The operation period is 35 years and the discount rate is 9.5% by both rules, which are officially advocated values for hydropower

feasibility studies in Türkiye [27]. With these values, the present worth of financial benefits on account of marketing the produced energy minus the present worth of the costs spent for the energy used for pumping by the night-shift-pumped-storage rule has turned out to be greater than the present worth of the marketed energy by the steady-rate rule. Table 4 presents the maximum values of the net financial benefits by both operation rules for all of 11 dams. As seen in this table, the night-shift-pumped-storage operation turns out to be financially more profitable for all of the analyzed dams, and the average increase in net profit is 28%.

Table 3 - Final parts of the output files of the runs for the operations by (a) the steady-rate and (b) the night-shift-pumped-storage rules for Yamula Dam

Regulation(*) (%)	**Average annual energy by steady-rate rule (GWh/year)**	**Average annual energy by night-shift-pumped-storage rule (GWh/year)**	**Average annual energy spent for pumping during NIGHT shift (GWh/year)**	**Average net head when active storage is half full (m)**
90	421.67	429.75	27.94	90.88
85	428.01	456.75	60.46	91.03
80	421.42	470.20	91.70	91.17
75	412.30	480.71	122.45	91.30
70	403.06	490.13	152.48	91.42
65	394.49	498.93	181.65	91.54
60	385.95	507.12	209.61	91.65
55	379.07	514.21	235.67	91.74
50	373.48	521.09	259.90	91.83
45	368.42	526.87	281.24	91.92
40	364.16	531.33	298.13	91.99

(*): Regulation = (outflow for energy generation, hm^3/day)/(average inflow, hm^3/day)

An ultimate goal of this study has been to obtain meaningful regression equations depicting the average annual produced energy in terms of a few explanatory variables given in the previous section. For the regression analyses we used the package program Minitab [30]. In the following, only the regression equations including the significant explanatory variables are presented, and the details like ANOVA (analysis of variance) tables are skipped in order not to extend the length of the paper.

Table 4 - Maximums of present worths of net financial benefits on account of marketing the energy produced by the operation rules of (a) the steady-rate and (b) the night-shift-pumped-storage for all of 11 dams studied (Operation period = 35 years, discount ratio = 0.095, unit prices of marketed energy are: 0.04 $/kWh for steady-rate rule, 0.04 $/kWh during 11-hour-long DAYTIME, 0.06 $/kWh during 5-hour-long PEAK shifts, and 0.02 $/kWh produced during 8-hour-long NIGHT shift in those days when the reservoirs is overflowing; unit cost of energy used for pumping during 8-hour-long NIGHT shift is: 0.02 $/kWh. Operations are simulated in daily time steps).

Dam	**Maximum present worth (PW) by steady-rate rule (Million Dollars)**	**Maximum of difference of PW of benefits minus PW of pumping costs by night-shift-pumped-storage rule (Million Dollars)**	**Relative Difference (Percent)**
Ağaçhisar	33.68	39.68	+18%
Altınkaya	636.71	972.94	+53%
Bahçelik	8.43	10.74	+27%
Berdan	44.26	48.57	+10%
Ermenek	469.88	568.43	+21%
Hasan Uğurlu	603.88	797.02	+32%
Karakurt	132.48	174.81	+32%
Kılıçkaya	170.83	216.73	+27%
Susurluk	28.63	37.89	+32%
Yamula	173.44	202.15	+17%
Yedigöze	380.49	516.15	+37%

Average relative difference = +28%

$$AESR = (-418.3) + (0.2112)*x_1 + (2.834)*x_3 + (78.01)*x_4 + (124.9)*x_5 + (-149.5)*x_6 \quad (65)$$

Degree of freedom = 121 − 6 = 115, R^2_{adj} (adjusted determination coefficient) = 0.985

t values of the coefficients of this regression equation and their significance probabilities:

−418.3, −10.7, 100%; 0.2112, 48.1, 100%; 2.834, 26.5, 100%, 78.01, 3.00, 99.7%;

124.9, 11.7, 100%; −149.5, −7.21, 100%

$$AENSPS = (-973.7) + (0.3509)*x_1 + (4.635)*x_3 + (330.5)*x_5 + (-277.2)*x_6 \quad (66)$$

Degree of freedom = 121 − 5 = 116, $R^2_{adj} = 0.954$

t values of the coefficients of this regression equation and their significance probabilities:

−973.7, −8.21, 100%; 0.3509, 27.9, 100%; 4.635, 20.8, 100%, 330.5, 10.1, 100%;

−277.2, −4.38, 100%

$$PWSR = (-146.5) + (0.08525)*x_1 + (1.297)*x_3 + (46.82)*x_5 + (-67.22)*x_6 \quad (67)$$

Degree of freedom = 121 − 5 = 116, $R^2_{adj} = 0.989$

t values of the coefficients of this regression equation and their significance probabilities:

−146.5, −10.8, 100%; 0.08525, 59.4, 100%; 1.297, 50.8, 100%, 46.82, 12.5, 100%;

−67.22, −9.30, 100%

$$PWNSPS = (-268.0) + (0.1215)*x_1 + (1.619)*x_3 + (89.05)*x_5 + (-94.57)*x_6 \quad (68)$$

Degree of freedom = 121 − 5 = 116, $R^2_{adj} = 0.981$

t values of the coefficients of this regression equation and their significance probabilities:

−268.0, −10.6, 100%; 0.1215, 45.2, 100%; 1.619, 33.9, 100%, 89.05, 12.7, 100%;

−94.57, −6.99, 100%

In these equations, the variables are: AESR: average annual energy produced by the steady-rate rule in GWh/year, AENSPS: average annual energy produced by the night-shift-pumped-storage rule in GWh/year, PWSR: present worth of financial benefits due to marketed energy at the beginning of a 35-year operation period by the steady-rate rule in $'s, PWNSPS: present worth of financial benefits due to marketed energy at the beginning of a 35-year operation period by the night-shift-pumped-storage rule in $'s, the explanatory variables x_i's are as explained before; and, the coefficients of the explanatory variables all are significant with a probability greater than 99.8% as given by the Confidence Intervals based on the Student's t test. Figures 3 and 4 show the scatter plots of average annual energy produced versus average annual inflow and the ratio of (maximum penstock discharge)/(average inflow) by the steady-rate rule and Figures 5 and 6 show the same plots by the night-shift-pumped-storage rule. The other graphs are not included in order to save space from the length of the paper.

The regression equations presented for the average annual energy produced by either the steady-rate or the night-shift-pumped-storage rule should be valid for a realistic initial estimate everywhere, while those for the present worth of financial benefits are specific for conditions used here. For example, the results of the night-shift-pumped-storage rule depend on the assumption that the target release for energy during the 11-hour-long DAYTIME shift equals 70% of the maximum penstock discharge capacity. Yet, the coded programs are flexible and they will run for any operation periods, for any unit energy prices and unit pumping costs, for any discount ratios, for any durations of the three shifts, and for any DAYTIME penstock discharge ratios within the boundaries of inequality (27).

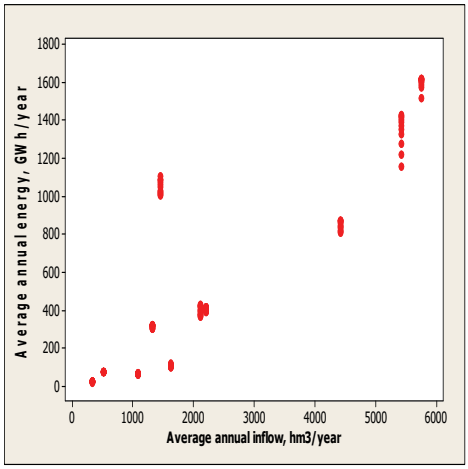

Figure 3 - Scatter plot of average annual energy versus average annual inflow for all 11 dams by the steady-rate rule

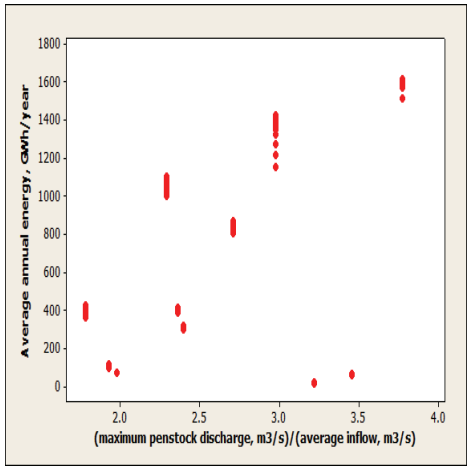

Figure 4 - Scatter plot of average annual energy versus ratio of (maximum penstock discharge) to (average inflow) for all 11 dams by the steady-rate rule

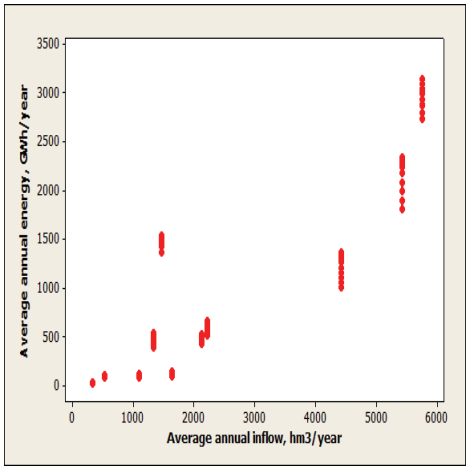

Figure 5 - Scatter plot of average annual energy versus average annual inflow for all 11 dams by the night-shift-pumped-storage rule

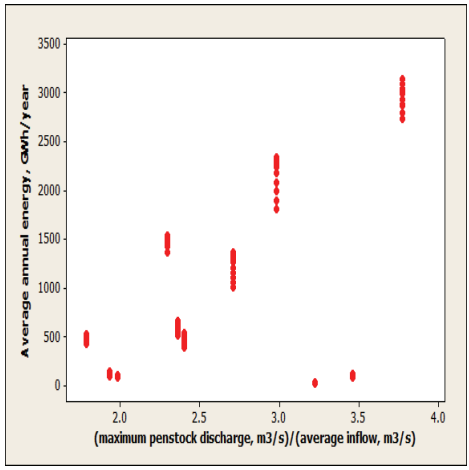

Figure 6 - Scatter plot of average annual energy versus ratio of (maximum penstock discharge) to (average inflow) for all 11 dams by the night-shift-pumped-storage rule

5. CONCLUSIONS

The technical details given in the final design projects of the selected dams are taken as the material of this study. Most of these dams are on unregulated streams. For only a couple of these dams, there are other dams at upstream locations quite far away. For example, Hirfanlı Dam is located on Kızılırmak River about 200 km upstream from Altınkaya Dam. So, the regulation effect of those upstream reservoirs on stream flows will be minimal.

After having applied our operation simulation models in daily time steps to these 11 dams, we have carried out the multiple regression analysis which we have summarized in the preceding section. It is impractical and almost impossible (1) to acquire or calculate the daily 35-year-long stream flow series coming to the dam, (2) to obtain the design projects, (3) to extract the necessary data from the project documents and prepare the input data files, (4) to execute the runs, and (5) to deduce the generalized relationships on all dams in the world with hydropower plants. However, as put forth in the previous section, we have still obtained statistically highly meaningful regression equations as the outcome of applying our models on these 11 dams. These particular dams have wide ranges of storage capacities, installed powers, and average stream flows. The ranges of active storage capacities, of ratios of (active storage capacity)/(average annual inflow), of net heads on the turbines when the volume of water in the active storage is as much as half of its capacity, and of ratios of (maximum penstock discharge)/(average inflow) of these 11 dams are: 80 hm^3 ~ 2900 hm^3, 0.07 ~ 1.20, 19 m ~ 342 m, 1.8 ~ 3.8, respectively. Hence, the regression equations obtained using the results of these dams cover such wide ranges, and therefore, these equations can be used for a plausible and reasonable prediction of hydroelectric energy potential of prospective projects.

For the night-shift-pumped-storage operation, the hydropower plant is running at maximum turbines capacity during the PEAK shift and it is running at 70% capacity during the DAYTIME shift. Yet, any value for this ratio between the lower bound given by expression (27) and 100% can be assigned by the program user. The turbines can be operated at full capacity during the DAYTIME shift also provided that the pumping capacity during the 8-hour NIGHT shift is large enough to pump back the volume of water equalling the full penstock discharge over a 16-hour period minus the target release further downstream from the tailwater reservoir. Because the computer programs are user-friendly and the execution time of a run takes about five seconds, sensitivity analyses with different DAYTIME penstock discharges, with different unit energy prices, with different discount rates, and with different operation periods can easily be done for any dam.

It has been shown that there are net positive relative financial benefits, varying between 10% and 50%, by the night-shift-pumped-storage rule over the conventional rule of steady-rate for all those 11 dams analyzed in this study. Since as of now, none of these dams are capable of pumping, for the conversion of them to the night-shift-pumped-storage rule, the cost of either installing a motor/pump unit or replacing the existing turbine/generator unit by a reversible (turbine/generator)↔(motor/pump) system must be smaller than the net financial benefits. The models and the coded programs provided can help the authorities to make feasible decisions about such possible conversions.

The models and the computer codes developed and presented in this study for the simulation of the operation of a dam with a hydropower plant either by the steady-rate or by the night-

shift-pumped-storage rules in daily steps and involve novelties and precise details peculiar to themselves. These codes, which are free to anybody interested, make up the major contribution of this study. The statistically significant regression equations obtained for a reasonable estimate of the annual average produced hydroelectric energy either by the steady-rate or by the night-shift-pumped-storage rules can also be mentioned as another contribution.

References

[1] IHA (2018) *The world's water battery: Pumped hydropower storage and the clean energy transition*. International Hydropower Association. www.hydropower.org/publications/

[2] Zhang S, Andrews-Speed P, Perera P (2015) The evolving policy regime for pumped storage hydroelectricity in China: A key support for low carbon energy. *Applied Energy*, 150, 15–24. http://dx.doi.org/10.1016/j.apenergy.2015.03.103

[3] Uria-Martinez R, Johnson M M, Shan R (2021) U.S. *Hydropower Market Report*. U.S. Department of Energy, Office of Energy Efficiency & Renewable Energy, Water Power Technologies Office, USA. http://www.osti.gov/bridge

[4] Gimeno-Gutierrez M and Lacal-Arantegui R (2015) Assessment of the European potential for pumped hydropower energy storage based on two existing reservoirs. *Renewable Energy*, 75, 856–868. http://dx.doi.org/10.1016/j.renene.2014.10.068

[5] DSI (2022) *General Activities Report of the Year 2021* (in Turkish). General Directorate of State Hydraulic Works, Ministry of Forestry and Water Works of Republic of Türkiye, Ankara, Türkiye.

[6] Ak M, Kentel E, Savasaneril E (2019) Quantifying the Revenue Gain of Operating a Cascade Hydropower Plant System as a Pumped-Storage Hydropower System. *Renewable Energy*. DOI: 10.1016/j.renene.2019.02.118

[7] Aydemir A, Acanal N, Haktanir T (2019) Efficient Use of Renewable Energy Sources: Pumped Storage Hydroelectric Power Plants. In E. Hüseyin & A. Nurlan (Eds.), *3rd International GAP Congress on Mathematical-Engineering-Technical-Medical Sciences, Proceedings,* 917–923. https://www.gapzirvesi.org/

[8] Aydemir A and Haktanir T (2019) Integration of Pumped Storage Hydropower Plant to Çamlıgöze Dam. *Internationally Participated The 1st Innovation, Sustainability, Technology and Education in Civil Engineering Conference*, *Proceedings,* 640–651. http://iste-ce2019.iste.edu.tr/

[9] Ayder E (2015) *Pumped Storage Hydroelectric Power Plants, Technical Report* (by Prof. Dr. Erkan Ayder) (In Turkish) Mechanical Engineering Department, Istanbul Technical University, Istanbul, Türkiye.

[10] Bozdemir M (2013) *Evaluation and Analysis of Pumped-Storage Hydroelectric Plants for Türkiye* (In Turkish). M.Sc. Thesis, Bilecik Seyh Edebali University, Graduate School of Sciences, Electrical and Electronics Engineering Program, Bilecik, Türkiye.

[11] Cicek O and Ozdemir M B (2021) Pumped Storage Hydroelectric Power Plant Design. *Gazi Journal of Engineering Sciences*, 7(1), 26-35. https://dx.doi.org/10.30855/gmbd.2021.01.04

[12] EIE (2008) *Elektrik İşleri Etüt İdaresi Genel Müdürlüğü İlk Etüt Raporları, 2008* (In Turkish). General Directorate of Electrical Works Planning and Reconnaissance, Ankara, Türkiye. http://www.eie.gov.tr/

[13] Firis F A, Karadol I, Sekkeli M (2022) Investigation of Unit Commitment Problem in Presence of Pumped Storage Hydroelectric Power Plants: The Case of Kahramanmaras. *Gazi Journal of Engineering Sciences*, 8(1), 110−121, doi:10.30855/gmbd.2022.01.10

[14] Haktanir T, Aydemir A, Acanal N (2021) A study on three different hydropower operation rules by monthly and daily time steps. *Proceedings of the Institution of Civil Engineers – Energy*, 174(1) 24−34. https://doi.org/10.1680/jener.19.00066

[15] Karacay P (2010) *Pumped Storage Power Plants and Their Status in Türkiye* (In Turkish). M.Sc. Thesis, Istanbul Technical University, Graduate School of Sciences, Civil Engineering Department, Hydraulics and Water Resources Program, Istanbul, Türkiye.

[16] Unver U, Bilgin H, Guven A (2015) Pumped-Storage Hydroelectric Systems (In Turkish). *Mühendis ve Makina* (A national journal in Turkish), 56(663), 57−64.

[17] Yenerji (2014) *The Project of Karakurt Dam and Hydropower Plant Revised Feasibility Report* (in Turkish) Yenerji Engineering and Consulting Co., Ankara, Türkiye, www.yenerji.com.tr

[18] USACE (1985) *Engineering and Design HYDROPOWER, EM 1110-2-1701*. U.S. Army Corps of Engineers, Washington, DC, 20314-1000.

[19] Sever S and Yurtal R (2022) Simulation of Multi-Purpose Multi-Reservoir System Operations by HEC-ResSim (In Turkish) *Teknik Dergi*, Paper 708, 12863-12875.

[20] Haktanir T, Aydemir A, Acanal N Versions of the drainage area ratio method for transfer of daily or monthly stream flows. *Proceedings of the Institution of Civil Engineers – Water Management*, https://doi.org/10.1680/jwama.21.00091, ahead of print.

[21] Openstreet, Openstreet map database 2022, Available under the Open Database Licence from: https://www.openstreetmap.org/copyright, accessed 10.09.2022

[22] HGM, General Directory of Mapping, Republic of Türkiye, Ministry of National Defense, Türkiye shape file: https://www.harita.gov.tr/urun/turkiye-mulki-idare-sinirlari/232, accessed 10.09.2022

[23] Haktanir T and Cobaner M (2007) Feasibility of hydropower plant installation to existing irrigation dams. *Water International*, IWRA, 32(2), 254–264. https://doi.org/10.1080/02508060708692205

[24] Elliott T C, Chen K, Swanekamp R C (1998) *Standard Handbook of Power Plant Engineering*, Section 7. Hydroelectric Power Stations, Second Edition. McGraw-Hill, New York.

[25] Coyne et Bellier (1986) *Sir Dam and Hydroelectric Project, Water Potential and Power Studies (Revision)*. Coyne et Bellier, Bureau d'Ingenieurs Conseils, Paris, France, Aknil Engineers Consultants, Ankara, Cukurova Elektrik A.Ş., Adana, Türkiye.

[26] Gulliver J S and Arndt R E A (1991) *Hydropower Engineering Handbook*. McGraw-Hill.

[27] DSI (2015) *Circular 2015/5 Criteria for Reconnaissance and Feasibility Studies* (in Turkish). Investigation, Planning and Allocations Department, General Directorate of State Hydraulic Works, Ministry of Forestry and Water Works of Republic of Türkiye, Ankara, Türkiye.

[28] Hydropower Europe (2019) *Hydropower Technologies The State-of-the-Art*. Document No. WP4-DIRp-02, Lead author: Emiliano Corà, Contributors: Jean Jacques Fry, Mario Bachhiesl, Anton Schleiss. A technical report prepared under grant agreement No 826010 supported by the European Union's Horizon 2020 research and innovation programme.

[29] European Clean Energy Alliance (2022) *Joint Declaration European Electrolyser Summit V9 public*. European Commission, Hydrogen Europe, Advent, Bosch, Convion, Cummins, DeNora, Elogen, Enapter, Genvia, Green Hydrogen Systems, Hydrogen & Energy Systems, H2B2, HyStar, John Cockerill, McPhy, NEL Hydrogen, Siemens Energy, Solid Power, Sunfire, Thyssenkrupp nucera, Topsoe, Brussels, 5 May 2022.

[30] Minitab: Data Analysis, Statistical & Process Improvement Tools, www.minitab.com Minitab, LLC 1829 Pine Hall Road, State College, PA, USA.

Turkish Journal of Civil Engineering, 2023 31-54, Yazı 745, ***Araştırma Makalesi***

Kuzey Kıbrıs'taki Havzaların Morfometrik Parametreler Kullanılarak Kümelenmesi

Hasan ZAİFOĞLU[1]

ÖZ

Hidrolojik açıdan birbirine benzer havzaların sınıflandırılması özellikle bilginin ölçüm yapılmış havzalardan ölçüm yapılmamış havzalara taşınması açısından önemlidir. Bu çalışmada Kuzey Kıbrıs'ta yer alan havzalar bir takım temel, çizgisel, alansal ve rölyef morfometrik havza özellikleri göz önüne alınarak hibrid hiyerarşik k-ortalamalar kümeleme yöntemi ile beş farklı kümede sınıflandırılmışlardır. Coğrafi bilgi sistemleri (CBS) kullanılarak elde edilen bu morfometrik parametreler ile havzaların ve oluşturulan havza kümelerinin hidrolojik ve morfolojik özellikleri detaylı bir şekilde incelenmiştir. Elde edilen sonuçlara göre havzaların büyük çoğunluğunda ana akarsu kollarının orta dereceli akarsulardan oluştuğu ve sadece Küme 1 içerisinde yer alan havzalar ile bazı Küme 4 havzalarının nehir olarak tanımlanabilecek ana akarsu kolları olduğu belirlenmiştir. Havzaların büyük çoğunluğunda ise iyi gelişmiş drenaj ağı ile düşük drenaj yoğunluklarının olduğu saptanmıştır. Ayrıca Küme 1 ve 3 içerisinde yer alan havzaların yüksek havza rölyef özellikleri ile taşkınlar gibi doğal afetlere karşı daha yatkın oldukları belirlenmiştir.

Anahtar Kelimeler: Kuzey Kıbrıs, morfometrik parametreler, coğrafi bilgi sistemleri, hibrid hiyerarşik k-ortalamalar kümeleme yöntemi.

ABSTRACT

Clustering of Basins in Northern Cyprus Using Morphometric Parameters

The classification of hydrologically similar basins is essential in transferring information from gauged basins to ungauged basins. In this study, the basins in Northern Cyprus were classified into five different clusters with the hybrid hierarchical k-means clustering method, taking into account some basic, linear, areal, and relief morphometric basin characteristics. With these morphometric parameters obtained using geographic information systems (GIS), the hydrological and morphological characteristics of the basins and the formed basin clusters were examined in detail. According to the results, it has been determined that the main stream branches in most of the basins are composed of medium streams. Only the basins in Cluster

Not: Bu yazı
- Yayın Kurulu'na 30 Ekim 2022 günü ulaşmıştır. 26 Mayıs 2023 günü yayımlanmak üzere kabul edilmiştir.
- 30 Kasım 2023 gününe kadar tartışmaya açıktır.

- https://doi.org/10.18400/tjce.1312155

1 Orta Doğu Teknik Üniversitesi, Kuzey Kıbrıs Kampüsü, İnşaat Mühendisliği Programı, Güzelyurt, KKTC
zhasan@metu.edu.tr - https://orcid.org/0000-0003-2615-5097

1 and some in Cluster 4 include streams that can be defined as rivers. It has been determined that most of the basins have a well-developed drainage network and low drainage densities. In addition, it has been determined that the basins in Clusters 1 and 3 are more prone to natural disasters, such as floods, with their high basin relief features.

Keywords: Northern Cyprus, morphometric parameters, geographic information systems, hybrid hierarchical k-means clustering method.

1. GİRİŞ

Dünya genelinde havzaların büyük çoğunluğunun hidrolojik ölçümlere sahip olmaması nedeniyle, su kaynakları sistemlerinin planlanması ve tasarımı, çoğunlukla doğrudan veya dolaylı bir şekilde ölçülen diğer havzalardan gelen veriler kullanılarak tahmin edilmektedir. Bu gibi durumlarda, ölçüm yapılmayan havzaların hidrolojik olarak bilgi sağlayan havzalara benzer olması beklenmektedir [1]. Bu bağlamda havzaların gelişen farklı meteorolojik olaylara benzer tepki veren gruplar halinde sınıflandırılması özellikle akım ölçümü yapılmamış havzalardaki akarsu akışı tahminleri açısından faydalı ve önemlidir. Ancak bugüne kadar geniş kabul gören bir havza sınıflandırma sistemi mevcut değildir [2]. Literatür incelendiğinde hidrolojik bölgeselleştirme farklı şekillerde yapılmakta ve genel olarak, üç kategori altında toplanmaktadır: benzerlik tabanlı, regresyon tabanlı ve hidrolojik imza tabanlı [3]. Benzerlik tabanlı yöntemlerde havzaların benzer mekansal ve fiziksel özelliklerinden yararlanılarak bir sınıflandırma gerçekleştirilmektedir [4, 5]. Regresyon tabanlı sınıflandırmada ise, regresyon model parametreleri ve havza parametreleri arasında belirli bir regresyon ilişkisi kurulmaktır. Bu ilişki, hedef havzaların model parametrelerini tahmin etmek ve daha sonra ölçülmemiş havzalarda akım tahminleri için kullanılmaktadır [6]. Diğer taraftan hidrolojik imza tabanlı sınıflandırma yöntemlerinde ise havzaların hidrolojik özelliklerini farklı zaman periyotlarında yansıtabilen statik (ortalama akış akışı, taşkın frekansı vb.) ve dinamik (taban akış endeksi, akış değişim hızı vb.) göstergelerden yararlanılarak bir bölgeselleştirme yapılmaktadır [7].

Gerçekleştirilen bölgeselleştirme çalışmalarının ciddi bir kısmı kümeleme teknikleri kullanılarak havzaların sınıflandırılmasından oluşmaktadır. Sonrasında ise bölgesel frekans analizi ile belli dönüş aralıklarına karşılık gelen taşkın debileri ve tasarım yağışları tahmin edilmektedir. Kümeleme analizi ayrıca, aşırı yağışların mekansal ve zamansal değişimlerini incelemek, şiddet-süre-frekans bağlantılarını elde etmek, havza özelliklerinin akış üzerindeki etkilerini anlamak gibi farklı amaçlar için de yaygın olarak uygulanmaktadır [8, 9]. Örneğin Saf [10] çalışmasında Batı Akdeniz Havzası'nı üç homojen bölgeye ayırmış ve daha sonra yıllık maksimum taşkın serilerine bölgesel frekans analizi uygulayarak taşkınların çeşitli dönüş aralıklarına karşılık gelen değerlerini tahmin etmiştir. Diğer bir çalışmada ise Fırat vd. [11] Türkiye'de yıllık toplam yağışları uygulanan kümeleme analizi ile sınıflandırmış ve homojen bölgeleri belirlemiştir.

Hosking ve Wallis [12] çeşitli sınıflandırma yöntemlerinin kendilerine özgü bir takım avantajları ve dezavantajları olduğunu ortaya koymuştur. Özellikle havzaların farklı özelliklerinin kullanılarak yapılacak kümeleme analizinin hidrolojik açıdan homojen havzaları elde etmenin en pratik yöntemi olduğunu öne sürmüştür. Bu noktada kümeleme, bir küme içindeki havzaların özellikleri bakımından mümkün olduğunca birbirine benzer ve

farklı kümelerdeki havzaların özelliklerindense mümkün olduğunca farklı olması için havzaların kümelere ayrıldığı bir yöntem şeklinde tanımlanabilir. Genellikle hidrolojide kullanılan kümeleme analizi havzanın fiziksel özellikleri, coğrafi konum özellikleri, havza tepki süresi ölçüleri, meteorolojik faktörler ve taşkın istatistikleri gibi havzayı betimleyici bir takım parametreler yardımıyla gerçekleştirilmektedir [13]. Literatürde yer alan çalışmaların çoğunda kullanılan küme analizi yöntemleri hiyerarşik kümeleme ve hiyerarşik olmayan kümeleme yöntemleridir. Ayrıca bulanık küme teorisinin kullanıldığı bulanık kümeleme ve doğrusal olmayan, örneğin kendini düzenleyen haritalar yöntemi gibi diğer kümeleme yöntemleri de uygulanmaktadır.

Drenaj morfometrisi, herhangi bir drenaj havzasının çizgisel, alansal ve rölyef özelliklerinin bir ölçümü olarak tanımlanır [14]. Özellikle havzaların hidrolojik özelliklerinin araştırılması, havzanın geliştirilmesi ve yönetimi açısından havzaların morfometrik özelliklerinin bilinmesi önemlidir [15, 16]. Son zamanlarda yapılan bazı çalışmalarda morfometrik parametreler yeraltı suyu potansiyelinin değerlendirilmesi, taşkın risk tahminleri, havza önceliklendirmesi, erozyon oranlarının tahmin edilmesi gibi konularda önemli faydalar sağlamıştır. Özellikle uzaktan algılama ve coğrafi bilgi sistemlerinin gelişmesiyle, sayısal yükseklik modelleri daha hızlı ve daha doğru havza analizleri sağlamaktadır. Bundan dolayı morfometrik analizlerde de bu gelişmeler sıklıkla kullanılmaya başlanmıştır [17].

Kuzey Kıbrıs'ta bulunan havzaların belirlenmesi, bu havzaların özelliklerinin ve benzerliklerinin irdelenmesi ve neticede benzer havzaların kümelenmesi ile bir bölgeselleştirmenin yapılması konularında literatürde sınırlı sayıda çalışma bulunmaktadır. Örneğin, Türker ve Hansen [18] Kıbrıs'ın kuzeyindeki meteorolojik koşulları ve topoğrafyayı dikkate alarak akarsu havzalarını dört ana havza altında toplamıştır. Ancak bu çalışmada herhangi bir kümeleme yaklaşımı kullanılmamıştır. Diğer bir çalışmada ise Nikolakis [19] Kıbrıs adasının tamamının belli yağış rejimleri ile karakterize edilen dört alt bölgeye ayrılabileceğini göstermiştir. Havza özelliklerinin dikkate alınmadığı bu çalışmada aylık ortalama yağış verilerinden elde edilen bir takım istatistiklere faktör analizi uygulanarak yağış temelli bir bölgeselleştirme yapılmıştır. Zaifoglu vd. [20] ise aylık yağış verilerine uygulanan zaman serisi kümeleme yöntemleriyle adanın kuzeyini beş farklı homojen bölgeye ayırmıştır. Buraki bölgeselleştirme de yine sadece benzer yağış davranışı gösteren istasyonların gruplanması şeklinde yapılmıştır. Bir başka deyişle yağış karakteristiğinin bölgeselleştirilmesidir. Dolayısıyla, bu çalışmada literatürde eksik olduğu saptanan, Kuzey Kıbrıs'ta yer alan havzaların morfometrik özelliklerinin incelenmesi ve ilgili havza özelliklerinin kullanılarak havza temelli bir bölgeselleştirmenin yapılması amaçlanmıştır. Bu bağlamda hibrid hiyerarşik k-ortalamalar kümeleme yöntemi kullanılarak havzalar morfometrik yakınlık bakımından kümelenmiş ve bölgeselleştirme gerçekleştirilmiştir. Çalışma alanı içerisindeki havzaların morfometrik analizi, havzalar içerisinde akım gözlem istasyonlarının bulunmaması ve geçmiş hidrolojik davranışları hakkında bilgi sahibi olunmaması nedeniyle özellikle önemlidir. Böylelikle uygulamacılar aynı homojen bölgede yer alan ve akım gözlem istasyonları ile ölçülen havzalarda gerçekleştirilen hidrolojik modelleri ve model parametrelerini ölçüm yapılmayan havzalardaki akım serilerini tahmin etmekte kullanabileceklerdir. Dolayısıyla bilgi daha hızlı şekilde ölçüm yapılmamış havzalara aktarılıp buralardaki sorunlara çözüm arayışlarını hızlandıracaktır. Bunun yanısıra elde edilen havza ve havza kümelerinin morfometrik özellikleri özellikle karar alıcılar tarafından incelenerek taşkınlara duyarlı havzalar belirlenip

önceliklendirilebilecektir. Benzer şekilde bu çalışmada elde edilen sonuçlar potansiyel erozyona eğilimli alanların belirlenmesi ve önceliklendirilmesi için de katkı sağlamaktadır.

2. ÇALIŞMA ALANI

Kıbrıs, Doğu Akdeniz'de yer alan ve yazları sıcak ve kurak, kışları ise ılıman ve az yağışlı Akdeniz iklimi etkisi altında bir adadır. Yıllık ortalama yağış miktarı 470 mm civarındadır [21] ve su kaynaklarının çoğu ise adanın yaklaşık %30'unu kaplayan Trodos Dağları'ndan kaynaklanmaktadır [22]. Kıbrıs adası, kuzey kıyı şeridine paralel uzanan Girne Dağları, Güney Kıbrıs'ta yer alan ve adanın ağırlıklı olarak merkez ve günaybatısında bulunan Trodos Dağları, iki dağ sırası arasında adanın merkezindeki düzlükleri içeren Mesarya Ovası ve Karpaz Yarımadası'ndan oluşan karmaşık bir topoğrafyaya sahiptir. Bu nedenle, yağış düzenleri dahil yerel meteorolojik özellikler büyük ölçüde farklılık göstermektedir.

Şekil 1'de de görüldüğü gibi çalışma alanı adanın kuzey kısmında yer alan ve adanın toplam havza alanının yaklaşık %54'ünü kaplayan havzalarla sınırlandırılmıştır. Adanın kuzey kısmındaki derelerin neredeyse tamamı yağışlı dönemlerde akan sürekli olmayan derelerdir. Çalışma alanı içerisindeki akarsuların çoğu Trodos Dağları'ndan adanın orta kısmına ve Güzelyurt Körfezi'ne doğru akmaktadır. Ancak Girne Dağları'ndan da kuzeye ve güneyde Mesarya Ovası'na doğru uzanan akarsular da vardır. Ayrıca iç kısımlardan Mağusa Körfezi'ne ve Girne Dağları'na doğru uzanan ve Karpaz Yarımadası içeresinde yer alan daha küçük akarsu havzaları da bulunmaktadır. Burada çalışma havzaları Kuzey Kıbrıs Türk Cumhuriyeti (KKTC) sınırları içerisinde yer alan derelerin havzaları olarak tanımlanmıştır.

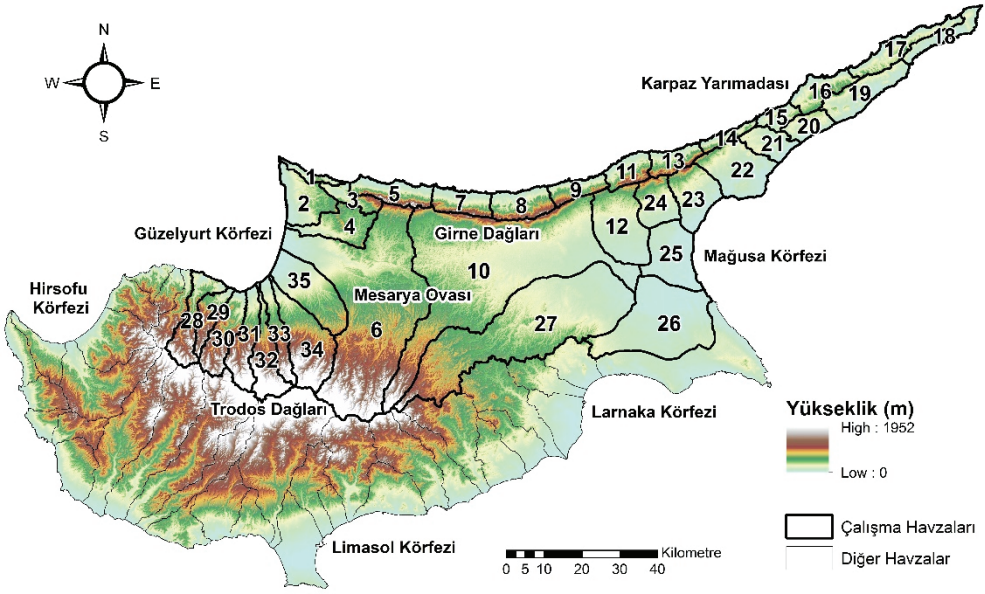

Şekil 1 - Çalışma alanının sayısal yükseklik haritası ve Kuzey Kıbrıs'taki çalışma havzaları

3. YÖNTEM

3.1. Havzaların Belirlenmesi

Çalışma alanını oluşturan havzaları ve drenaj ağını elde etmek için Kuzey Kıbrıs Türk Cumhuriyeti Harita Dairesi'nden 1/25,000 ölçekli haritalardan üretilen 12.5 m çözünürlüğe sahip sayısal yükseklik modeli kullanılmıştır. Bu model ArcGIS 10.5 coğrafi bilgi sistemleri (CBS) tabanlı yazılıma aktarılmış ve yazılım içerindeki çeşitli coğrafi veri işleme araçlarıyla Kuzey Kıbrıs'ta yer alan havzalar otomatik olarak üretilmiştir. Bu aşamada, öncelikle her hücre için hakim akım yönü saptanmıştır. Bununla birlikte akım toplamı haritası için, 0.0156 km^2'ye karşılık gelen 100 hücrelik bir eşik değeri kullanılarak akarsu ağı oluşturulmuştur. Görece olarak küçük ve içerisinde akarsu ağı bulunmayan havzalar ise coğrafi ve fiziksel durumları değerlendirilerek kendilerine komşu havzalarla birleştirilmiş ve Şekil 1'de de görülebileceği gibi çalışma alanı toplamda 35 havzaya ayrılmıştır.

3.2. Morfometrik Parametrelerin Hesabı

Kuzey Kıbrıs'taki havzaların çeşitli morfometrik parametrelerini belirlemek için ArcGIS ortamında yer alan bir takım coğrafi işlem araçları kullanılmıştır. Parametre hesaplanmasında kullanılacak devamlı ya da geçici tüm akarsu kollarını içeren akarsu ağı oluşturulmuş ve akarsu ağının incelenmesi için ilgili kollar derecelendirilmiştir. Ayrıca eğim özelliklerinin elde edilmesi için ArcGIS'teki mekansal analiz araçlarından yararlanılmıştır. Böylece havzaların temel, çizgisel, alansal ve rölyef özelliklerinin değerlendirilmesi için ilgili morfometrik parametreler hesaplanmıştır. Bunlar havzaların temel özellikleri olan havza alanı (A), havza çevresi (P), havza genişliği (W), havza uzunluğu (L_b); çizgisel özellikleri temsil eden akış dizilimi (u), akış numarası (N_u), çatallanma oranı (R_b), toplam akış uzunluğu (L_u); alansal özellikleri gösteren biçim faktörü (F_f), uzama oranı (R_e), dairesellik oranı (R_c), drenaj yoğunluğu (D_d), tekstür oranı (R_t), akarsu sıklığı (S_f), kompaktlık katsayısı (C_c); rölyef özellikleri ifade eden havza rölyefi (H), rölyef oranı (R_h) ve engebelilik oranıdır (R_n). Tablo 1'de verilen formüller veya yaklaşımlar kullanılarak havzaların morfometrik özellikleri hesaplanmıştır.

Tablo 1 - Havzaların morfometrik parametreleri

Parametre	Formüller	Birim	Referans
Temel özellikler:			
Havza alanı (A)	CBS Araçları	km^2	[23]
Havza çevresi (P)	CBS Araçları	km	[23]
Havza genişliği (W)	CBS Araçları	km	[23]
Havza uzunluğu (L_b)	$L_b = 1.312 \times A^{0.588}$	km	[24]
Çizgisel özellikler:			
Akış dizilimi (u)	Hiyerarşik sıralama	-	[25]
Akış numarası (N_u)	$N_u = N_{u1} + N_{u2} + \cdots + N_{un}$	-	[25]
Çatallanma oranı (R_b)	$R_b = N_u/N_u + 1$	-	[26]
Toplam akış uzunluğu (L_u)	$L_u = L_{u1} + L_{u2} + \cdots + L_{un}$	km	[24]

Tablo 1 - Havzaların morfometrik parametreleri (devam)

Parametre	Formüller	Birim	Referans
Alansal özellikler:			
Biçim faktörü (F_f)	$F_f = A/L_b^2$	-	[24]
Uzama oranı (R_e)	$R_e = 2/L_b \times \sqrt{A/\pi}$	-	[26]
Dairesellik oranı (R_c)	$R_c = 4\pi A/P^2$	-	[25]
Drenaj yoğunluğu (D_d)	$D_d = L_u/A$	km^{-1}	[24]
Tekstür oranı (R_t)	$R_t = N_u/P$	km^{-1}	[24]
Akarsu sıklığı (S_f)	$S_f = N_u/A$	km^{-2}	[24]
Kompaktlık katsayısı (C_C)	$C_C = 0.282 \times P/\sqrt{A}$	-	[27]
Rölyef özellikleri:			
Havza rölyefi (H)	$H = R - r$	m	[26]
Rölyef oranı (R_h)	$R_h = H/L_b$	-	[26]
Engebelilik oranı (R_n)	$R_n = H \times D_d$	-	[26]

3.3. Kümeleme Analizi

Çalışmada hidrolojik açıdan benzer havzaların belirlenmesi için hibrid hiyerarşik k-ortalamalar kümeleme yöntemi kullanılmıştır. Burada denetimsiz öğrenme yöntemleri içerisinde yer alan birleştirici hiyerarşik Ward kümeleme yöntemi [28] ve hiyerarşik olmayan kümeleme yöntemlerinden k-ortalamalar yöntemi [29] birlikte uygulanmıştır. Böylece, hibrid kümeleme yaklaşımı kullanılarak her iki yöntemin bir takım dezavantajlarının giderilmesi hedeflenmiştir. Ayrıca bu yaklaşım ile iki yöntemden en iyi şekilde faydalanılması amaçlanmıştır [30].

Hibrid yöntemin ilk kısmında hiyerarşik Ward yöntemi uygulanarak küme sayısı ve küme merkezleri belirlenmektedir. Başlangıç olarak havza sayısı kadar tek üyeli küme oluşturulmuştur. Başka bir deyişle her havza tek bir kümede ayrı ayrı konumlandırılmıştır. Ardından aralarındaki benzerlik uzaklığına göre en yakın iki küme birleştirilmektedir. Bu işlem neticede hiyerarşik yapıya dayalı tüm havzaları içeren tek bir küme elde edilene kadar tekrarlanmaktadır. Hiyerarşik Ward yöntemi uygulanırken mesafe matrisi adı verilen ve kümeler arası benzerlik uzaklıklarını gösteren bir matris oluşturulmaktadır. Buradaki değerler Karesel Öklid uzaklık ölçüsü (d_{ij}) kullanılarak şu şekilde hesaplanmaktadır:

$$d_{ij} = \sum_{k=1}^{p} \left(x_{ik} - x_{jk}\right)^2 \quad (1)$$

Burada $i = 1, 2, \dots, n$; $j = 1, 2, \dots, n$; $k = 1, 2, \dots, p$ olmak üzere n nesne sayısını, p de değişken sayısını göstermektedir. Formül içerisinde yer alan x_{ik} i'inci nesnenin k'inci değişkendeki değerini, x_{jk} ise j'inci nesnenin k'inci değişkendeki değerini ifade etmektedir. Birbirine yakın olan havzalar mesafe matrisine göre aşamalı olarak birleştirilmekte ve adım adım yeni kümeler üretilmektedir. Her adımda, yeni küme ve diğer kümeler kullanılarak uzaklık matrisleri yeniden hesaplanmaktadır. Daha sonra ise tüm istasyonları içeren en büyük kümeye ulaşmak için birleştirme işlemi gerçekleştirilmektedir. Bu çalışmada yapılan

kümeleme analizinde havzaların benzerliği morfometrik parametreler ve coğrafi konum değişkenleri üzerinden değerlendirilmiştir. Ayrıca yöntem içerisinde kullanılan Öklid uzaklık ölçüsü, değişkenlerin farklı ölçü birimlerinden etkilenebileceğinden ilgili değişkenler analize sokulmadan önce standartlaştırılmıştır. Bu işlem değişkenlerin her bir değerinden ortalama değerin çıkarılıp elde edilen farkın standart sapmaya bölünmesi ile gerçekleştirilmektedir.

Hiyerarşik Ward kümeleme yönteminde amaç tüm parametreler üzerinden hesaplanan iki küme merkezi arasındaki sapmanın (hatanın) karelerinin toplamının minimize edilmesidir. Bu bağlamda oluşturulan amaç fonksiyonu şu şekilde ifade edilebilir [31]:

$$E = \sum_{m=1}^{g} E_m \tag{2}$$

Burada $m = 1, 2, \dots, g$ olmak üzere E tüm kümelerin hata kareler toplamıdır. E_m ise küme içi hata karaler toplamıdır ve şu şekilde hesaplanmaktadır:

$$E_m = \sum_{l=1}^{n_m} \sum_{k=1}^{p_k} \left(x_{ml,k} - \bar{x}_{m,k}\right)^2 \tag{3}$$

Burada $l = 1, 2, \dots, n_m$ olmak üzere $\bar{x}_{m,k}$ m'inci kümedeki k'inci değişkene ait ortalamayı ve $x_{ml,k}$ ise m'inci kümedeki l'inci nesne için k'inci değişkenin değerini göstermektedir.

Hiyerarşik kümelemenin sonuçları genellikle kümelerin hangi düzende birleştiğini gösteren ve dendrogram olarak bilinen diyagramlar kullanılarak verilir. Havzaların kümelenmesi dendrogramın istenilen yükseklikte kesilmesi ve düğümlerden kümeler oluşturacak şekilde ayrılmasıyla gerçekleştirilir. Ancak dendrogramın hangi düğüm noktasından ayrılacağı yani havzaların kaç küme altında sınıflandırılacağı belli değildir ve literatürde bu konuda genel kabul görmüş bir yöntem bulunmamaktadır. Dolayısıyla bu çalışmada toplam havza kümesi sayısının belirlenmesi için yaygın olarak kullanılan bir yaklaşım olan küme geçerlilik indekslerinden yararlanılmıştır. Kullanılan bu indeksler küme sayısı, benzerlik uzaklığı ölçüleri ve kümeleme yöntemlerinin tüm kombinasyonlarını deneyerek en uygun kümelemeyi önermektedir. Temelde bu indisler küme içi ve kümeler arası varyans değerlerini birlikte dikkate alarak kümeleme analizi sonuçlarının veriye ne kadar uyumlu olduğunu değerlendirmektedir [32]. Bu aşamada NbClust R programlama paketi [33] kullanılarak 30 farklı indeks eş zamanlı olarak hesaplanmış ve indeksler tarafından en fazla önerilen küme sayısına göre optimum havza küme sayısı kararlaştırılmıştır.

Hibrid yöntemin ikinci kısmında ise hiyerarşik yöntem ile elde edilen kümelerin her biri için küme merkezleri hesaplanarak k-ortalamalar yönteminde başlangıç değer olarak kullanılmaları sağlanmıştır. Aslında bu adım hibrid yöntem kullanılarak yapılacak ikinci bir sınıflandırmanın sağlayacağı avantajı ortaya çıkarmak için gerçekleştirilmektedir. Böylece başlangıç aşamasında küme sayısı ve küme merkezlerinin bu rasgele seçimine karşı oldukça duyarlı olan ve sonuçları zaman zaman etkilenen k-ortalamalar yönteminin en önemli dezavantajı ortadan kaldırılmaktadır. Bunun yanında k-ortalamalar yönteminde özellik vektörleri bir kümeden diğerine amaç fonksiyonunu minimize etmek için dinamik bir şekilde değişebilmektedir. Buna karşın Ward yöntemi gibi hiyerarşik yöntemlerde belli kümelere atanan özellik vektörleri kümeler arasında hareket edememektedir [34]. Hibrid yöntem uygulaması bu bağlamda her iki yaklaşımın olumlu yönlerini kullanıp sonuçların doğruluğunu olabildiğince artırmayı amaçlamaktadır.

Sınıflandırma algoritması içerisinde her havza önceden tanımlanmış sayıdaki kümelere, küme merkezlerine olan uzaklıklarına göre dahil edilmektedir. Daha sonra oluşturulan kümelerin yeni küme merkezleri hesaplanarak havzaların yeni merkezlere uzaklıkları güncellenmekte ve tekrar havzaların sınıflandırılması gerçekleştirilmektedir. Burada amaç fonksiyonunun değeri en aza indirilerek her bir özellik vektörünün ait olduğu kümenin merkezine olan uzaklığı minimize edilmektedir. Amaç fonksiyonu J şu şekilde hesaplanmaktadır [35]:

$$J = \sum_{j=1}^{n} \sum_{i=1}^{n} \left\| X_i^{(j)} - C_j \right\|^2 \quad (4)$$

Burada $\left\| X_i^{(j)} - C_j \right\|^2$ bir veri noktası $X_i^{(j)}$ ve küme merkezi C_j arasındaki seçilen mesafenin ölçüsüdür. Her havza için küme merkezine olan mesafe hesaplanır ve en yakın küme merkezine göre sınıflandırma gerçekleştirilir. Bu işlem havza sınıflandırılmasında herhangi bir değişiklik olmayıncaya kadar devam etmektedir.

Literatürde hibrid kümeleme yöntemleri kullanılarak yapılan birçok hidroloji temelli çalışma bulunmaktadır. Örneğin Rao ve Srinivas [36] hibrid kümeleme analizinin bölgeselleştirme üzerindeki etkinliğini, Amerika Birleşik Devletleri Indiana eyaletinde yer alan havzalardan alınan veriler kullanarak araştırmıştır. Bu çalışma hibrid hiyerarşik Ward ve k-ortalama yönteminin amaç fonksiyonunu optimize etmedeki genel performansının, aynı algoritmaların ayrı ayrı çalıştırılarak elde edilen sonuçlarından daha iyi olduğunu ortaya koymuştur. Smith vd. [37] global ölçekte farklı dönüş aralıklarına karşılık gelen taşkın debilerinin tahmini için taşkın indeksi yöntemiyle birlikte hibrid kümeleme yaklaşımı kullanmıştır. Hibrid Ward ve k-ortalamalar yöntemiyle uygun şekilde oluşturulmuş havza kümelerine uygulanan bölgesel taşkın frekans analizi ile, küresel ölçekte makul taşkın debisi tahminlerinin yapılabileceği gösterilmiştir. Diğer bir çalışmada ise Kebebew ve Awass [38] hibrid Ward ve k-ortalamalar yöntemiyle çeşitli havza özelliklerini dikkate alarak Etiyopya'daki havzaların bölgeselleştirilmesini gerçekleştirmiştir ve taşkın istatistiklerini kullanarak bu bölgelerin hidrolojik açıdan homojenliği test edilmiştir.

4. BULGULAR VE TARTIŞMALAR

4.1. Havzaların Morfometrik Analizi

4.1.1. Temel Havza Özellikleri

Kuzey Kıbrıs'ta yer alan havzaların morfometrik parametreleri önceden belirtilmiş yöntemlerle hesaplanmış ve Tablo 2'de verildiği gibi bir takım istatistikler üzerinden özetlenmiştir. Buna göre öncelikle havzaların temel özellikleri incelendiğinde çalışma alanı içerisinde bulunan havzaların büyük bir kısmının 29.06 km^2 ile 176.38 km^2 arasında değişen havza alanlarına sahip olduğu, en büyük havzanın ise 1302.09 km^2'lik havza alanıyla hem Girne Dağları'ndan hem de Trodos Dağları'ndan beslenen ve Kıbrıs'ın en uzun deresi olan Kanlıdere'yi de içerisinde barındıran 10 numaralı havza olduğu görülmektedir. Diğer temel havza özellikleri arasında yer alan havza çevresi, havza genişliği ve havza uzunluğu da, sırasıyla 254.00 km, 16.89 km ve 77.10 km değerleri ile yine bu havzada en yüksek değerlere sahiptir. Diğer havzalarla kıyaslandığında bu değerler ortalama değerlerin bir hayli üzerindedir. Bunların yanında 1 numaralı havzanın en küçük havza alanına, 15 numaralı

havzanın en küçük havza çevresine, 33 numaralı havzanın en küçük havza genişliğine ve 1 numaralı havzanın ise en küçük havza uzunluğuna sahip oldukları belirlenmiştir.

4.1.2. Havzaların Çizgisel Özellikleri

Çizgisel özellikler içerisinde incelenen akış dizilimi, akarsuların hiyerarşik sıralamasına dayalı Strahler yöntemi [25] kullanılarak belirlenmiştir. Buna göre sadece toprak yüzeyinden gelen suları alan kollar birinci derece olarak numaralandırılmıştır. İkinci derece kol ise iki birinci derece kolun birleşmesiyle meydana gelmektedir. İki ikinci derece kol birleştiğinde üçüncü derece kolu oluşturur ve bu şekilde derecelendirme devam eder. Bu yönteme göre çalışma alanı içerisindeki akarsu kolları üçüncü dereceden sekizinci dereceye kadar derecelendirilmiştir. Ortalama akarsu derecesi ise havzaların çoğunda görülen beşinci derece olarak saptanmıştır. Diğer bir taraftan, havzanın en büyük akış dizilimi değeri, havzanın ana akış kolunun türünü belirlemek için de kullanılabilir. Burada üçüncü dereceye kadar akış dizilimi değerine sahip olan akarsular memba suyu, dördüncü ile altıncı derece arası akarsu kolları orta dereceli akarsular ve altıncı dereceden büyük akarsu kolları ise nehirler olarak tanımlanabilir. Bu bağlamda Kuzey Kıbrıs'taki havzaların çoğunda yer alan akarsular orta dereceli akarsulardır. En büyük havzalar olan 6, 10 ve 27 numaralı havzalar ile 10 ve 27 numaralı havzaların içerisinden geçen akarsu kollarının daha mansabında yer alan Havza 25 ve 26'daki ana akarsu kolları altıncı dereceden büyük akış dizilimi değerleri ile nehir olarak tanımlanabilir.

Tablo 2 - Kuzey Kıbrıs'taki havzaların morfometrik parametre istatistikleri

Parametre	Minimum	1. Kartil (Q_1)	Medyan	Ortalama	3. Kartil (Q_3)	Maksimum
A (km^2)	29.06	80.80	120.38	214.89	176.38	1302.09
P (km)	38.45	48.47	65.55	76.43	72.86	254.00
W (km)	3.27	4.99	6.04	6.87	7.41	16.89
L_b (km)	8.89	15.89	19.94	24.47	24.74	77.10
u	3	4	5	4.97	5	8
N_u	141	416	643	1153	857	7155
R_b	1.67	2.06	2.52	3.78	4.00	13.21
L_u (km)	48.80	146.47	239.83	426.81	362.08	2664.33
F_f	0.22	0.28	0.30	0.30	0.32	0.37
R_e	0.53	0.60	0.62	0.62	0.64	0.68
R_c	0.16	0.30	0.38	0.40	0.52	0.69
D_d (km^{-1})	1.63	1.80	1.90	1.92	2.06	2.22
R_t (km^{-1})	3.05	7.67	10.24	11.94	14.11	29.65
S_f (km^{-2})	4.06	4.96	5.30	5.20	5.47	6.08
C_C	1.20	1.39	1.62	1.67	1.83	2.48
H (m)	70	359	714	800	1138	1954
R_h	0.003	0.018	0.031	0.037	0.054	0.090
R_n	0.15	0.70	1.41	1.52	2.10	3.58

Akış numaraları incelendiğinde havzaların farklı derecelerde toplam 40,354 adet akarsu kolu içerdiği, en küçük havzanın 141 (Havza 1) en büyük havzanın (Havza 10) ise 7,155 adet akarsu koluna sahip olduğu görülmektedir. Bu drenaj ağı içerisinde yer alan akarsu kollarının %51.6'sı birinci derece, %23.6'sı ikinci derece, %12.3'ü üçüncü derece, %6.6'sı dördüncü derece, %3.8'i beşinci derece, %1.4'ü altıncı derece, %0.5'i yedinci dereece ve %0.2'sinin sekizinci derece kollara sahip olduğu belirlenmiştir. Açıktır ki, akış dizilimi arttıkça akarsu kollarının sayısı azalmaktadır [24].

Çatallanma oranı, belirli bir derecedeki akış numarasının bir sonraki üst derecedeki akış numarasına oranını ifade etmektedir [26]. Bu da akış ağındaki dallanma miktarının bir ölçüsüdür. Bu parametre temelde drenaj ağının jeolojik yapılardan etkilenmediği anlamına gelen düşük sınıf ve jeolojik yapılar tarafından kontrol edildiği anlamına gelen yüksek sınıf şeklinde sınıflandırılır. Strahler [39] drenaj ağının iyi gelişmiş olduğu havzalarda ortalama çatallanma oranının 2 ile 5 arasında değiştiğini gözlemlemiştir. Çalışma alanını oluşturan 35 havzanın beş havzası hariç diğer tüm havzaları bu aralıkta olduğu için çalışma alanının genelinde drenaj ağının iyi gelişmiş olduğu söylenebilir. En düşük çatallanma oranı 1.67 olarak 4 numaralı havzada, en büyük çatallanma oranı ise 13.21 olarak 27 numaralı havzada hesaplanmıştır.

Toplam akış uzunluğu havza içerisinde derecelendirilen akarsu kollarının toplam uzunluğu olarak belirlenmektedir [24]. Havzalardaki toplam akış uzunluğu havza büyüklüğüne bağlı olarak 48.80 km ile 2664.33 km arasında değişmektedir. Mesarya Ovası içerisinde yer alan nispeten büyük havzalar haricinde genel olarak havzaların çoğunun 362.08 km'nin altında toplam akış uzunluğuna sahip oldukları görülmektedir. Toplam akış uzunluğunun yüksek değerler aldığı havzalarda ortalama akış değerlerinin diğer havzalara oranla daha yüksek olacağı söylenebilir.

4.1.3. Havzaların Alansal Özellikleri

Alansal morfometrik özellikler arasında bulunan biçim faktörü, havza alanının havza uzunluğunun karesine oranıdır. Dolayısıyla havzalardaki akış hidrografları her zaman havza formunun etkisi altındadır. Mükemmel dairesel bir havza için biçim faktörü değeri her zaman 0.7854'ten küçük olmalıdır. Havzanın daireselliğini belirten biçim faktörünün değeri ne kadar küçükse, havza o kadar uzun olacaktır [40]. Yüksek biçim faktörlü havzalar daha kısa süreli yüksek pik debili akımlara sahipken, düşük biçim faktörüne sahip uzun havzalarda daha uzun süreli ve daha düşük pik debiler gözlemlenmektedir. Kuzey Kıbrıs'taki havzaların 0.22 ile 0.37 arasında değişen biçim faktörü değerleriyle daha çok uzun ve orta daireselliğe sahip olduğu söylenebilir.

Diğer taraftan havza ile aynı alana sahip bir dairenin çapının maksimum havza uzunluğuna oranı olarak hesaplanan uzama oranı [26] sıfır (en yüksek uzama) ile bir (en yüksek dairesellik) arasında değişen bir morfometrik parametredir. Bire yakın uzama oranı değerleri havzada daha az jeomorfolojik kontrol olduğunu göstermektedir [25]. Çalışma alanı içerisinde yer alan havzalarda hesaplanan uzama oranları en düşük 0.53, en yüksek 0.68 ve ortalama ise 0.62 olarak bulunmuştur. Bu da havzaların kısmen dairesel havza özelliği taşıyabileceğini yani yüksek debili akım potansiyelini göstermektedir.

Dairesellik oranı havzanın alanının aynı çevreye sahip bir dairenin alanına oranı olarak tanımlanır [25]. Bu oran sıfır (en az dairesellik) ile bir (en fazla dairesellik) arasında değişir

ve yüksek, orta ve düşük olarak sırasıyla yaşlı, olgun ve genç jeomorfolojik gelişim evrelerini tanımlayacak şekilde sınıflandırılır. Adanın kuzeyinde yer alan havzaların çoğunluğunda dairesellik oranı 0.52 değerinin altında ve ortalama değer 0.40 olduğundan genel olarak havzaların jeomorfolojik açıdan daha çok genç veya olgun oldukları söylenebilir.

Drenaj yoğunluğu havza içindeki tüm akarsuların uzunluklarının toplamı ile toplam havza alanı arasındaki oran olarak tanımlanmıştır [24]. Herhangi bir havzanın drenaj kapasitesi, bu alanın drenaj yoğunluğuna bağlıdır. Yüksek drenaj yoğunluğu değeri, yağış olaylarına nispeten hızlı bir hidrolojik yanıta sahip büyük ölçüde parçalanmış bir havzayı işaret eder. Nispeten düşük drenaj yoğunluğu ise, yavaş hidrolojik tepkiye sahip daha düşük drenaj kapasiteli bir havzayı gösterir [41]. Çalışma alanındaki havzaların ortalama drenaj yoğunluğu 1.92 km^{-1}, en düşük değer 1.63 km^{-1} ve en büyük değer ise 2.22 km^{-1} olarak hesaplanmıştır. Havzaların çoğu 2.06 km^{-1} değerinin altındadır. Bu sonuç havzaların çoğunun düşük drenaj yoğunluğuna sahip dolayısıyla yağış olaylarına yavaş hidrolojik tepki gösterdiklerini ortaya koymaktadır. Diğer bir grup havza ise orta derecede hidrolojik tepkiye sahip orta drenaj kapasiteli havzalardır.

Tekstür oranı akış numarasının havzanın çevresine oranı olarak tanımlanır ve herhangi bir havzanın drenaj ağının göreli aralığını gösteren önemli bir morfometrik parametredir. Bu oranı etkileyen en önemli faktör havzanın sızma kapasitesidir [24]. Tekstür oranı 2'den küçükse çok kaba, 2 ile 4 arasında kaba, 4 ile 6 arasında orta, 6 ile 8 arasında iyi, 8'den büyük ise çok ince olarak nitelendirilir [42]. Çalışma havzalarının tekstür oranları 3.05 ile 29.65 km^{-1} arasında değişen değerler olduğundan Kuzey Kıbrıs'ta kaba ile çok ince arasında değişen çeşitli tekstür özellikleri görülmektedir. Ayrıca büyük alan kaplayan havzaların daha yüksek tekstür oranına sahip oldukları saptanmıştır. Bu yüksek değerler ayrıca havzaların düşük sızma kapasitelerini, kayalarının daha az geçirgenliğini ve yüksek rölyef özelliklerini işaret etmektedir.

Akarsu sıklığı birim alandaki toplam akarsu sayısıdır [24]. Çalışma alanındaki havzaların 4.06 ile 6.08 km^{-2} arasında değişen değerler aldıkları belirlenmiştir. Bu değerler adanın kuzeyinin yüksek akarsu sıklığına sahip olduğunu göstermektedir. Ayrıca akarsu sıklığının akış ile doğru, yıllık ortalama yağış ile ters orantılı olarak ilişkilendirildiği bilinmektedir [43, 44]. Dolayısıyla yüksek akarsu sıklığı değerleriyle havzaların daha düşük ortalama yıllık yağışa ve daha yüksek akış potansiyeline sahip olması muhtemeldir. En yüksek akarsu sıklığı Gazimağusa Körfezi'ne dökülen akarsu kollarıyla 25 numaralı havzadadır.

Kompaktlık katsayısı havzanın çevresinin havzaya eşdeğer alana sahip dairenin çevresine oranı olarak tanımlanabilir [27]. Bu parametrenin düşük olması ilgili havzanın daha uzun olduğuna ve düşük erozyon yatkınlığına işaret etmektedir. Diğer taraftan yüksek kompaktlık katsayısı havzanın daha az uzun ve yüksek erozyon özelliğini belirtmektedir. Çalışmada yer alan havzalarda bu parametre en yüksek 2.48 (Havza 17), en düşük ise 1.20 (Havza 24) olarak hesaplanmıştır.

4.1.4. Havzaların Rölyef Özellikleri

Havza rölyefi, havza içerisinde yer alan en yüksek nokta ile en düşük nokta arasındaki yükseklik farkıdır ve havzanın altında yatan jeoloji, jeomorfoloji ve bir takım drenaj özellikleri ile ilişkilidir. Dolayısıyla özellikle havzanın erozyon aşamalarının ve yatkınlığının

önemli bir göstergesi olarak düşünülebilir. Kuzey Kıbrıs'ta bulunan havzalar genellikle iki dağ kütlesi arasında ve Girne Dağları'nın kuzey yamaçlarında yer aldığından orta ve yüksek rölyef değerlerine sahip oldukları görülmektedir. Havza rölyefi 70 ile 1954 m arasında ve ortalama 800.1 m olarak hesaplanmıştır. En yüksek havza rölyefi Trodos Dağları'ndan Güzelyurt Körfezi'ne uzanan 32 numaralı havzadadır. Yüksek rölyef jeomorfik gelişimin genç aşamalarını ve daha yüksek erozyon potansiyelini göstermektedir. Ayrıca ani rölyef değişiklikleri içeren, özellikle Girne ve Trodos dağlarından düzlüklere uzanan havzaların, taşkın gibi doğal afetlere jeomorfolojileri gereği daha yatkın oldukları söylenebilir.

Rölyef oranı havza rölyefinin havza uzunluğuna bölünmesiyle hesaplanmaktadır. Bu parametre kayaç türleri ve havza eğimi ile ilişkilendirilebilir. Böylece yüksek rölyef oranı değerleri dağlık bölgeleri, düşük değerler ise vadi ve düzlükleri yansıtmaktadır [45]. Çalışma havzaları incelendiğinde rölyef oranının çok geniş bir aralıkta değerler aldığı görülmektedir. En düşük 0.003 rölyef oranı aynı zamanda en düşük havza rölyefine de sahip Mağusa Körfezi'nde bulunan 25 numaralı havzada hesaplanmıştır. En yüksek rölyef oranı 0.090 değeri ise en yüksek havza rölyefine de sahip 32 numaralı havzada bulunmaktadır. Genel olarak havzaların ortalama rölyef oranı ise 0.037 olarak bulunmuştur. Ayrıca yüksek rölyef oranları havzaların yüksek akış potansiyeline de işaret etmektedir.

Engebelilik oranı havza rölyefi ile drenaj yoğunluğunun çarpımı ile elde edilmektedir [26]. Çalışma alanındaki havzaların engebelilik oranları 0.15 ile 3.58 değerleri arasında ve ortalama 1.52 olarak hesaplanmıştır. Özellikle düşük engebelilik oranları daha çok eğimin düşük olduğu havzalarda, yüksek oranlar ise yamaçların dik ve uzun olduğu havzalarda gözlemlenmektedir. Diğer havza rölyef parametrelerinde olduğu gibi en büyük engebelilik oranı 32 numaralı havza için, en düşük oran ise 25 numaralı havza için hesaplanmıştır. Ek olarak yüksek engebelilik oranı pik debinin nispeten yüksek olabileceğini de göstermektedir.

4.2. Havzaların Kümelenmesi

4.2.1. Kümeleme Analizi

Benzer morfometrik özelliklere sahip havzaların oluşturacağı kümlerin sayısını bulmak için 30 farklı indis değerlendirilmiş ve en anlamlı küme sayısının beş olduğu çoğunluk prensibi gözetilerek belirlenmiştir. Böylece morfometrik veriye uygulanan hibrid hiyerarşik k-ortalamalar yöntemi ile Kuzey Kıbrıs'ta yer alan tüm havzalar beş kümede gruplanmıştır. Şekil 2'de kümeleme analizinin dendrogramı görülmektedir. Dendrogram incelendiğinde Karpaz Yarımadası içerisinde yer alan 20 ve 21 numaralı havzaların birbirlerine en çok benzeyen havzalar oldukları görülmektedir. Ayrıca Girne Dağları'nın kuzeye bakan yamaçlarında bulunan 11 ve 13 numaralı havzaların da aralarındaki uzaklığın çok az olduğu dolayısıyla birbirlerine çok yakın morfometrik özellikler gösterdiği belirlenmiştir. Diğer taraftan oluşturulan kümeler incelendiğinde, Havza 27'nin daha yakın özellikler gösteren 6 ve 10 numaralı havzalar ile bir araya gelerek bir küme oluşturduğu ortaya çıkmıştır. Havza 28, 29, 30, 31, 32, 33 ve 34'ün yakın kümeler arası uzaklık değerleri ile benzer oldukları ve aynı küme içinde yer aldıkları belirlenmiştir. Aynı şekilde 15, 16, 17, 18, 19, 20 ve 21 numaralı havzalar da benzer havza morfometrisine sahip oldukları ortaya konmuştur. Burada Havza 17 ve 18 diğer havzalara göre görece olarak daha uzak bir mesafede kümeye dahil olmuşlardır. Bunun yanında Havza 12, 22, 23 ve 24 yakın morfometrik özellikler göstererek kendi içlerinde gruplanmış ve ardından Havza 25 ve 26 ile birleşerek yeni bir küme

oluşturmuşlardır. Bu kümedeki Havza 25 ve 26 öteki havzalara kıyasla daha uzak özelliklere sahiptir. Son olarak 1, 2, 3, 4, 5, 7, 8, 9, 11, 13, 14 ve 35 numaralı havzaları içerisinde barındıran bir küme elde edilmiştir. Bu havzalar genel olarak yakın özellikler gösterip aynı küme içerisinde bulunsalar da küme içerisinde bir takım alt kümelerden de söz etmek mümkündür. Örneğin Havza 5 ve 35; Havza 1 ve 14; Havza 7, 8, 9, 11 ve 13; Havza 2, 3 ve 4 kendi içlerinde daha benzer havza karakteristiklerine sahip oldukları söylenebilir.

4.2.2. Havza Küme Özellikleri

Kümeleme analizi neticesinde elde edilen beş farklı havza kümesinin Kuzey Kıbrıs'taki mekansal dağılımı Şekil 3'te gösterilmektedir. Buna göre Küme 1, Girne ve Trodos Dağları arasında yer alan Mesarya Ovası'nın orta kısmını kapsayan üç havzadan meydana gelmektedir. Bu havzaların diğerlerine kıyasla havza alanlarının önemli ölçüde büyük olduğu görülmektedir. Küme 2 içerisinde ise 12 havza bulunmaktadır. Buradaki havzaların büyük çoğunluğu Girne Dağları'nın Kuzey'e bakan yamaçlarında yer almakta ve topladıkları suyu adanın kuzey sahilinden denize deşarj etmektedir. Bu noktada Havza 2, 4 ve 35 ise Güzelyurt Körfezi doğrultusundaki akış yönleriyle diğerlerinden farklılaşmaktadır. Küme 3'ü Trodos Dağları'ndan Güzelyurt Körfezi'ne doğru akan derelerin havzaları oluşturmaktadır. Burada birbirine çok benzeyen ve komşu yedi farklı havza söz konusudur. Küme 4'te gruplanan havzaların ise adanın doğusunda bulunan Mağusa Körfezi'ne doğru akış yönüne sahip oldukları belirlenmiştir. Bu kümedeki havzalar Mesarya Ovası'nın doğu kısmını oluşturmaktadır. Son olarak, Küme 5 ise esasen Karpaz Yarımadası'nı temsil eden havzaları içermektedir. Buradaki yedi adet havzanın ortak akış yönlerinden bahsetmek pek mümkün değildir. Havza 15, 16, ve 17'nin kuzeye, Havza 19, 20 ve 21'in ise güneye doğru akış yönlerinin olduğu görülmektedir.

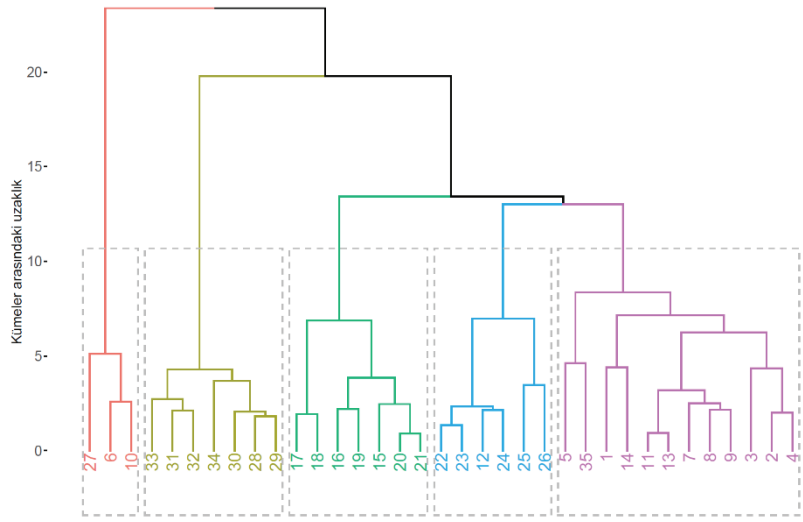

Şekil 2 - Kuzey Kıbrıs'taki havzaların morfometrik özelliklerine uygulanan hibrid hiyerarşik k-ortalamalar küme analizinin dendrogramı

Diğer bir taraftan belirlenen havza kümelerinin kendilerine özgü morfometrik özelliklerinin belirlenmesi ve kümeler arasındaki farkların daha iyi anlaşılması adına oluşturulan kümelerin temel, çizgisel, alansal ve rölyef havza özelliklerinin medyan değerleri hesaplanmış ve karşılaştırılmıştır. Örneğin Şekil 4'te kümelerin dört farklı temel havza özelliklerinin medyan değerleri verilmiştir. Buna göre açık bir şekilde Küme 1'in diğer kümelere kıyasla çok daha büyük havza alanı, havza çevresi, havza genişliği ve havza uzunluğuna sahip olduğu açıkca ortaya çıkmıştır. Diğer kümelerin ise birbirlerine daha yakın temel havza özellikleri taşıdıkları görülmektedir. Ancak bu noktada da Küme 2 içerisinde yer alan havzalar genellikle Girne Dağları ile kuzey kıyı şeridi arasına sıkışmış olarak bulunduğundan görece olarak en küçük temel havza özelliklerini taşımaktadır.

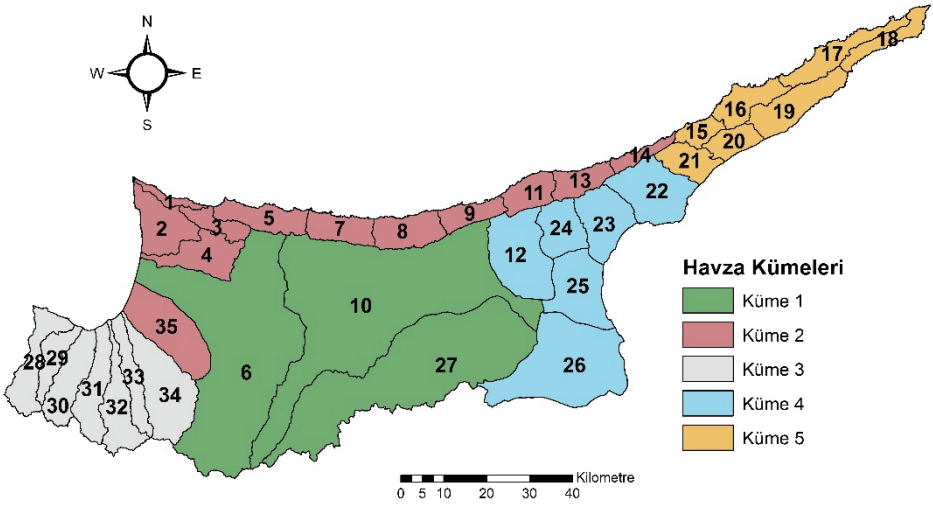

Şekil 3 - Kuzey Kıbrıs'taki havzaların morfometrik özellikleri temelinde oluşturulan havza kümeleri

Şekil 5'te verilen kümelerin çizgisel havza özellikleri incelendiğinde Küme 1 havzalarının sahip oldukları büyük temel havza özelliklerinden dolayı akış numaralarının diğer kümelere kıyasla oldukça büyük olduğu açıkça görülmektedir. Benzer şekilde akış dizilimi de temel havza özellikleriyle doğru orantılı olarak Küme 1 için en büyük durumdadır. Küme 1 içerisinde bulunan akarsular detaylı incelendiğinde kolların altıncı derceden büyük akış dizilimine sahip oldukları saptanmıştır. Bu da ana akarsu tipinin nehir olduğu sonucunu ortaya çıkarmaktadır. Geriye kalan kümelerde ise bahsedilen iki çizgisel havza özelliği için Küme 4'teki havzaların diğerlerinden daha büyük değerlere sahip oldukları saptanmıştır. Küme 4'te de yine nehir tipinde akarsular vardır. Diğer dikkat çekici sonuç ise en küçük temel havza özelliklerine sahip Küme 2'nin en büyük çatallanma oranına sahip olmasıdır. Bu noktada Küme 2'de yer alan havzaların kısa konsantrasyon süresine sahip oldukları ve dolayısıyla akışın daha erken pik debiye ulaşmasıyla taşkın yaratma olasılığının daha yüksek olduğu söylenebilir [46]. Toplam akış uzunluğu için ise kümeler arasında ciddi bir fark bulunmamaktadır.

Kümelerin alansal havza özellikleri Şekil 6'da verilmektedir. Bu bağlamda özellikler sorgulandığında Küme 1'deki havzaların tekstür oranlarının diğerlerine göre daha büyük olduğu belirlenmiştir. Bu sonuç ilgili havzaların yüksek akış ve erozyon potansiyeline sahip oldukları şeklinde yorumlanabilir. Kıbrıs'ın en uzun ve en yüksek akış potansiyeline sahip deresi olan Kanlıdere de bu küme içerisinde yer almaktadır. Ancak havzaların biçim faktörü ve uzama oranları kıyaslandığında Küme 1'e dahil olan havzaların nispeten daha küçük değerler aldığı saptanmıştır. Bu da havzaların uzun ve gerçekleşecek akışlardaki pik debilerin genellikle daha geç meydana geleceği şeklinde yorumlanabilir [24]. Usul [47] havza şeklinin hidrograf şekli ve pik değeri ile ilişkili olduğunu belirtmiştir. Burada uzun havzaların dairesel havzalara oranla daha yayvan ve daha düşük pik değerlere sahip olacaklarını göstermiştir. Bu sayede uzun havzaların pike ulaşma süreleri de daha fazla olacaktır. Diğer taraftan Küme 4'ün diğer kümelere kıyasla daha yüksek dairesellik oranı ve drenaj yoğunluğuna sahip olduğu görülmüştür. Genel anlamda bu küme içerisindeki havzaların daha yüksek akış hızı, daha düşük havza gecikme süresi ve daha yüksek pik debiye sahip olabilecekleri söylenebilir [48]. Kompaktlık katsayıları ise tüm kümelerde birbirine yakın olarak hesaplanmıştır. Sadece Küme 4 diğerlerine kıyasla daha küçüktür.

Şekil 7'de gösterilen kümelerin rölyef havza özelliklerine bakıldığında Küme 1 ve 3'ün havza rölyefi ve engebelilik oranlarının birbirlerine yakın olduğu, diğer kümelerden ise daha fazla olduğu görülmektedir. Bunun yanında Küme 3'teki havzaların rölyef oranları da diğer havzalara oranla daha yüksek olarak hesaplanmıştır. Bu çerçevede, Trodos Dağları'ndan Güzelyurt Körfezi'ne doğru akan bu havzaların ayrıca yüksek sediment ve akış potansiyelleri taşıdığı söylenebilir. Küme 5 içerisindeki havzaların ise en düşük rölyef havza özelliklerine sahip oldukları belirlenmiştir.

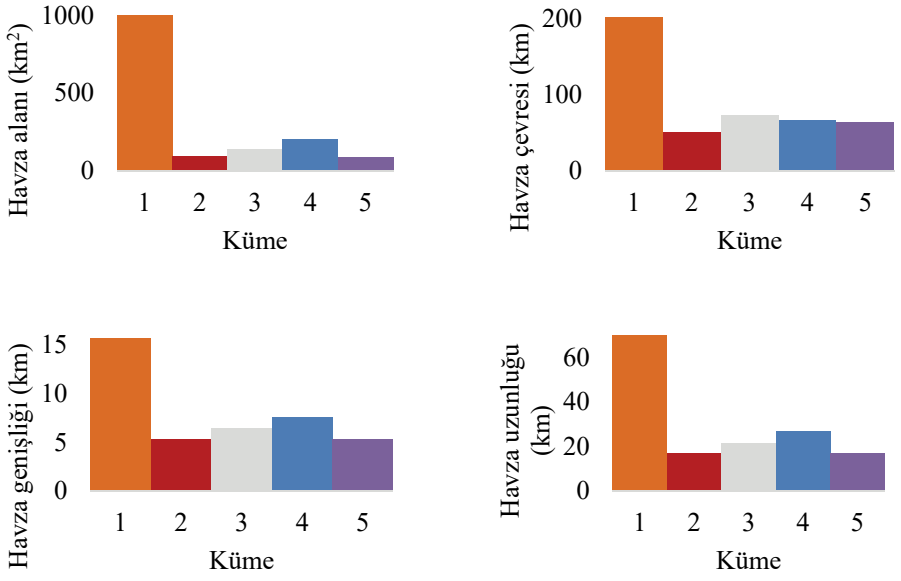

Şekil 4 - Kümelerin temel havza özelliklerinin medyan değerleri

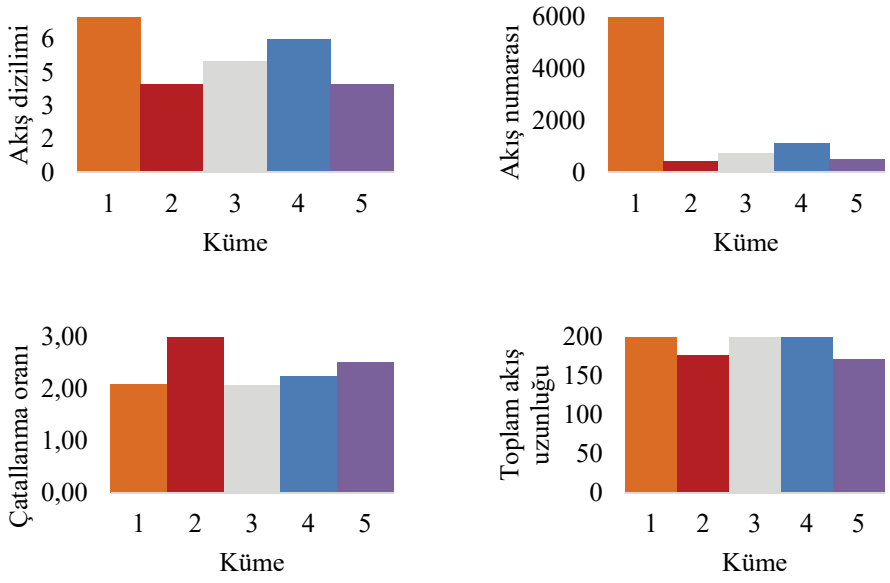

Şekil 5 - Kümelerin çizgisel havza özelliklerinin medyan değerleri

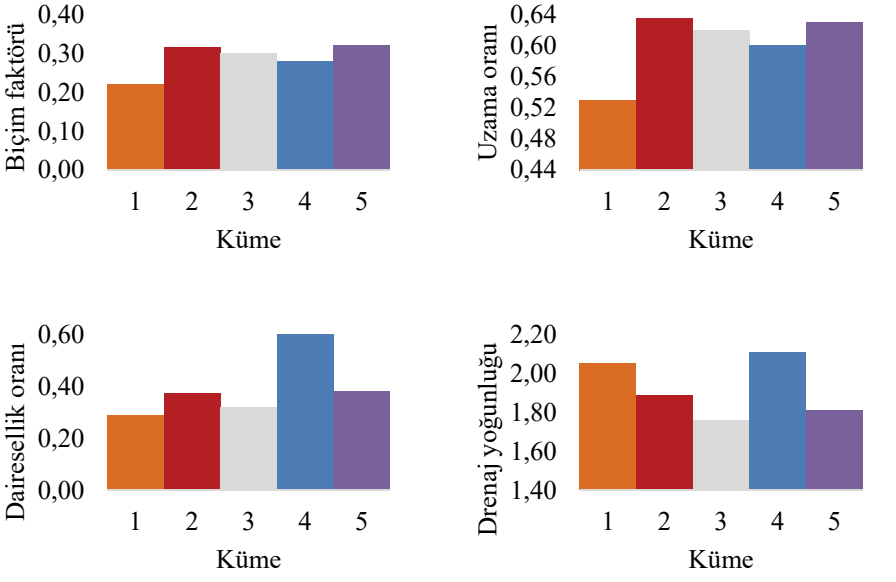

Şekil 6 - Kümelerin alansal havza özelliklerinin medyan değerleri

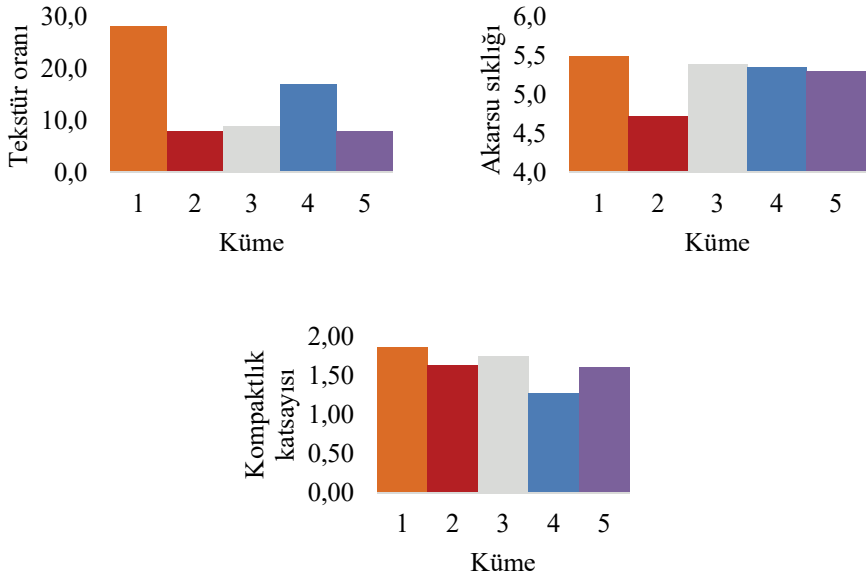

Şekil 6 - Kümelerin alansal havza özelliklerinin medyan değerleri (devam)

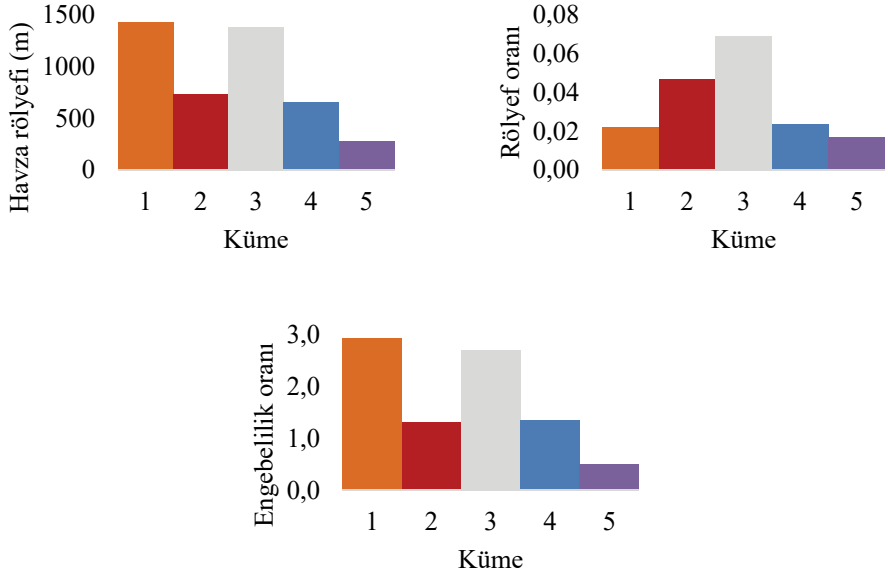

Şekil 7 - Kümelerin rölyef havza özelliklerinin medyan değerleri

5. SONUÇLAR

Bu çalışmada Kuzey Kıbrıs'ta yer alan havzaların temel, çizgisel, alansal ve rölyef morfometrik havza özellikleri coğrafi bilgi sistemleri kullanılarak elde edilmiş ve detaylı bir şekilde incelenmiştir. Böylelikle havzaların esasen jeomorfoloji, jeoloji, rölyef ve hidrolojik açıdan özellikleri ve davranışları anlamaya çalışılmıştır. Tüm bunları bilmek havza bazlı yapılacak gelişim planları ve ortaya çıkabilecek sel ve taşkın olayları gibi olumsuz durumlara karşı plan ve strateji geliştirilmesi açısından da önem arz etmektedir. Bu nedenle havzalar önce teker teker, ardından ise kümelenip bölgesel olarak değerlendirilmiştir. Bu bağlamda gerek havza bazlı gerekse bölgesel bazda taşkın potansiyelleri morfometrik analiz sonuçlarına göre önceliklendirilmelidir. Böylelikle karar vericilerin önlem almaya bu sonuçlara bağlı olarak yapılacak öncelik sırasına göre başlamaları sağlanabilir. Ayrıca bu çalışmada elde edilen sonuçlar, taşkınların sorun olduğu ve veri eksikliği nedeniyle yapılacak taşkın tahminlerinin güvenilirliğinin sağlanamadığı KKTC'de sürdürülebilir bir taşkın yönetimi geliştirme çalışmaları için de oldukça önemlidir. Çalışma neticesinde ulaşılan homojen bölgelerde yer alan tüm istasyonlardaki verilerin bir arada dahil olduğu bölgesel analiz gelçekleştirilir. Bu da en sık karşılaşılan sorunlardan biri olan ölçüm istasyonlarındaki veri eksikliğinin ve yetersizliğinin aynı homojen bölgedeki diğer istasyonların katkısı ile giderilmesini sağlayacaktır.

Çalışma neticesinde şu sonuçlara ulaşılmıştır:

- Hibrid hiyerarşik k-ortalamalar kümeleme yöntemi ile gerçekleştirilen ve 18 morfometrik parametre ve havzaların coğrafi konumları temelinde yapılan kümeleme analizi neticesinda Kuzey Kıbrıs'taki 35 havza beş kümede sınıflandırılmıştır. Küme 1'de 3, Küme 2'de 12, Küme 3'te 7, Küme 4'te 6 ve Küme 5'te ise 7 havza morfometrik özellikler açısından birbirlerine benzer havzalar olarak belirlenmiştir. Burada orta Mesarya bölgesindeki havzalar Küme 1'i, Girne Dağları ile kuzey kıyı şeridi arasında kalan havzalar Küme 2'yi, Trodos Dağları'ndan Güzelyurt Körfezi'ne uzanan havzalar Küme 3'ü, Doğu Mesarya bölgesinden Mağusa Körfezi'ne uzanan havzalar Küme 4'ü ve Karpaz Yarımadası'nda yer alan havzalar ise Küme 5'i oluşturmuştur. Elde edilen havza kümeleri içerisinde bulunan havzaların hidrolojik açıdan benzer oldukları düşünüldüğünde az da olsa akım gözlem istasyonlarına sahip havzalardaki verilerinin bir araya getirilmesiyle belli bir havza kümesinin istatistiksel olarak davranışı modellenebilir. Böylece gerçekleştirilecek bölgesel analiz ile gözleme sahip olmayan veya sınırlı verisi olan bir istasyonun davranışı hakkında da bilgi sahibi olunabilir. Bu sonuçlar özellikle su kaynaklarının planlanması açısından önem arz etmektedir.

- Çalışma alanı içerisinde yer alan havzaların çok çeşitli havza alanlarına sahip oldukları görülmektedir. Özellikle orta Mesarya bölgesinde yer alan ve Küme 1'i de oluşturan havzaların havza alanı, havza çevresi, havza genişliği ve havza uzunluğu gibi temel havza özellikleri diğer havzalara kıyasla oldukça büyüktür. Bu havzalar Girne ve Trodos Dağları'ndan adanın batısına ve doğusuna su ileten havzalardır. Bunun yanında Girne Dağları ile kuzey kıyı şeridi arasında bulunan havzalar (Küme 2) ise nispeten küçük temel havza özellikleri taşımaktadır.

- Akış dizilimi ve özellikle akış numarası Küme 1'deki havzalarda diğerlerine göre daha yüksektir. Küme 1 içerisinde yer alan akarsu kollarının akış dizilimi altıncı dereceden büyük olduğundan ana akarsu kollarının tamamının nehirlerden oluştuğu belirlenmiştir.

Ayrıca Kuzey Kıbrıs'taki havzalar içerisinden geçen ve nehir olarak tanımlanabilecek akarsuların bir kısmı da Küme 4'te bulunmaktadır. Ancak tüm çalışma alanı dikkate alındığında havzaların büyük çoğunluğunun ana akarsu kolu orta dereceli akarsulardan oluşmaktadır. Bunlara ek olarak, yüksek çatallanma oranları ile Küme 2'deki havzaların düşük konsantrasyon sürelerine sahip oldukları ve daha yüksek taşkın potansiyeli taşıdıkları söylenebilir. Genel olarak ise çatallanma oranı temelinde çalışma alanı içerisindeki havzaların büyük çoğunluğunda drenaj ağının iyi gelişmiş olduğu görülmektedir. Buradan elde edilen sonuçlar ile hangi bölgelerin taşkına duyarlı olduğu belirlenmiştir. Dolayısıyla öncelikle buralardaki havzalarda geliştirilecek hidrolojik ve hidrolik modeller ile taşkınlar analiz edilebilir ve alınabilecek yapısal ve yapısal olmayan önlemler ile olası taşkın etkileri azaltılabilir.

- En yüksek tekstür oranlarıyla Küme 1 içerisinde yer alan havzalar aynı zamanda en yüksek erozyon ve akış potansiyellerine de sahip havzalar olarak belirlenmiştir. Buna karşın biçim faktörü ve uzama oranları ise diğer kümelere kıyasla daha düşük olduğu saptanmıştır. Kuzey Kıbrıs ölçeğinde havzaların biçim faktörü değerleri daha çok uzun ve orta daireselliğe sahip oldukları yönünde fikir vermektedir.

- Küme 4'teki havzalar genel olarak daha yüksek dairesellik oranı ve drenaj yoğunluğu olan havzalar olarak ortaya çıkmaktadır. Küme 2'deki havzalar ise diğer havzalarla kıyaslandığında genel olarak en düşük akarsu sıklığına sahip havzalar olarak bulunmuştur. Adanın kuzeyinde yer alan havzaların genel olarak dairesellik oranları havzaların jeomorfolojik açıdan daha çok genç veya olgun havzalar olduklarını göstermektedir. Ayrıca havzaların çoğunluğunun sahip olduğu düşük drenaj yoğunlukları yağış sonrası yavaş hidrolojik tepkiler gösterdiklerini ortaya koymaktadır. Bu bulgular taşkın araştırmaları içinde önem arz eden havza davranışlarının anlaşılması konusuna katkı sağlamaları açısından değerlidir.

- Havza rölyef özellikleri incelendiğinde Küme 1 ve Küme 3 içerisinde yer alan havzaların diğerlerine kıyasla daha yüksek rölyef havza özelliklerine sahip oldukları belirlenmiştir. Bu havzalar genellikle Girne ve Trodos Dağları'nın Mesarya Ovası'na doğru olan yamaçlarında veya Doğu Mesarya'dan Mağusa Körfezine doğru uzanmış şekilde konumlanmışlardır. Buralardaki ani eğim değişiklikleri havzaların taşkınlar gibi doğal afetlere karşı daha yatkın olduklarını göstermektedir. Diğer bir taraftan en düşük rölyef değerlerine sahip havzalar Karpaz Yarımadası'nı temsil eden Küme 5 içerisindeki havzalardır. Burada ulaşılan sonuçlar çeşitli doğal afetlere karşı havzaların yatkınlığını göstermektedir ve alınacak önlemler bağlamında havzaların önceliklendirilmesi için kullanılabilir.

Tüm bunlara ek olarak, elde edilen sonuçlar hidrolojik değişkenler ile morfometrik parametreler arasındaki ilişkinin daha iyi anlaşılması açısından önemlidir. Böylelikle aynı küme grupları içerisinde yer alan ve ölçüm değerleri olmayan havzalar için farklı hidrolojik değişkenlerin tahminlerinde elde edilen bu bulgular kullanılabilir. Örneğin ileride yapılacak bir çalışma ile akım gözlem istasyonu bulunan havzaların yağış-akış ilişkileri hidrolojik model geliştirilerek elde edilebilir ve aynı kümedeki diğer havzalar için bu ilişkilerin benzerliği araştırılabilir. Aynı uygulamada ayrıca farklı kümeleme yöntemlerinin sonuçlar üzerindeki etkileri de incelenebilir. İlave olarak, bu çalışmanın sonucunda elde edilen bulgular ve sonuçlar; Kuzey Kıbrıs'taki havzaların ve benzerlerinin karar vericiler tarafından daha iyi anlaşılmasını sağlayabilir. Dolayısıyla havzalar için üretilecek kalkınma, yönetim ve

koruma politikalarının önceliklendirilip uygulanması noktasında referans alınması açısından faydalı olacaktır.

Bunun yanı sıra, bu çalışmada gerçekleştirilen kümeleme analizinde morfometrik özellikler kullanılsada ortaya çıkan havza kümelerinin harita üzerindeki konumları temelde coğrafi ve iklimsel faktörlerin de havza benzerliklerinde etkili oldukları konusunda fikir vermektedir. Bu çalışmada morfometrik özellikler temelinde yapılan bölgeselleştirme ile Zaifoglu vd. [20] tarafından yağış serileri kullanılarak elde edilen homojen bölgeler büyük ölçüde örtüşmektedir. Dolayısıyla Kuzey Kıbrıs'ta hidrolojik açıdan benzer havzalar üzerindeki yağış karakteristiğinin de benzer olabileceği görülmektedir. İlerde yapılacak bir çalışma ile bu ilişkinin anlamlılığı araştırılabilir. Ayrıca topoğrafik özelliklerle birlikte farklı iklimsel, jeolojik ve yüzey özellikleri gibi daha çeşitli veri setleriyle de havzalar sınıflandırılabilir. Özellikle iklim değişikliğinin havzaların farklı özellikleri üzerinde yaratacağı etkilerin çalışılması sürdürülebilir havza yönetimi açısından değerli olacaktır.

Semboller

A : Havza alanı

C_C : Kompaktlık katsayısı

C_j : j'inci kümenin merkezi

D_d : Drenaj yoğunluğu

d_{ij} : Karesel Öklid uzaklık ölçüsü

E : Tüm kümelerin hata kareler toplamıdır

E_m : Küme içi hata karaler toplamı

F_f : Biçim faktörü

H : Havza rölyefi

J : K-ortalamalar yöntemindeki amaç fonksiyonu

L_b : Havza uzunluğu

L_u : Toplam akış uzunluğu

N_u : Akış numarası

n : Nesne sayısı

P : Havza çevresi

p : Değişken sayısı

R : Havza içerisindeki en yüksek kot

R_h : Rölyef oranı

R_b : Çatallanma oranı

R_c : Dairesellik oranı

R_e : Uzama oranı

R_n : Engebelilik oranı

R_t : Tekstür oranı

r : Havza içerisindeki en düşük kot

S_f : Akarsu sıklığı

u : Akış dizilimi

W : Havza genişliği

$X_i^{(j)}$: j'inci kümeye ait i'inci özellik vektörü

x_{ik} : i'inci nesnenin k'inci değişkendeki değeri

x_{jk} : j'inci nesnenin k'inci değişkendeki değeri

$x_{ml,k}$: m'inci kümedeki l'inci nesne için k'inci değişkenin değeri

$\bar{x}_{m,k}$: m'inci kümedeki k'inci değişkene ait ortalama

Teşekkür

Bu çalışmanın gerçekleştirilmesi için gerekli topoğrafik haritaları sağlayan Kuzey Kıbrıs Türk Cumhuriyeti Harita Dairesi'ne teşekkür ederiz.

Kaynaklar

[1] Papageorgaki, I., Nalbantis, I., Classification of Drainage Basins Based on Readily Available Information. Water Resour. Manag., 30(15), 5559-5574, 2016.

[2] Hrachowitz, M., Savenije, H. H. G., Blöschl, G., McDonnell, J. J., Sivapalan, M., Pomeroy, J. W., ... Cudennec, C. A decade of Predictions in Ungauged Basins (PUB)-A review. Hydrol. Sci. J, 58(6), 1198-1255, 2013.

[3] Guo, Y., Zhang, Y., Zhang, L., Wang, Z. Regionalization of Hydrological Modeling for Predicting Streamflow in Ungauged Catchments: A Comprehensive Review. WIREs Water, 8(1), e1487, 2021.

[4] Randrianasolo, A., Ramos, M. H., Andréassian, V. Hydrological Ensemble Forecasting at Ungauged Basins: Using Neighbour Catchments for Model Setup and Updating. Adv. Geosci., 29, 1-11, 2011.

[5] Merz, R., Blöschl, G. Regionalisation of Catchment Model Parameters. J. Hydrol., 287(1-4), 95-123, 2004.

[6] He, Y., Bárdossy, A., Zehe, E. A Review of Regionalisation for Continuous Streamflow Simulation. Hydrol. Earth Syst. Sci., 15(11), 3539-3553, 2011.

[7] Zhang, Y., Chiew, F. H., Li, M., Post, D. Predicting Runoff Signatures Using Regression and Hydrological Modeling Approaches. Water Resour. Res., 54(10), 7859-7878, 2018.

[8] Hailegeorgis, T. T., Thorolfsson, S. T., Alfredsen, K. Regional Frequency Analysis of Extreme Precipitation with Consideration of Uncertainties to Update IDF Curves for the City of Trondheim. J. Hydrol., 498, 305-318, 2013.

[9] Wang, Z., Zeng, Z., Lai, C., Lin, W., Wu, X., Chen, X. A Regional Frequency Analysis of Precipitation Extremes in Mainland China with Fuzzy C-means and L-moments Approaches. Int. J. Climatol., 37, 429-444, 2017.

[10] Betül, S. A. F. Batı Akdeniz Bölgesi Taşkın Tahminlerinde Homojenlik İrdelemesi. Tek. Der., 22(109), 5587-5611,2011.

[11] Fırat, M., Dikbaş, F., Koç, A. C., ve Güngör, M. Classification of Annual Precipitations and Identification of Homogeneous Regions Using K-means Method. Tek. Der., 23(115), 1609-1622, 2012.

[12] Hosking. J.R.M., Wallis. J.R. Regional Frequency Analysis: An Approach Based on L-moments. New York. Cambridge University Press, 2005.

[13] Rao, A. R., Srinivas, V. V. Regionalization of Watersheds by Hybrid-cluster Analysis, J. Hydrol., 318(1-4), 37-56, 2006.

[14] Clarke. J. J. Morphometry from Map. Essays in Geomorphology, New York. Elsevier, 1966.

[15] Soni, S. Assessment of Morphometric Characteristics of Chakrar Watershed in Madhya Pradesh India Using Geospatial Technique. Appl. Water Sci., 7(5), 2089-2102, 2017.

[16] Rekha, B. V., George, A. V., Rita, M. Morphometric Analysis and Micro-watershed Prioritization of Peruvanthanam Sub-watershed, the Manimala River Basin, Kerala, South India. Environ. Res. Eng. Manag., 57(3), 6-14, 2011.

[17] Prasannakumar, V., Vijith, H., Geetha, N. Terrain Evaluation Through the Assessment of Geomorphometric Parameters Using DEM and GIS: Case Study of Two Major Sub-watersheds in Attapady, South India. Arab. J. Geosci., 6(4), 1141-1151, 2013.

[18] Türker, U., Hansen, B. R. River Basin Management and Characterization of Water Bodies in North Cyprus. In 10th International Congress on Advances in Civil Engineering, Ankara, Türkiye, 2012.

[19] Nikolakis, D. A Statistical Study of Precipitation in Cyprus, Hell. J. Geosci., 43, 67-74, 2008.

[20] Zaifoglu, H., Akintug, B., Yanmaz, A. M. Regional Frequency Analysis of Precipitation Using Time Series Clustering Approaches. J. Hydrol. Eng., 23(6), 05018007, 2018.

[21] Camera, C., Bruggeman, A., Hadjinicolaou, P., Pashiardis, S., Lange, M. A. Evaluation of Interpolation Techniques for the Creation of Gridded Daily Precipitation (1×1 km^2); Cyprus, 1980–2010. J. Geophys. Res. Atmos., 119(2), 693-712, 2014.

[22] Christofi, C., Bruggeman, A., Kuells, C., Constantinou, C. Hydrochemical Evolution of Groundwater in Gabbro of the Troodos Fractured Aquifer. A Comprehensive Approach. Appl. Geochemistry, 114, 104524, 2020.

[23] Djokic, D., Ye, Z., Dartiguenave, C. Archydro Tools Overview Version 2.0, California. Esri, 2011.

[24] Horton, R. E. Erosional Development of Streams and Their Drainage Basins; Hydrophysical Approach to Quantitative Morphology. Geol. Soc. Am. Bull., 56(3), 275-370, 1945.

[25] Strahler, A. N. Part II. Quantitative Geomorphology of Drainage Basins and Channel Networks. Handbook of Applied Hydrology, New York. McGraw-Hill, 1964.

[26] Schumm, S. A. Evolution of Drainage Systems and Slopes in Badlands at Perth Amboy, New Jersey. Geol. Soc. Am. Bull., 67(5), 597-646, 1956.

[27] Magesh, N. S., Chandrasekar, N., Soundranayagam, J. P. Morphometric Evaluation of Papanasam and Manimuthar Watersheds, Parts of Western Ghats, Tirunelveli District, Tamil Nadu, India: A GIS Approach. Environ. Earth Sci., 64(2), 373-381, 2011.

[28] Ward, J. H. Hierarchical Grouping to Optimize An Objective Function. J. Am. Stat. Assoc., 58(301), 236-244, 1963.

[29] MacQueen, J. Classification and Analysis of Multivariate Observations. 5th Berkeley Symposium on Mathematical Statististics and Probability. California, 1967.

[30] Chen, B., Tai, P. C., Harrison, R., Pan, Y. Novel Hybrid Hierarchical-K-means Clustering Method (HK-means) for Microarray Analysis. 2005 IEEE Computational Systems Bioinformatics Conference-Workshops. California. 2005.

[31] Everitt, B.S., Dunn G., Applied Multivariate Analysis, London. Edward Arnold, 1991.

[32] Theodoridis S., Koutroubas K. Pattern Recognition. 4th edition. Academic Press, 2008.

[33] Charrad, M., Ghazzali, N., Boiteau, V., Niknafs, A. NbClust: An R Package for Determining the Relevant Number of Clusters in A Data Set. J. Stat. Softw., 61, 1-36, 2014.

[34] Rao, A. R., Srinivas, V. V. Regionalization of Watersheds: An Approach Based on Cluster Analysis, Berlin. Springer Science and Business Media, 2008.

[35] Ralambondrainy, H. A Conceptual Version of the K-means Algorithm. Pattern Recognit. Lett., 16(11), 1147-1157, 1995.

[36] Rao, A. R., Srinivas, V. V. Regionalization of Watersheds by Hybrid-Cluster Analysis. J. Hydrol., 318(1-4), 37-56, 2006.

[37] Smith, A., Sampson, C., Bates, P. Regional Flood Frequency Analysis at the Global Scale. Wat. Resour. Res., 51(1), 539-553, 2015.

[38] Kebebew, A. S., Awass, A. A. Regionalization of Catchments for Flood Frequency Analysis for Data Scarce Rift Valley Lakes Basin, Ethiopia. J. Hydrol. Reg. Stud., 43, 101187, 2022.

[39] Strahler, A. N. Quantitative Analysis of Watershed Geomorphology. Eos, Trans. Am. Geophys. Union, 38(6), 913-920, 1957.

[40] Chopra, R., Dhiman, R. D., Sharma, P. K. Morphometric Analysis of Sub-watersheds in Gurdaspur District, Punjab Using Rremote Sensing and GIS Techniques. J. Indian Soc. Remote Sens., 33(4), 531-539, 2005.

[41] Melton, M. A. (1957). An Analysis of the Relations Among Elements of Climate, Surface Properties, and Geomorphology, New York. Columbia University, 1957.

[42] Smith, K. G. Standards for grading texture of erosional topography. Am. J. Sci., 248(9), 655-668, 1950.

[43] Biswas, S., Sudhakar, S., Desai, V. R. Prioritisation of Subwatersheds Based on Morphometric Analysis of Drainage Basin: A Remote Sensing and GIS Approach. J. Indian Soc. Remote Sens., 27(3), 155-166, 1999.

[44] Morisawa, M. E. (1962). Quantitative Geomorphology of Some Watersheds in the Appalachian Plateau. Geol. Soc. Am. Bull., 73(9), 1025-1046, 1962.

[45] Kumar, A., Darmora, A., Sharma, S. Comparative Assessment of Hydrologic Behaviour of Two Mountainous Watersheds Using Morphometric Analysis. Hydrology Journal, 35(3-4), 76-87, 2012.

[46] Bogale, A. Morphometric Analysis of A Drainage Basin Using Geographical Information System in Gilgel Abay Watershed, Lake Tana Basin, Upper Blue Nile Basin, Ethiopia. Appl. Water Sci., 11(7), 1-7, 2021.

[47] Usul, N. Mühendislik Hidrolojisi, Ankara. ODTÜ Yayıncılık, 2013.

[48] Chorley RJ (1969) The Drainage Basin As The Fundamental Feomorphic Unit, London. Methuen Co. Ltd, 1969.

Turkish Journal of Civil Engineering, 2023 55-79, Paper 746, ***Research Article***

Identifying Interrelated Factors of Fatal and Injury Traffic Accidents Using Association Rules

Zeliha Cagla KUYUMCU[1]
Hakan ASLAN[2]
Nilufer YURTAY[3]

ABSTRACT

This study aims to investigate the possible relationships of risk factors related to traffic accidents playing important roles in increasing the likelihood of accidents. In the previous studies, parametric models are mostly used to investigate the causes of traffic accidents. As a non-parametric data mining model with its increasing usage in recent years; association rule mining was employed in this study to analyse the traffic accident data for the period of 2015 and 2020 in the city of Sakarya, Turkey. The analysis of the data studied revealed the relationships among the external/environmental, driver, road, vehicle and nature of accident factors. Some important rules regarding accidents occurring on daylight came into prominence within the scope of this study. In addition, the correlations between the driver casualties and their education level and ages are established. The findings are beneficial for transportation authorities to apply effective operational strategies and campaigns to increase the road safety.

Keywords: Traffic accidents, road crashes, traffic safety, data mining, association rules, driver faults.

1. INTRODUCTION

According to the data given by World Health Organisation (WHO) while around 1.35 million people die each year due to traffic accidents world-wide, more than around 35 million people are also involved in traffic accidents not fatal but leave many disabled. The data also state that although car ownership and trip rates are relatively higher in industrialized countries, more than 90% of road-traffic related deaths occur in low and middle-income countries.

Note:
- This paper was received on November 1, 2022 and accepted for publication by the Editorial Board on June 23, 2023.
- Discussions on this paper will be accepted by November 30, 2023.
- https://doi.org/10.18400/tjce.1322965

1 Sakarya University, Civil Engineering Department, Sakarya, Türkiye, caglacaglar@sakarya.edu.tr - https://orcid.org/0000-0002-9851-6843

2 Sakarya University, Civil Engineering Department, Sakarya, Türkiye haslan@sakarya.edu.tr - https://orcid.org/0000-0001-9444-6908

3 Sakarya University, Computer Engineering Department, Sakarya, Türkiye nyurtay@sakarya.edu.tr - https://orcid.org/0000-0002-7577-7506

Similarly, in high-income industrialized countries, people from low socioeconomic backgrounds are more likely to be involved in road accidents. These accidents are the leading causes of deaths for children and young people aged between 5 and 29. Males world-wide are more likely to be involved in traffic accidents than the same age group of young females. The figures obtained across the world and presented by WHO state that about three-quarters (73%) of all road traffic fatalities are caused by young males under 25 years old who are almost 3 times more likely to die in a road traffic accident than young females [1].

To reflect the effect of road injuries for the life quality of the people, it was stated by a study conducted in 2019 involving 204 countries from all over the world that they are the seventh causes of disability-adjusted life [2].

According to the report of injuries related to the European Union countries for the period of 2009-2018, as shown in Figure 1, the average traffic accident rate (TAR) is 5.74 per 1000 people. On the other hand, this average figure doubles as almost 10 per 1000 people in Turkey, making it as the second highest country in Europe [3].

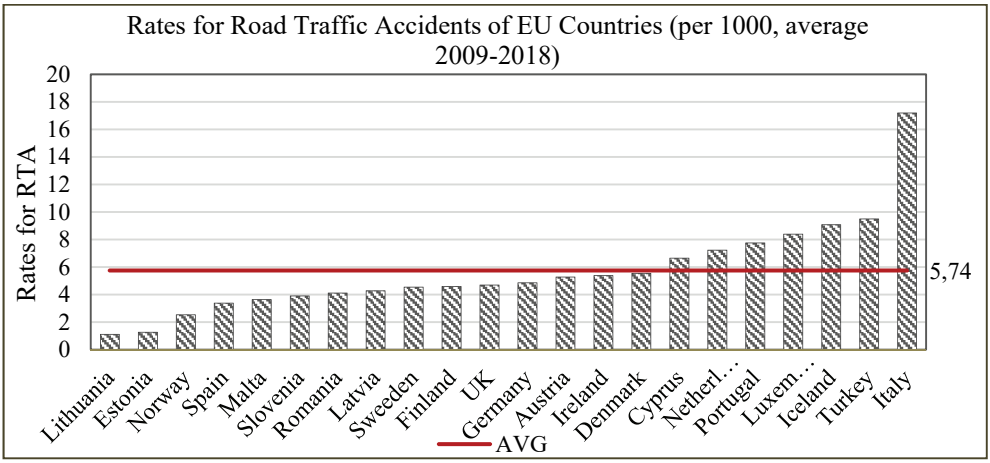

Figure 1 - Average road traffic accident rates of non-fatal traffic injuries for EU countries for the period of 2009-2018 [3]

In 2018, while the number of deaths in traffic per 100 thousand people was 4.9 in EU countries, Turkey had the figure of 8.1 [4].

The total number of fatal and injury related accidents occurred in Turkey, an upper-middle-income country [5], with regard to 2015, 2016, 2017, 2018, 2019 and 2020 are given as 183,011, 185,128, 182,669, 186,532, 174,896, 150,275, respectively. It is important to note that, the quarantine enforced in many countries in effect of the Covid-19 pandemic caused the number of traffic accidents dropped drastically [6]. In addition, driver fault rates for these stated years are given as 89.76, 90.02, 90.29, 89.64, 88.89 and 88.65 percent, respectively [7]. These high rates of the accidents involving driver faults led the accidents without driver faults to be excluded for the analysis in this study. Furthermore, as non-faulty drivers simply

do not have any contribution to the occurrence of the accidents, this study mainly analysed the correlations between the characteristics of the faulty drivers involved in the accidents and the nature of the accidents without considering the features of the drivers having no responsibility or fault. However, if the accident reports give responsibility to all the drivers in the accident to some extend then each of these drivers are taken into consideration through the analysis.

A wide range of parametric methods such as regression and logit models have been used by numerous researchers in order to control and reduce the number of traffic accidents [8, 9, 10, 11].

The dataset used in this study provides ample contents with regard to numerous attributes having effect on the occurrence of the traffic accidents. In addition, it is needed to note that a meticulous data pre-processing was carried out by excluding noisy data, by both combining the attributes to get meaningful rules when needed, and by converting numerical data into categoric one, etc. to prevent the biased results to be attained.

The dataset was also divided into groups to obtain different inter-correlations. Furthermore, after pre-processing, the analysis was carried out by changing support and confidence values repeatedly through the evaluations of the rules produced by the software, R, so that the best and comprehensive association rules are assured to be acquired.

2. LITERATURE REVIEW

In the literature there are numerous studies with regard to traffic accidents. In these studies, a lot of factors were investigated to analyse their potential effects to traffic accidents. The literature review is divided into two sections: 1) studies on traffic violations and prediction of accident severity and 2) studies on identifying co-occurring accident factors.

2.1. Studies on Traffic Violations and Prediction of Accident Severity

Alver et al. examined the relationship of four major traffic rule violations with the characteristics of the traffic accidents involving young drivers through the data collected from 2057 participants of their questionary survey conducted as face-to-face interview. They employed binary logit model to establish the correlation between the socio-demographic background of the young adults and their behaviours in traffic leading to an accident [12].

Katanalp et al. used a dataset of bicycle accidents recorded for the period of 2013-2017 for the assessment of the classification of injury-severity in accidents involving cyclists by employing DT-based hybrid-fuzzy models (DT-CFL and DT-RFL). C4.5 decision tree algorithm was used both to classify the injury-severity level and to obtain all splitting conditions to set up the DT-CFL fuzzy prediction model. The analysis illustrated the performance of the injury-severity classification in terms of accuracy, precision, recall, and F-measure values [13].

Kadilar examined the factors having effect on the severity of drivers in traffic accidents via ordinary logistic regression assessment model. The study modelled the Turkish driver fatalities and the meaningful estimations of the accident severity levels in Turkey for the first

time. According to the findings of the research it was determined that age and education level of the driver, existence of alcohol-drug usage, availability of seat belt, condition and type of the roadway, location and type of the collision are among the important factors having major effect on the accident severity to be considered for the analysis. On the other hand, it is engrossingly claimed that gender, roadway surface, weather condition and vehicle age do not have statistically significant effect on the accident severity [8].

Zhang et al. identified main risk factors causing traffic violations and their relations with the severity of the accidents. In this study, stepwise logistic regression model was applied to reveal the most important factors affecting the probability of traffic violations. The results indicated that drivers with less than two-years of experience have less risk of getting involved with severe accidents although they tend to perform higher possibility of rule violations. Another important finding of the study is that morning rush hours involve the probability of more violations with unimportant effect on accident severity [9].

Ma et al. investigated different age groups of drivers involved with accidents resulted in pedestrian injury. Pedestrian age, vehicle type and weather conditions were pointed out as important variables for pedestrian injury types. Another finding is that number of vehicles and traffic type as independent variables affect young and middle-aged drivers` behaviours at intersections. Moreover, hit-and-run pedestrian involved accidents caused by young and older drivers are related to a significant variable of whether the roadway is divided or not. With the developed probit regression models, it was revealed that education level of the drivers along with control and intersection design measures are effective in the decision-making processes to increase the safety of pedestrians at intersections [10].

Adanu et al. explored frequent and improper lane-changing behaviours having a profound impact on both the operation and safety of traffic. The analysis of severity of injuries due to lane changing-related accidents involving young and old drivers resulted in two models for young and old drivers. According to the model estimation results, young male drivers are more likely to be injured in terms of lane changing-related accidents compare to older male drivers. This is mainly due to the fact that older drivers are more careful when changing the lanes for different purposes preventing them to get involved that kind of accidents [14].

Chiou et al. analysed parameters of both of the vehicles causing the accident rather than concentrating on only one of them by employing Generalized Estimating Equations (GEE) to examine level of severity. The accident data included variables like driver features (for both parties), type of vehicles, road-intersection-lighting conditions, and type of collision. According to this study, the most influential factors on accident severity are vehicle type (motorcycle), speeding, angle impact type of accident, and drunk driving [15].

AlKheder et al. investigated accident severities by employing Decision Trees, Bayesian Network and Linear Support Vector Machine (SVM) as data mining analysis methods. Among these, Decision Trees have many advantages over traditional statistical approaches. This method can work with different types of variables like binary, categorical, ordinal, and continuous ones. Another advantage of applying decision trees is the ability to indicate the importance of the selected predictors. Age (under 17, 18-30, 31-60, over 60), seat belt, seat/place of the injured person (driver, front/back seat, pedestrian, etc.), road class, speed limit, number of lanes, type of accident (pedestrian, T-bone, side-by-side, rear-end collision and other) were regarded as variables. The performances of these three used methods were

compared through different parameters. While Bayesian network produced the most successful results for predictions of the severity of the accidents, SVM resulted in the most unsuccessful. It was stated that pedestrians are more vulnerable road users compared to drivers and passengers. Another finding of the research is that male drivers and front seat passengers are more exposed to severe and fatal consequences. Likewise, older drivers are shown to be more likely to get involved in severe injuries and fatalities [16].

Batouli et al. conducted research in Colorado, USA. In this study the factors affecting the hitting pedestrian accident severity were examined through the data for the period of time from 2006 to 2016. Probability ratios of occurrence of fatal and non-fatal pedestrian accidents were calculated through the established logistic regression model by considering the proximity of the accident to the intersection, daylight condition, vehicle type and vehicle speed as the variables. The outcomes of the paper state that since the older drivers` involvement within car technological devices and mobile phones is less than the younger drivers, the older drivers are less distracted improving their reaction time and vision ability leading them to get involved in less severe accidents. Another interesting finding of the research is that pedestrian severity is affected by the impairment of both pedestrian himself and driver [11].

2.2. Studies on Co-Occurring Accident Conditions

Cai examined the effect of type and location of accident, season, time of the day, weather condition, lighting, visibility distance, barrier positions, type of road pavement and intersection with the rules of association. The rules specify that fatal accidents occur when "driving with other behaviours that undermine driving safety". Furthermore, "collision with moving vehicles" results in more fatality when season is summer and time of the day hour is deep night. Another remarkable outcome of the study points out that the fatality rate of the accidents increases when weather is sunny, terrain is plain, time is evening without street lighting [17].

Yu et al. applied a priori algorithm to analyse features and factors affecting severity of traffic accidents in Wisconsin, United States. According to study results, male drivers aged between 16 and 29 are more tend to be involved in accidents on roadways with no median. The other important findings state that fatal accidents are more likely to happen at towns while property damage accidents in the cities [18].

Das et al. examined pedestrian deaths between 2014 and 2018 through association rules applied to 4 groups of the most common fatal accident scenarios. This study developed all twenty best rules for 4 subgroups using a priori algorithm and taking lift as a performance measure. Some key variable categories are considered as; lighting, straight moving vehicles, turning vehicles, local municipality streets, and pedestrian age range. Patterns of rules differed according to the position of the pedestrian being inside and outside the crosswalk. When the pedestrian is in a place other than a crosswalk, the absence of lighting at night is associated with many accidents [19].

Kong et al. with the naturalistic driving dataset, investigated the potential rules between fast driving behaviour and journey/driving/road characteristics by employing classification-based association rules algorithms. One of the findings of the study is that the fatigue and distraction

that occurs on long journeys with the combination of fast driving on high class roads can cause severe accidents [20].

Zhu derived association rules to find accident-related features that increase the probability of vehicle-bike hit-and-run accidents. One of the rules expresses that the likelihood of vehicle-bicycle hit-and-run accidents reduces when the collision type is rear-end occurring at morning peak hours [21].

Hong et al. produced worthful outcomes by explaining the fundamental rules in the field of freight vehicle accident data. According to the study, a priori algorithm as an association rule mining method is an acceptable method for analysing features of freight vehicle accidents. They also spotted that the accidents involving young freight vehicle drivers in their 20s and 30s are linked with specific regions having well-designed roadway geometry, excluding vertical and horizontal curves. Furthermore, the study indicates the connection between young freight vehicle drivers' traffic violations and good conditions of roadways [22].

Das et al. developed an effective way of discovering important association rules explaining accidents when the weather is rainy. One of the remarkable findings is that drivers from the age group in between 15 to 44 get involved in the accidents during rainy weather when the illumination is poor, and roadway has curves [23].

According to the study conducted by Xu et al., factors associated with traffic accidents involving serious casualty include road user behaviour, condition of the vehicles, road geometric design, and environmental features. The factors associated with poor vehicle operation conditions such as flat tires, braking-related problems, and faulty steering systems may cause severe accidents on even high standard roads having relatively decent safety facilities [24].

3. METHODOLOGY AND DATA

In this study, the association rule mining was chosen as the data mining method to determine the co-occurrence pattern of traffic accidents with regard to related attributes stated in the accident reports. The association rule analysis, which has recently been increasingly applied in road traffic safety research, is designed to investigate a set of elements that typically occur together in a given incident. Association rule mining is a suitable method to investigate road traffic accidents when the large amount of data makes it difficult to extract a latent hypothesis for the research analysis. This makes association rules to be extremely useful tool for a big set of unsupervised data [19].

The raw data in this research covers 6 years of traffic accident data having over 23,551 rows representing accidents and 26 columns of attributes designating the possible factors contributing to the occurrence of the accidents. As the association rules in this sense provides profound and effective analysis of the big data, it was employed for the analysis of the data available within the concept of this study.

3.1. Study Area

Covering 4817 km^2 area and residing 1.06 million people, Sakarya is located in the northwest part of Turkey [25].

While the car ownership rate per 1000 people was 162 in Turkey in 2021, it was 151 in Sakarya, making the city to characterize Turkey's average with that respect [25].

The highway network of Sakarya consists of highways, state roads, provincial roads and urban roads. The motorways passing through Sakarya are O-4 (TEM) and O-7 (NMM), the state roads, on the other hand, passing through Sakarya are D-100, D-650 and D-020 [26].

Another important fact to be mentioned is that Sakarya is a transit point of four major cities of Turkey, Kocaeli (37 km), İstanbul (148 km), Bursa (158 km), Bolu (114 km) and Ankara (306 km). Sakarya is 110 km from Istanbul Kurtköy Sabiha Gökçen Airport and 176 km from Istanbul Airport [26]. This important location of the city led to one of the 20 accident black spots planned to be investigated across Turkey in 2021 to be in city of Sakarya [27].

The total number of the registered motor vehicles in the city is 312,552 out of them 160,200 being automobile. The total number of accidents, number of people killed, and number of people injured in 2021 are given as 15,758 (43 per day), 2727 (59 per day; 33 at the accident scene, 26 accident follow-up) and 3972 (11 per day), respectively [25].

These facts establish the background of why city of Sakarya was chosen for the analysis. The study area covers all the transportation network of the city and available roads on it, streets, avenues and state roads are all investigated.

3.2. Data Description and Processing

The raw accident data for this study was provided from the Republic of Turkey General Directorate of Security. All traffic accident reports recorded after 2015 in Turkey, hence in Sakarya, include the 30-day hospital follow up period to see whether any further fatal results are the case for the accidents involving serious injury at the accidents. Thus, the dataset used in this study covers fatal or injury related accidents in city of Sakarya for 6 years of time period from 2015 to 2020 by covering this 30 day follow up period.

Since the number of fatal accidents involving drivers, pedestrians or passengers constitutes only 126 records out of 14,226 being considerably lower than the total number of injury and non-injury accidents, all fatal accidents are included in the dataset of injury accident classes.

There are two raw datasets; one with 14,226 records which signify the characteristics of all real accidents, and the other with 23,551 records involving driver’s characteristics. As many accidents involved more than one car, hence drivers, the second raw data had more rows than the initial one. These two datasets with 14,226 and 23,551 rows consist of 43 and 26 columns, respectively, as presented in Table 1.

Finally, these two raw datasets were combined to acquire the dataset to be used for the analysis purposes. The combination was carried out through the common accident ID numbers. In this way an actual analysis data involving 14,387 records with 11 columns symbolising all the attribute related features were obtained.

In this dataset used in the analysis, each row covers the information related to only the accidents and involved one unique driver faulty. For example, if two vehicles are involved in an accident and both drivers are at fault, they are represented by 2 rows in the dataset used in the analysis. If one of the drivers is responsible for the occurrence of the accident, however, those drivers are represented in the dataset as a single row. It should be mentioned that each row arranged in this way includes the related "driver severity", "driver age" and "vehicle damage level*"* information.

Table 1 - Summary of frequencies and distributions of some important attributes of raw data

Attribute	F	%	Attribute	F	%
Driver Gender			**Illumination**		
Male	20,950	89	Good street-lighting	8815	62
Female	1627	7	No street-lighting	5411	38
Unknown	974	4	**Traffic Signal**		
Driver Age Range			Yes	1636	12
Young	6264	27	No	12,371	87
Middle-aged-1	8492	36	Broken	219	2
Middle-aged-2	7591	32	**Weather**		
Elderly	1204	5	Sunny	11,975	84
Driver Lapses			Rainy	1802	13
Following too close	1298	5	Cloudy/foggy	300	2
Failure to yield	2556	11	Snowy	152	1
Improper turn	1675	7	**Vehicle Type**		
Speeding	5172	22	Car	12,986	55
Improper lane changing	1670	7	Heavy vehicle	1985	8
Drunk driving	183	1	Van	4031	17
Other	1842	8	Others	4549	19
No lapse	9155	39	**Vehicle Damage**		
Driver Severity			Major damaged	3528	15
Injured	9816	42	Minor damaged	9857	42
Non-injured	12,671	54	None damaged	2857	12
Fatal	68	0	Functional damaged	1720	7
Unknown	996	4	Can't move	5067	22
			Not identified	552	2

Table 1 - Summary of frequencies and distributions of some important attributes of raw data (continued)

Attribute	F	%	Attribute	F	%
Driver Education			**Municipality Type**		
Primary school	7862	34	Urban	11,886	84
Middle school	2371	10	Rural	2340	16
High school	6546	28	**Pavement Condition**		
Higher education	2623	11	Dry	11,561	81
Unknown	4149	17	Wet	2479	17
Seatbelt/Helmet Usage			Snowy	96	1
Yes (Seatbelt)	847	4	Ice	55	0
No (Seatbelt)	157	1	Puddle	20	0
Yes (Helmet)	142	1	Other slippery cond.	15	0
No (Helmet)	124	1	**Alcohol Usage**		
Unknown	22,281	95	Yes	1058	4
Driver License			No	18,060	77
Yes	19,753	84	Unknown	4433	19
No	2723	12	**Lighting Condition**		
Unknown	1075	5	Daylight	9503	67
Collision Type			Night	4331	30
Rear	1717	12	Twilight	392	3
Side collision	5115	36	**Season of the Year**		
Rsr	2325	14	Winter (dec-feb)	2760	20
Head on Collision	835	6	Spring (mar-may)	3188	23
Hitting Pedestrian	2756	19	Summer (june-aug)	4181	31
Boo	1478	10	Autumn (sep-nov)	3578	26

Rsr: Rollover/ skidding/run off road, Boo: Bumping into fixed objects and others

As some variables in raw data are in unbalanced nature expressing the dominant structure of the classes available in these attributes, the related association rules lead to only the same type of classes. This is why these attributes are not included in the final dataset for the analysis. The final data contain 2854, 2919, 2660, 2430, 1949 and 1575 samples for each year for the analysis period, respectively.

The dataset includes information regarding the factors related to external and environmental conditions, road conditions, vehicle and driver characteristics and nature of accident features. The data examined within the scope of this study are related only with the accidents involving driver faults. To find effective and meaningful association rules; attributes such as accident

ID, vehicle ID, hours and coordinates of the accidents, number of the road section were excluded since these attributes have individual values and do not create a group of datasets resulting in extremely small percentage values in the general dataset.

On the other hand some attributes; such as vehicle type, district of accidents, geometrical structure of the roadway (vertical or horizontal sections, etc.), availability of the pedestrian crossings and traffic signs, weather conditions, types of road surface, number of involved vehicles, infrastructural road degradations, existence of road maintenance works, barriers, road lines, shoulders, traffic police and obstacles, along with gender and license type of drivers are all used at the elementary stages of the analysis but removed for further detailed investigation due to overwhelmingly unbalanced nature that they have.

Moreover, the remaining number of some attributes might be enough to be evaluated in the analysis but the percentage of the missing data for them are so high that their inclusion for the analysis may lead to deceptive results. These attributes related to road width, the physical condition of the vehicles, recorded alcohol levels, the psychological and physical states of the drivers, the usage of the driver seat belt were also excluded from thorough analysis.

Attributes regarding the date of accidents converted to seasons that they belong to.

Classes set up by discrete continuous numerical data with respect to the age of drivers and vehicles were required to apply a priori algorithm for association rule mining analysis. Some variables were integrated because of necessity. For example, if the accident occurred at day time under daylight conditions and the illumination variable recorded as the lighting exists or not, then a new variable named “revised lighting condition” was derived by combining these two variables. This is simply because of the fact that there is no need to check whether the street was lightened or not for the accidents occurred during day time, as it is against the nature of the day time conditions. In this way by eliminating the day time situation, it was possible to evaluate the accidents in terms of the availability of the lighting. Accordingly, if the accident occurred at night-time, the new variable allows us to determine whether lighting was available at the time of the accident. In the same manner, existence of intersection and traffic sign variables were also integrated.

The summary statistics of the obtained latest data used in this study are illustrated in Table 2. Data was divided into subsections to identify how the severity of traffic accidents correlate with the attributes under external and environmental, driver, road and vehicle factors as accident-causing factors along with the other group of factors.

External and environmental factors are related to the Seasons of the year, Lighting conditions at Daylight or night-time in that accident occurred. Seasons of the year are defined as Spring (march-may), Summer (june-august), Autumn (september-november) and Winter (December-February). Revised lighting condition is classified into Daylight, Good and Bad Street Lighting at night.

Driver factors are related to the driver age and driver-education level. Ages, one of the driver related factors, are divided into four groups: 18-25, 26-40, 41-64 and 65+ years described as young, middle-aged-1, middle-aged-2 and elderly, respectively. As another driver factor, education level is classified into four groups: Primary school, Middle school, High school and Higher education.

While road types are mainly divided into three groups: Divided, Two-way, One-way, the availability of intersections were also included in dataset. Signal type of intersection was

divided into three groups: Unsignalized, Signalized and No-intersection (any section of the roadway apart from intersections).

Age of vehicle was obtained by subtracting the manufacturing years of the vehicle from the accident year.

Driver severity was categorised as Injured and Fatal (first group), and No-injured (second group). The accident causes are classified as Ftc (Following too close), Fty (Failure to yield), Improper Turning, Speeding, Ilc (Improper lane changing), Drunk driving and other. Collision types are taken into consideration under six allocated parts: Rear (Rear end), Sc (Side collision), Rsr (Rollover/skidding/run off Road), HC (Head on Collision), Hitting pedestrian, Boo (Bumping into fixed objects and others).

As can be seen from Table 2, the vehicle damage variable from the raw accident dataset having six classes as Major, Minor, None damaged, Functional damage, Can't move and Not identified, has been reduced to three classes due to the fact that some of them share similar concepts. This reduction was carried out by combining Major and Can't move as Major, Minor and Functional damage as Minor, None damaged and Not identified as None Damaged classes.

Table 2 - Summary of frequencies and distributions of key attributes

Attribute	**F**	**%**	**Attribute**	**F**	**%**
Nature of Accidents			*Driver Factors*		
Driver Severity			**Age Range**		
Injured and Fatal	7050	49	Young	3453	24
Non-injured	7337	51	Middle-aged-1	5035	35
Accident Cause			Middle-aged-2	4604	32
Following too close	1150	8	Elderly	719	5
Failure to yield	2446	17	Unknown	576	4
Improper turn	1583	11	**Education**		
Speeding	4748	33	Primary school	5323	37
Improper lane changing	1583	11	Middle school	1439	10
Drunk driving	1007	7	High school	4172	29
Other	1870	13	Higher education	1583	11
Collision Type			Unknown	1870	13
Rear	2014	14	*Vehicle Factor*		
Side collision	6474	45	**Age of Vehicle**		
Rsr	2014	14	3orLess	2877	20
Head on collision	1007	7	4 between 10	4604	32
Hitting pedestrian	1439	10	11orMore	6906	48
Boo	1439	10			

Table 2 - Summary of frequencies and distributions of key attributes (continued)

Attribute	F	%	Attribute	F	%
Nature of Accidents (continued)			*Road Factors*		
Vehicle Damage			**Road Section**		
Major damaged	5899	41	Divided	4172	29
Minor damaged	6618	46	Two-way	2590	18
None damaged	1870	13	One-way	432	3
External and Environmental Factors			Intersection	5323	37
Revised Lighting Condition			Roundabout	1151	8
Daylight	9639	67	Other intersections	719	5
Good street lighting	3309	23	**Signal type of Intersection**		
Bad street lighting	1439	10	Signalized	1151	8
Season of the Year			Unsignalized	5899	41
Winter (dec-feb)	2877	20	No-intersection	7337	51
Spring (mar-may)	3309	23			
Summer (june-aug)	3741	26			
Autumn (sep-nov)	4460	31			

F: Frequency, Rsr: Rollover/ skidding/run off road, Boo: Bumping into fixed objects and others

The proportional rate of the accidents occurred each year from 2015 to 2020 with respect to the total number of accidents for this period of time are obtained as 0.19/0.20 /0.19/0.17/0.14/0.11, respectively. Hangi Tablo?

The definition and variety of the values of eleven attributes are listed in Table 2. Some of the items like Day light condition, Unsignalized, 11orMore, Speeding, Sc (Side collision) have high support values. Although some other factors have been analysed, they have not been illustrated at this table due to their relatively low values being under the determined lowest support and confidence criteria selected for the analysis.

3.3. Data Mining

Data mining is exploration of hidden, attractive or worthful patterns in big datasets. The structure of data is important for an effective analysis. Furthermore, it is expected that the importance of collecting quality data will be better understood with the increasing popularity of data mining [28]. Raw data generally have missing and irrational items. To handle this, records should be processed into structured data. Figure 2 indicates one of the mostly used data mining processes proposed by Yu [18].

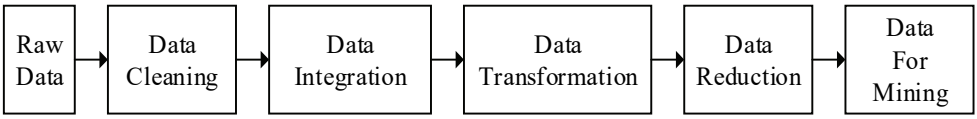

Figure 2 - The process of data mining [15]

The methods to be used for the analysis of the main data mining problems are Regression, Classification, Clustering, Association rule mining, and attribute selection [23]. In this study, Association Rule Mining method (ARM) was chosen for the data analysis of traffic accidents. This method is a combination of nonparametric technique and a machine learning method suggested by Agrawal and Srikant [29].

Within the scope of this research, the outcomes obtained through ARM are evaluated to reveal the interrelationships between the antecedents and consequents of traffic accidents.

The method, on the one hand, ensures to find most effective group of components causing accidents, on the other hand, effectively releases critical and concealed knowledge from the big dataset. The main decisive concepts of association rule mining method are support, confidence and lift. The rules with high support values point out a high frequency of mutual occurrence of the related attributes setting up those association rules. In the same manner, high confidence values state the likelihood of happening of a consequent incident when the antecedent element occurs in an accident. The support of the rule X →Y is the percentage of the records that include both X and Y within the whole dataset of $|D|$. The confidence of the rule X →Y is the ratio of total records of X and Y occurring together on the condition that X is already at hand to the total records of |X| in the whole dataset. The concept of "*lift*" has been developed to overcome some problematic analysis of the generation of useless association rules. This is mainly due to the fact that some specific circumstances may be contradictory to the nature of the mutual interaction of the attribute pairs although the confidence values may have the same figures for the related attribute pairs. If lift > 1, the association rules are identified as creditable rules. As the value of lift gets higher, the strength of the association rules regarding the related variables becomes more meaningful and worthy [18].

Lift in the concept of data mining analysis represents the amount of times a given rule comes to light to be true in practice over the number of times that related attribute or attributes of the rule appears in the whole dataset. Hence, to evaluate, for example, the frequency of the mutual coexistence of two attributes to the frequency of one of them in terms of all the elements in the dataset, lift values play an important role. As a result of this fact the association rules obtained through the data mining analysis were ordered according to the lift values revealing the set of the most common nature and the structure of the accidents.

The dataset is initially subdivided through a threshold value in a way that those attributes having equal or higher values than this value are considered to be investigated in detail further. In the literature, the predetermined critical support value was taken between 0.001 and 0.05 depending on the main dataset [20, 22, 24, 30-34]. Within the scope of this research, this value has been determined as 0.05 by trying some other higher and lower values, too. The higher values resulted in more but repeating rules. The less values, on the other hand,

produced inadequate rules causing the analysis having quite limited meaningful outcomes. Considering the structure and volume of the main dataset of this study, the threshold confidence and lift values are taken as 0.07 and 1.0 respectively.

Although the support and confidence values by themself may produce numerous association rules, it is required to eliminate them in order to obtain the most important and valuable ones. The concept of lift is used for this purpose. While support values express the importance degree of single or combined attributes within the whole dataset, confidence values state the intercorrelation of these attributes regardless of their influence within the available full dataset. On the other hand, lift values evaluate this correlation in terms of its weighted effect within the total dataset. The lift value with this regard plays more important role to determine the strength of an association rule compared to support and confidence values.

The followings express the way how support, confidence and lift values are calculated.

$$Support(X \rightarrow Y) = \frac{|X \cup Y|}{|D|} \qquad Confidence(X \rightarrow Y) = \frac{|X \cup Y|}{|X|} \qquad Lift = \frac{Conf(X \rightarrow Y)}{Sup(Y)}$$

4. RESULTS OF DATA ANALYSIS

Association rule mining is one of the most prevalent methods used to generate useful and unseen knowledge from a large dataset. This method was preferred to generate valuable and meaningful outcomes through the data analysis of this study.

Initially, as shown in Figure 3 the data were grouped into five main groups to acquire association rules. Four of them are considered as the groups with the attributes causing the accidents. The fifth one consists of the layers as shown in Table 2 to represent the nature and structure of the accidents.

The interrelationships between each attribute in the four groups and the fifth group are sought through the association rules to release the important factors causing different type of the collisions. In this way, the relationships between the attributes of driver factors, for example, and driver wounding severity or damage level of the vehicles can be obtained.

At this stage it is quite important to state that the dataset consists of accidents with at least one casualty. In the analysis, the driver related attributes whether they are antecedent or consequent are all only related to the drivers involved in the accidents. With that regard it can be concluded that if, for example, the non-injured-attribute related rules are the case, it means that at least one of the drivers is definitely injured or dead unless there are no injured passengers or pedestrians in the accidents. Even in the case of both drivers are non-injured, then there must be at least either one injured passenger or pedestrian.

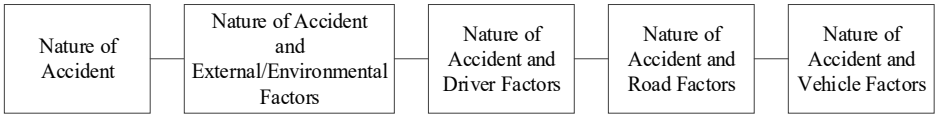

Figure 3 - Five main groups of attributes to obtain association rules

A priori algorithm was used to create the association rules with R Studio package program.

This algorithm iteratively scours the dataset to find frequent items playing important and comprehensive role in the occurrence of the accidents [35].

As shown in Figure 4, 13 association rules were obtained by employing only the attributes regarding the nature of the accident with threshold values of support and confidence equal to 0.05 and 0.70, respectively, and lift greater than 1.0.

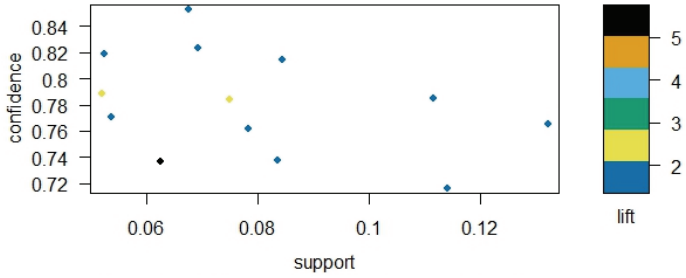

Figure 4 - Scatter plot for 13 association rules regarding the nature of the accident

The top 9 association rules with the highest lift values obtained from the subgroup data based on the nature of the accidents are illustrated in Table 3 in descending order.

In the same way, the top 10 association rules concerning accident and external-environmental features, the top 4 association rules regarding accident and driver features, the top 11 association rules with regard to accident and road features, the top 4 association rules relating accident and vehicle features are also shown in Table 4, 5, 6 and 7, respectively, in terms of the lift values they have.

Table 3 -Top 9 association rules having highest lift values related to nature of the accident

Rule	Antecedent	Consequent	Support	Confidence	Lift
1	Fty	Rear	0.06	0.74	5.38
2	Fty, Minor d.	Sc	0.07	0.78	1.76
3	Non-injured, Fty, Minor d.	Sc	0.05	0.79	1.76
4	Speeding, Rsr	Injured	0.07	0.85	1.74
5	Rsr, Major d.	Injured	0.07	0.82	1.68
6	Improper turn, Minor d.	Non-injured	0.05	0.82	1.62
7	Hitting pedestrian	Non-injured	0.08	0.81	1.61
8	Speeding, Major d.	Injured	0.11	0.72	1.46
9	Improper turn	Non-injured	0.08	0.74	1.46

Ftc: Following too close, Fty: Failure to yield, Minor d: Minor damaged, Rsr: Rollover/skidding/run off road, Major d.: Major damaged

The analysis of results from Table 3 can be summarized as; (1) The highest lift value, 5.38, is related with the Following too close (Ftc) as an antecedent and Rear as a consequent reflecting the relatively strong correlation between Rear collisions and Following too close driving faults. In the same way, high lift value indicates the relatively high weigh of the connection between the Ftc (Following too close) correlated Rear collision to the general weigh of the rear collision accidents in the whole dataset. As can be seen from the support value between these two attributes, 74 rear collision accidents out of 100 rear collision type of accidents are related to following the car in front too closely. (2) Non-injured, Fty (Failure to yield) and Minor damage accidents are mostly related with Sc (Side collision) type of collisions; (3) Speeding and Rsr (Rollover/skidding/run off road) accidents often lead to driver injury. Although there are some other rules with lift values over 1, they have not been included at this table simply because they are the elements of the combinations of the sets constituted by the attributes of the list at the table above. It is worthwhile to mention that the same criterion also applied for all the lists given below.

As shown in Figure 5, there were 72 pieces of association rules that were obtained from the accident and external and environmental factors with the same threshold values as the previous scatter plot has (Figure 4).

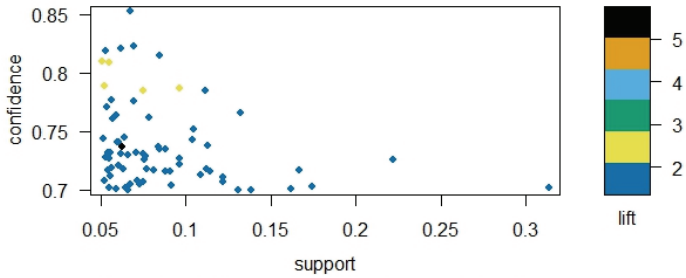

Figure 5 - Scatter plot for 72 association rules between the accident and external and environmental features

Out of these 72 rules, the following ones are the most remarkable ones to mention considering mutual relationship of the attributes with respect to support, confidence and lift values.

As can be seen from Table 4 the highest lift value, 1.81, is related to the interrelation between daylight, Fty (Failure to yield) and Minor damaged attributes leading to Sc (Side collision). The support and confidence values are 0.05 and 0.81, respectively. Another rule reveals the fact that accidents involving daylight and hitting pedestrian attributes result in mostly non-driver injury accidents. On the other hand, daylight and Rsr (Rollover/skidding/run off road) inclusive accidents often lead to driver injuries. There is a strong interdependence between Daylight, Fty (Failure to yield), Minor damaged vehicle and side collision accidents.

Figure 6 demonstrates the 18 pieces of association rules with regard to accidents related to driver factors.

Table 4 - Strong association rules between accident and external-environmental-related attributes

Rule	Antecedent	Consequent	Support	Confidence	Lift
1	Daylight, Fty, Minor d.	Sc	0.05	0.81	1.81
2	Daylight, Fty	Sc	0.10	0.79	1.76
3	Daylight, Hitting pedestrian	Non-injured	0.06	0.82	1.62
4	Daylight, Rsr	Injured	0.07	0.78	1.58
5	Daylight, Speeding, Major d.	Injured	0.08	0.72	1.46
6	Summer, Non-injured, Sc	Daylight	0.06	0.76	1.15
7	Spring, Non-injured	Daylight	0.09	0.73	1.12
8	Summer, Minor d.	Daylight	0.10	0.74	1.11
9	Spring, Speeding	Daylight	0.05	0.73	1.11
10	Summer, Speeding	Daylight	0.07	0.73	1.10

Fty: Failure to yield, Minor d: Minor damaged, Rsr: Rollover/skidding/run off road, Major d.: Major damaged, Sc: Side collision.

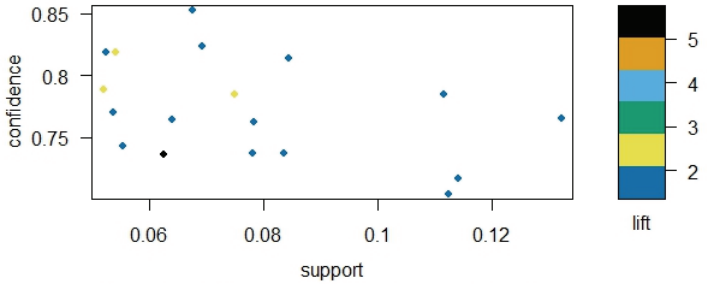

Figure 6 - Scatter plot for 18 association rules related to driver factors

Four rules reflecting important noteworthy relationship based on the lift values have been selected out of these 18 rules and represented in Table 5.

Table 5 - Strong association rules for accident and driver-related attributes

Rule	Antecedent	Consequent	Support	Confidence	Lift
1	Primary School, Fty	Sc	0.05	0.82	1.83
2	Middle-aged-1, Sc, Minor d.	Non-injured	0.06	0.76	1.51
3	Young, Major d.	Injured	0.08	0.74	1.50
4	Middle-aged-2, Sc, Minor d.	Non-injured	0.05	0.74	1.47

Fty: Failure to yield, Minor d: Minor damaged, Major d.: Major damaged, Sc: Side collision.

Regarding the attributes of driver factors causing the accidents, it is worth mentioning that people are less obedient to give way to other vehicles as the education level gets relatively low.

As for the young drivers, it should be noted that they get involved with major damage and injury accidents pointing out the importance of their education and enforcement regarding the way of driving vehicles and obeying the rules. Although middle-aged drivers also involve with side collision types of collisions, the severity of them are relatively low causing generally non-injury accidents.

As shown in Figure 7, there are 128 pieces of association rules obtained from the attributes of road factors triggering the accidents investigated.

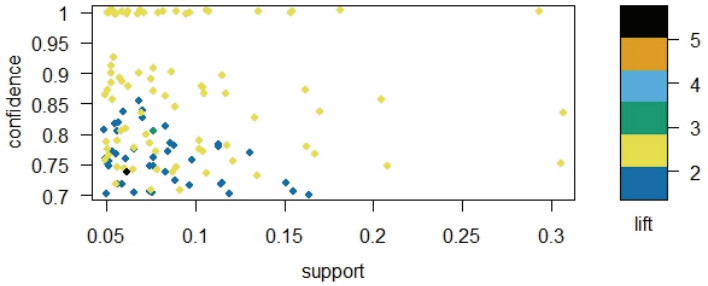

Figure 7 - Scatter plot for 128 association rules regarding road factors

Table 6 - Strong association rules between road factors and nature of the accidents

Rule	Antecedent	Consequent	Sup.	Conf.	Lift
1	Intersection, Fty, Minor d.	Unsignalized	0.05	0.92	2.27
2	Intersection, Fty, Sc	Unsignalized	0.08	0.91	2.24
3	Intersection, Speeding, Sc	Unsignalized	0.07	0.9	2.21
4	Intersection, Non-injured, Sc, Minor d.	Unsignalized	0.07	0.89	2.19
5	Intersection, Injured, Speeding	Unsignalized	0.05	0.88	2.17
6	Unsignalized, Injured	Intersection	0.13	0.73	1.99
7	Divided, Boo	No-intersection	0.05	1	1.96
8	Divided, Ilc	No-intersection	0.05	1	1.96
9	Intersection, Unsignalized, Fty	Sc	0.08	0.87	1.95
10	Intersection, Severe	Unsignalized	0.11	0.77	1.90
11	Roundabout	Sc	0.06	0.72	1.61

Sup: Support, Conf: Confidence, Fty: Failure to yield, Minor d: Minor damaged, Sc: Side collision, Rsr: Rollover/skidding/run off road, Major d.: Major damaged, Boo: Bumping into fixed objects and others, Ilc: Improper lane changing.

Among these numerous rules, the selected ones by taking into consideration the criteria mentioned above have been illustrated in Table 6.

Through the analysis of the results from Table 6, it can be seen that the rule with the highest lift value, 2.27, reflects the strong interaction between Intersection, Fty and Minor damaged with Unsignalized intersections. Failure to give way at intersections leads to minor damaged accidents at unsignalized junctions. The support value in Table 6 indicates that 8 percent of all the accidents are related to side collision accidents occurred on unsignalized intersections due to failure to yield behaviour of the drivers. When the roads are divided, the accidents are generally related to bumping and caused by improper lane changing at any section of the roadway apart from intersections. The location of these type of accidents is denoted as No-intersection. This class term may, obviously, also be used for any accidents occurred at the locations apart from intersections. Rules also state that the accidents at roundabouts are mostly side collision type.

Figure 8 illustrates 17 pieces of association rules for the accidents obtained from vehicle factors.

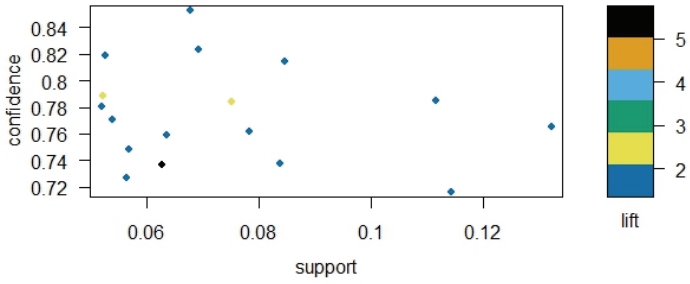

Figure 8 - Scatter plot for 17 association rules regarding the vehicle features and the accidents

Table 7 shows the age of vehicle and the resulted type of the collisions.

Table 7 - Strong association rules between accident and vehicle-related attributes

Rule	Antecedent	Consequent	Support	Confidence	Lift
1	11orMore, Fty	Sc	0.06	0.76	1.7
2	11orMore, Rsr	Injured	0.05	0.78	1.59
3	11orMore, Speeding, Major d.	Injured	0.05	0.73	1.48
4	4-10, Sc, Minor d.	Non-injured	0.06	0.75	1.48

11orMore, 4-10: Age of vehicle, Fty: Failure to yield, Rsr: Rollover/skidding/run off road, Major d.: Major damaged, Sc: Side collision, Minor d: Minor damaged.

As can be seen through the rules from the above table, older vehicles may involve comparatively severe accidents than the newer vehicles. Rule 1 illustrates that the driving attitude of the drivers of the old vehicles seems to be more reckless. This may be related to the perception of the drivers of the old vehicles when they get involved with an accident as the cost of the vehicle damage will be relatively low. On the other hand, with high speed, accidents involving older vehicles result in severe accidents with injuries. New model vehicles, however, get involved with minor accidents resulting in non-injured drivers.

5. CONCLUSIONS

Traffic accidents are quite complex phenomenon with combination of numerous attributes generally recorded on the police reports. The essence of this study is to investigate the mutual effects of the important factors/attributes causing traffic accidents by using association rule mining. After the data preparation process with respect to the attributes either not having proper or balanced contents along with combination of some of them representing the same coverage, the dataset finally had 11 attributes grouped into 5 main factors. These factors are related at least one of the scopes of the nature of the accidents, external and environmental factors, driver related factors, road factors and vehicle conditions. In this study, a priori algorithm was rigorously applied to identify the most frequently appearing attributes setting up the association rules in the dataset affecting traffic accidents occurred in city of Sakarya.

Some of the essential outcomes of this study can be summarized as below:

- Some of the noteworthy attributes to set up the association rules are found to be related to the type of collision, lighting condition, and violations by drivers.
- There exists a significant correlation between speeding, damage of vehicle as Major and severity level of driver`s injury as Injured. In accordance with this finding, Albuquerque et al. also stated that speeding is one of the most important parameters of injury severity in fixed object and run-off-road accidents [36].
- Rollover/skidding and run off road (Rsr) accidents are intercorrelated with damage of vehicle as Major and severity of driver injury as Injured. Karabulut et al. found that accidents involving motorcycles, fixed objects, and run-off-road accidents were the main factors significantly associated with injury and fatality of the drivers [37].
- It has been found that there is a strong correlation between close Following too close and Rear-end collisions. Yu et al. also found the same correlation between these classes [18].
- Hitting pedestrian collisions resulted in Non-injured drivers. In the same manner, Karabulut et al., obtained that drivers are less severely injured in pedestrian accidents [37].
- Most of the accidents occurred when the attributes are in conjunction with Daylight, type of collision Fty, damage of vehicle Minor and Side collision are in effect together. This is mainly because of the inclination of the drivers to take risky manoeuvres as they have relaxed in terms of spiritual and mental conditions for daytime driving [34].

- The evaluation of the obtained rules revealed the fact that Fatal and Injury accidents occur mostly in Spring and Summer months. In addition, the rules clearly made it known that drivers tend to speed during daylight hours in Spring and Summer periods. In harmony with our findings, Celik et al., states that fatal injuries are two times more likely to happen in summer compared to the 'no injury' severity level. In addition, they express that the probability of non-fatal injuries increases by 6.3% in the summertime [38].
- An interesting outcome acquired through the analysis of this research is that the faulty drivers responsible for the accident generally cause the other vehicles` drivers to have more serious Fatal or Injury effect than themselves. This may be due to the fact that as those drivers are aware of the imminent accidents, they are about to cause, they adjust their maneuvers to get the least negative effect of the accident just about to happen. As stated earlier, the analysis process carried out in this research is based upon the data related only to the faulty drivers not the other drivers. The combination of these two facts resulted in this outcome.
- Another rule was revealed in the results that drivers with prominently Primary-educated level were involved in Fatal and Injury accidents as these drivers tend to violate yield rule and were involved in Side collision accidents. Celik et al. also share the same conclusion by remarking that primary-educated drivers increase the probability of fatal injuries [38].
- Eight percent of all accidents are related to Side collision accidents occurring at Unsignalized intersections due to the failure to yield by drivers. Yu et al. also verify the fact that 15% of accidents are resulted from failing to yield at intersections [18].
- Drivers generally involved in Side collisions are from the group of people aged between 26 and 40 (middle-aged-1 group). This may mainly be attributed to the risk-taking behaviour of this group of drivers especially at intersections.
- Accidents involving young drivers between 18-25 years old were resulted in injuries and Major vehicle damage. This is mainly related to the fact that these drivers tend to have relatively speedy drive. Hence, this finding verifies the strong connection between speed and severity type of accidents resulting in severely injured drivers as stated above. Yu et al. state that the drivers aged between 16-25 are more likely to violate driving rules in comparison with other drivers, hence involving more numerous and severe accidents [18]. The results obtained by Celik et al. highlighted the need for education campaigns to address all road users, especially older drivers by taking successful implications as a role model [38]. On the other hand, the finding of this research emphasizes the fact that the campaigns or enforcements are needed more for young drivers.
- As far as the location of the accidents are concerned, it has been obtained that the overwhelming majority of the accidents occurred at Unsignalized intersections including roundabouts. No rule was acquired with regard to Signalized intersection in terms of Fatal or injury accidents. This supports the fact that, Signalised intersections decrease the likelihood of Fatal and injury accidents. Celik et al. also stated that traffic signals at accident locations reduce the probability of fatal injuries by 41.8% [38].
- Mostly, accidents involving older vehicles with high-speed result in severe accidents with injuries. In contrast to the results of this study, the outcomes of the research carried

out by Bédard et al. point out that the "vehicle age" variable was statistically insignificant by investigating the relationship between driver, accident and vehicle characteristics in fatal accidents [39]. This may mainly stem from the fact that they only investigated the fatal accidents.

The most crucial factor of the accidents with regard to side collision types is related to the failure to give way to the vehicles having right of way. This behaviour may be considered to be related to two different attitudes. First one is due to aggressive driving and disobeying the traffic rules. Second one, on the other hand, is associated with lack of education and awareness. While increasing traffic enforcement and fines might have positive effect on solving these problems, education and awareness campaigns for the middle age group drivers might play an important role to reduce the violations of the rules [40,41].

Traffic sign/signal violation is one of the main factors associated with injury and fatality of the drivers [37]. Furthermore, standardization of warning and informative traffic signs is essential to make sure that they are understood by the drivers easily and correctly [42]. In Sakarya, as it is in Turkey, there are different applications of yield signs and majority of them don't contain written notification of "yield" or "give way". The lack of this written information related to yield signs reduces the drivers` awareness. Changing the standardization with added notification of written warning might reduce the violation of give way behaviour of the drivers [43].

This study does not provide any information in connection with level of injury severity along with property damage-only accidents. The outcomes provide the general structure and nature of the accidents` causes in terms of the mutual correlation among the effective attributes of the accidents recorded in Sakarya, Turkey. Hence, the results provide the authorized institutions with the appropriate precautions to be taken to reduce both the number and severity of the traffic accidents. In future studies, predictions regarding the interaction of the attributes will be studied to evaluate the possible accidents and their nature by using machine learning techniques such as decision trees and deep learning methods.

Acknowledgments

The authors are grateful to Republic of Turkey General Directorate of Security for sharing the traffic accident data. The authors would like to thank the reviewers for their invaluable suggestions leading to improve the manuscript.

References

[1] World Health Organization (WHO) 2022. https://www.who.int/news-room/fact-sheets/detail/road-traffic-injuries (accessed August 15, 2022).

[2] Global burden of 369 diseases and injuries in 204 countries and territories, 1990–2019: a systematic analysis for the Global Burden of Disease Study 2019. 2020.

[3] Injuries in the European Union 2009-2018. EuroSafe; 2021.

[4] Ministry of the Interior. Turkey Road Traffic Safety Strategy Report (2021-2030). 2021.

[5] The World Bank. World Bank 2022. https://data.worldbank.org/country/turkiye (accessed August 25, 2022).

[6] International Transport Forum. Road Safety Annual Report. IRTAD-OECD; 2020.

[7] Turkey Traffic Accident Report-2021. Turkey General Directorate of Highways. 2022.

[8] Kadilar GO. Effect of driver, roadway, collision, and vehicle characteristics on crash severity: a conditional logistic regression approach. Int J Inj Contr Saf Promot 2016;23:135–44. https://doi.org/10.1080/17457300.2014.942323.

[9] Zhang G, Yau KKW, Chen G. Risk factors associated with traffic violations and accident severity in China. Accid Anal Prev 2013;59:18–25. https://doi.org/10.1016/j.aap.2013.05.004.

[10] Ma Z, Lu X, Chien SI-J, Hu D. Investigating factors influencing pedestrian injury severity at intersections. Traffic Inj Prev 2018;19:159–64. https://doi.org/10.1080/15389588.2017.1354371.

[11] Batouli G, Guo M, Janson B, Marshall W. Analysis of pedestrian-vehicle crash injury severity factors in Colorado 2006–2016. Accid Anal Prev 2020;148:105782. https://doi.org/10.1016/j.aap.2020.105782.

[12] Alver Y, Demirel MC, Mutlu MM. Interaction between socio-demographic characteristics: Traffic rule violations and traffic crash history for young drivers. Accid Anal Prev 2014;72:95–104. https://doi.org/10.1016/j.aap.2014.06.015.

[13] Katanalp BY, Eren E. The novel approaches to classify cyclist accident injury-severity: Hybrid fuzzy decision mechanisms. Accid Anal Prev 2020;144:105590. https://doi.org/10.1016/j.aap.2020.105590.

[14] Adanu EK, Lidbe A, Tedla E, Jones S. Factors associated with driver injury severity of lane changing crashes involving younger and older drivers. Accid Anal Prev 2021;149:105867. https://doi.org/10.1016/j.aap.2020.105867.

[15] Chiou Y-C, Fu C, Ke C-Y. Modelling two-vehicle crash severity by generalized estimating equations. Accid Anal Prev 2020;148:105841. https://doi.org/10.1016/j.aap.2020.105841.

[16] AlKheder S, AlRukaibi F, Aiash A. Risk analysis of traffic accidents' severities: An application of three data mining models. ISA Trans 2020;106:213–20. https://doi.org/10.1016/j.isatra.2020.06.018.

[17] Cai Q. Cause Analysis of Traffic Accidents on Urban Roads Based on an Improved Association Rule Mining Algorithm. IEEE Access 2020;8:75607–15. https://doi.org/10.1109/ACCESS.2020.2988288.

[18] Yu S, Jia Y, Sun D. Identifying Factors that Influence the Patterns of Road Crashes Using Association Rules: A case Study from Wisconsin, United States. Sustainability 2019;11:1925. https://doi.org/10.3390/su11071925.

[19] Das S, Tamakloe R, Zubaidi H, Obaid I, Alnedawi A. Fatal pedestrian crashes at intersections: Trend mining using association rules. Accid Anal Prev 2021;160:106306. https://doi.org/10.1016/j.aap.2021.106306.

[20] Kong X, Das S, Jha K, Zhang Y. Understanding speeding behavior from naturalistic driving data: Applying classification based association rule mining. Accid Anal Prev 2020;144:105620. https://doi.org/10.1016/j.aap.2020.105620.

[21] Zhu S. Investigation of vehicle-bicycle hit-and-run crashes. Traffic Inj Prev 2020;21:506–11. https://doi.org/10.1080/15389588.2020.1805444.

[22] Hong J, Tamakloe R, Park D. Discovering Insightful Rules among Truck Crash Characteristics using Apriori Algorithm. J Adv Transp 2020;2020:1–16. https://doi.org/10.1155/2020/4323816.

[23] Das S, Dutta A, Sun X. Patterns of rainy weather crashes: Applying rules mining. J Transp Saf Secur 2020;12:1083–105. https://doi.org/10.1080/19439962.2019.1572681.

[24] Xu C, Bao J, Wang C, Liu P. Association rule analysis of factors contributing to extraordinarily severe traffic crashes in China. J Safety Res 2018;67:65–75. https://doi.org/10.1016/j.jsr.2018.09.013.

[25] Turkish Statistical Institute 2021. https://cip.tuik.gov.tr/# (accessed December 16, 2022).

[26] Sakarya City Guide. Sakarya Metropolitan Municipality. https://www.sakarya.bel.tr/ (accessed March 10, 2023).

[27] Turkey General Directorate of Highways. http://yol.kgm.gov.tr/KazaKaraNoktaWeb/ (accessed March 1, 2022).

[28] Hand DJ. Principles of Data Mining 2007:2.

[29] Srikant R, Agrawal R. Mining Generalized Association Rules. 1995.

[30] Geurts K, Thomas I, Wets G. Understanding spatial concentrations of road accidents using frequent item sets. Accident Analysis and Prevention 2005; 37:787–99. https://doi.org/10.1016/j.aap.2005.03.023.

[31] Montella A. Identifying crash contributory factors at urban roundabouts and using association rules to explore their relationships to different crash types. Accid Anal Prev 2011;43:1451–63. https://doi.org/10.1016/j.aap.2011.02.023.

[32] Montella A, Aria M, D'Ambrosio A, Mauriello F. Analysis of powered two-wheeler crashes in Italy by classification trees and rules discovery. Accid Anal Prev 2012;49:58–72. https://doi.org/10.1016/j.aap.2011.04.025.

[33] Pande A, Abdel-Aty M. Market basket analysis of crash data from large jurisdictions and its potential as a decision support tool. Saf Sci 2009;47:145–54. https://doi.org/10.1016/j.ssci.2007.12.001.

[34] Das S, Dutta A, Jalayer M, Bibeka A, Wu L. Factors influencing the patterns of wrong-way driving crashes on freeway exit ramps and median crossovers: Exploration using 'Eclat' association rules to promote safety. Int J Transp Sci Technol 2018;7:114–23. https://doi.org/10.1016/j.ijtst.2018.02.001.

[35] Agrawal R, Imieliński T, Swami A. Mining association rules between sets of items in large databases. ACM SIGMOD Rec 1993;22:207–16. https://doi.org/10.1145/170036.170072.

[36] Albuquerque FDB de, Awadalla DM. Roadside Fixed-Object Collisions, Barrier Performance, and Fatal Injuries in Single-Vehicle, Run-Off-Road Crashes. Safety 2020;6:27. https://doi.org/10.3390/safety6020027.

[37] Karabulut NC, Ozen M. Exploring Driver Injury Severity Using Latent Class Ordered Probit Model: A Case Study of Turkey. KSCE J Civ Eng 2023;27:1312–22. https://doi.org/10.1007/s12205-023-0473-6.

[38] Celik AK, Oktay E. A multinomial logit analysis of risk factors influencing road traffic injury severities in the Erzurum and Kars Provinces of Turkey. Accid Anal Prev 2014;72:66–77. https://doi.org/10.1016/j.aap.2014.06.010.

[39] Bédard M, Guyatt GH, Stones MJ, Hirdes JP. The independent contribution of driver, crash, and vehicle characteristics to driver fatalities. Accid Anal Prev 2002;34:717–27. https://doi.org/10.1016/S0001-4575(01)00072-0.

[40] Factor R. The effect of traffic tickets on road traffic crashes. Accid Anal Prev 2014;64:86–91. https://doi.org/10.1016/j.aap.2013.11.010.

[41] Paleti R, Eluru N, Bhat CR. Examining the influence of aggressive driving behavior on driver injury severity in traffic crashes. Accid Anal Prev 2010;42:1839–54. https://doi.org/10.1016/j.aap.2010.05.005.

[42] Manual on Uniform Traffic Control Devices. MUTCD.pdf 2009.

[43] Cakici Z, Murat YS. An Investigation on the Awareness of Traffic Signs: Denizli Sample. Bitlis Eren Üniversitesi Fen Bilim Derg 2017;6:21–21. https://doi.org/10.17798/bitlisfen.305485.

Turkish Journal of Civil Engineering, 2023 81-106, Paper 747, ***Research Article***

Operational Barriers against the Use of Smart Contracts in Construction Projects

Handan KUNKCU[1]
Kerim KOC[2]
Asli Pelin GURGUN[3]
Houljakbe Houlteurbe DAGOU[4]

ABSTRACT

As an emerging but embryonic way of contract administration, smart contracts can play a prominent role in managing construction projects in an effective manner. However, there are still some barriers preventing the implementation of them in the life cycles of construction projects. This study investigates operational barriers against the adoption of smart contracts in construction projects and explores the challenges in this process. Operational barriers against smart contract implementation are identified through a comprehensive literature review and a focus group discussion is performed to refine the identified barriers. These barriers are evaluated through fuzzy analytical hierarchy process analysis. Finally, a framework is proposed for the adoption of smart contracts effectively in construction projects. 20 operational barriers were attained based on four main barrier categories: technical, financial, security/technological, and time. The results show that financial and technical aspects establish the most significant categories hindering the adoption of smart contracts, while expensive and clunky drafting and registration process, and cost of upskilling are the most significant barriers. Overall, the proposed framework might be useful for practitioners and project managers, who decide to use smart contracts in managing construction projects. The motive behind understanding critical operational barriers is to assist construction practitioners in automating contract execution processes. This study provides a basis for recommending the necessary strategies for the use of smart contracts in the industry to researchers in the construction management field.

Note:
- This paper was received on November 8, 2022 and accepted for publication by the Editorial Board on June 23, 2023.
- Discussions on this paper will be accepted by November 30, 2023.
- https://doi.org/10.18400/tjce.1322972

1 Eskisehir Technical University, Department of Civil Engineering, Eskisehir, Türkiye
handan424@eskisehir.edu.tr - https://orcid.org/0000-0001-9839-640X

2 Yildiz Technical University, Department of Civil Engineering, Istanbul, Türkiye
kerimkoc@yildiz.edu.tr - https://orcid.org/0000-0002-6865-804X

3 Yildiz Technical University, Department of Civil Engineering, Istanbul, Türkiye
apelin@yildiz.edu.tr - https://orcid.org/0000-0002-0026-4685

4 Yildiz Technical University, Department of Civil Engineering, Istanbul, Türkiye
houljakbe.dagou@std.yildiz.edu.tr - https://orcid.org/0000-0003-1249-2615

Keywords: Blockchain, operational risks, contract administration, construction management, Fuzzy AHP, Construction 4.0.

1. INTRODUCTION

Many construction projects are complicated, large-scale, long-lasting, and characterized by a higher level of uncertainties. Therefore, strategic decisions require the involvement of project stakeholders to manage construction projects effectively [1]–[3]. These features make it more difficult to achieve project objectives in the context of planning, management, and contract administration. Therefore, project managers and construction professionals are in search of robust project management tools and managerial support techniques [4]. Integrating various methods and technologies to have profitable outcomes is a must in construction projects [5], performance of which rely on different dimensions of project management [6]. In this vein, management of construction projects has gradually encompassed a broad range of elements related to sustainable project governance [1], with contract management playing a central role [7]. Forestalling all adversities and uncertainties and including them in contract management with the participation of project stakeholders become a difficult task [8], threatening the recovery from or adjustment to setbacks or changes in construction projects. These unprecedented drawbacks may lead to productivity loss, payment problems, delays, cost overruns, and inevitably project disputes [9].

Mutikanga et al. [10] pointed out that many contractual issues exist in engineering, procurement, and construction projects, such as insufficient project scope and goals, and poor compliance with contractual obligations by project parties. McKinsey Global Institute [11] highlights that misalignment of the structure of contract documents is one of the major causes of low productivity in construction projects. A recent report by Arcadis [3] underlined that poorly drafted documents, errors and/or omissions in contracts, and liabilities misunderstood by clients, contractors or sub-contractors were the top causes of disputes in construction projects. Due to the inherent incompleteness of construction contracts [12], organizations that use traditional contracts may face many setbacks hindering effective management of iron triangle (i.e., time, cost, and quality) [13]. To deal with these challenges, smart contracts are one of the technological tools that are developed through distributed ledger technology and offer great potential for many industries including the construction industry [14]. Smart contracts leading to innovative solutions have drawn considerable attention in various industries, including education, energy, healthcare, banking, and financial services, public management, construction, supply chain, and entertainment [15], [16]. Compared with other industries, the development and implementation of smart contracts in the construction industry can be relatively slow and challenging due to their complex, unique, and dynamic characteristics.

The dominance of digital age on global commerce portends that smart contracts could have a prominent place in the future business environment [17] since the underlying blockchain technology is practical in many ways and able to provide a mechanism that is more secure than traditional contracts [18]. Many aspects of the requirements, terms, and clauses of a contract can be managed technologically by smart contracts [19]. This would not only support the coordination of several contract administration processes but also organize the payments through improved payment pipeline in construction projects, where late payments are

inherent culture [20]. By considering the traceability, security, and immutability of the blockchain technology, blockchain-enabled smart contracts also contribute to elevating the confidence level of the stakeholders [21]. On the other hand, smart contracts can be used as an effective tool in resolving or reducing conflicts/disputes among parties included [22]. Improved transparency through transaction credibility, efficiency, intelligence, and automation can also be an additional advantage in several processes. However, some issues such as the initial investment cost or the inefficiency of the consensus mechanism can still be considered as major inhibitors against their application [23]. Similarly, lack of qualified human resource or capabilities of organizations regarding smart contracts may also pose an obstacle for stakeholders desiring to rely on smart contracts.

The efficiency of smart contracts and their ability to overcome a number of current challenges in traditional contracts put them in a place that could take over traditional contracts [24]. However, many research in the literature highlighted the significant operational challenges that might limit the adoption of smart contracts in construction projects [14], [22]. This study aims to have a deeper understanding on smart contracts by evaluating operational barriers and developing a conceptual model for construction companies to adopt smart contracts with the guidance of the findings. A multi-step framework has been followed to achieve the study objective. First, a comprehensive literature review and focus group discussion (FGD) were performed to identify challenges against smart contract adoption. Then, fuzzy analytical hierarchy process (AHP) was used to evaluate identified barriers. Finally, a conceptual smart contract adoption framework was developed based on the analysis results. The findings of the analysis steps make several contributions to the current literature on smart contract, contract administration, and project management by proposing a way to operate smart contracts in construction projects. With the study findings, construction projects can be better managed with smart contracts by eliminating risks of adopting them since contract life-cycle management requires more robust and automated processes in today's competitive environment. Besides, construction managers can use the results of this study in terms of minimizing inefficient paper-based procedures, dealing with conflicts through analytical methods, preventing unexpected cost increases, and preserving privacy of contracts. Overall, the outcomes of this study are expected to raise awareness among construction industry practitioners and develop improved risk mitigation strategies based on the contract life cycle of construction projects.

2. BACKGROUND

2.1. Definition and Role of Smart Contracts

In 1994, an American computer scientist, lawyer, and cryptographer, Nick Szabo [25], coined the term smart contract. Szabo [26] defined smart contract as a computer-based transition protocol executing the clauses of a contract. Fundamentally, smart contracts are designed to meet or fulfil common contractual requirements and abate accidental or malicious peculiarities. These contracts are primarily characterized by their digital forms and are embedded in hardware and software as code [27]. Rule-based operations and the underlying blockchain technology enable the release of payments securely, fulfil the contract terms visibly, and thereby reduce contractual conflicts. Smart contracts are expected to have a vast effect on contract law and the economy with more efficiency, traceability, and

confidentiality, which are little explored [28]. Containing electronic clauses and triggering processes according to the terms of the contract, a smart contract is a self-executing contract and works depending upon automated conditional performance management. Smart contracts work in a way to allow the triggering of an obligation, once the task associated with the obligation is fulfilled [29]. For example, the ownership of real assets can be digitally controlled with smart contracts based on the terms of the agreement and these contracts provide stakeholders with clear information management systems.

Smart contracts are written as codes in both hardware and software [30], and accessed through an agreed data source unlike traditional contracts that are written in legalese language [31]. The blockchain technology keeps the identical and dynamic copies of the contract and included parties can check the amendments according to a consensus algorithm. Therefore, comparison software is needed for the verification of documents to avoid or prevent unapproved contract term changes made by other parties in blockchain-enabled smart contracts [32]. The status of the contracts can be viewed optionally and dynamically, and monitored by the project stakeholders, which allows them to adjust to the changing conditions. Blockchain technology is the stepping stone of smart contracts. Therefore, a secure blockchain and coding are essential. All these requirements are usually considered as barriers for construction companies, limiting the investments in blockchain technology and adoption of smart contracts in their business operations.

2.2. Studies about Smart Contracts in the Construction Industry

Smart contracts can be regarded as a prominent tool of self-executing digital transformation initiatives by coding contract terms and conditions that reduce cost and time overruns, while addressing contractual risks and disputes during contract management life-cycle [22]. Smart contracts can add significant value to the construction projects with their ability to decentralize the execution of contract requirements [33]. Existing literature mostly highlights their impacts on the security, traceability, and automation in the process of construction projects. For instance, Bolhassan et al. [22] investigated various benefits and implementation challenges in the Malaysian construction industry. The study suggested the use of smart contracts in short-term projects. Chong and Diamantopoulos [34] performed a case study to automate the payment process for façade panel supply by incorporating several advanced technologies such as smart contracts, smart sensors, BIM, and blockchain. Mason and Escott [35] investigated the stakeholder perceptions of smart contracts in the construction industry and highlighted their fear about the full automation in contract administration. Similarly, Nanayakkara et al. [36] conducted a workshop with six groups to exhibit stakeholder perceptions of smart contracts for construction supply chains and found that stakeholders mostly addressed efficiency, trust, fairness, security, transparency, accountability, compliance, and standardization features of smart contract-based solutions. Li and Kassem [37] employed a systematic review analysis and stated that smart contracts as supplementary technologies can be used with other technological systems, which were still immature to be used with smart contracts. Li et al. [38] developed a model that integrated smart contracts with BIM, IoT, and DLT to automate installation activities in construction and addressed that the proposed approach could minimize several challenges such as late payments, lack of trust, and inadequate collaboration.

In another study, Rathnayake et al. [39] conducted a systematic literature review and highlighted that past studies usually focused on drivers, barriers, implications, and benefits affecting the adoption smart contracts in the construction industry. They found that lack of security, lack of observability, incompatibility, inactive government collaboration and storage capacity restrictions were the most frequently identified barriers in smart contract implementation. Similarly, Shang et al. [40] concentrated on institutional factors influencing the adoption of smart contracts in the Singapore construction industry. The researchers also underlined the barriers of poor knowledge of smart contracts, lack of industry-specific standards, and lack of observability. Ameyaw et al. [41], using statistical analyses, investigated the drivers for blockchain-based smart contracts applications in construction projects. Considering the opinions of experts in the field, the researchers specified trialability of smart contract (such as ability to try, and a trial period before adoption), transparency in project delivery, facilitation in payments, and security of payment as the top critical factors. Gurgun and Koc [42] presented a multi-criteria approach to identify and evaluate administrative risks of the smart contracts based on contractual, cultural, managerial, planning, and relational main risk groups. The researchers emphasized the necessity of handling the managerial risks diligently to increase the adoption of smart contracts in the projects.

Various studies also proposed solutions using smart contracts regarding payment issues, which is one of the challenges inherent in construction projects. For instance, Hamledari and Fischer [33] examined their effects on enhancing visibility of payments in the supply chain and stated that although smart contracts cannot fully ensure information latency yet, they are effective instruments for information completeness. Ahmadisheykhsarmast and Sonmez [43] presented a smart contract-based payment security system to minimize payment problems (i.e., non-payment and/or late payment) by using the schedule and cost data. Similarly, Luo et al. [44] proposed a smart contract-based interim payment management framework to automate the process in a blockchain environment. The comprehensive literature review illustrates that operational barriers against the adoption of smart contracts have not been researched systematically, which formed the research motivation of this study.

3. METHODOLOGY

The steps of the study are illustrated in Figure 1 and each step is explained in the following sub-sections.

3.1. Literature Review

In the first step of the study, a comprehensive literature survey was performed to identify initial list of operational barriers against smart contract implementation in construction projects. For this purpose, search engine Scopus was used to gather relevant research articles since it is one of the widely used search tools in nearly any domain and shows an effective performance compared to other search engines [45]–[47]. As a preliminary search step, two main search strings were considered as (i) “Smart contract” AND (ii) “Risk OR “Barrier” OR “Challenge”. This search retrieved 809 publications, which was reduced to 336 articles by limiting the results with only journal papers. Then, another search string i.e.,

"Construction" was inserted, and the number of studies was reduced to 24 that are directly related to the construction industry. Hence, 24 articles were investigated in detail, while the remaining 312 articles were examined on an abstract level. The reference list of 24 articles was also explored as part of snow-balling approach in order not to exclude any of the relevant past research. Accordingly, the initial list of operational barriers was ensured mainly based on the studies of Mason [48], Mason and Escott [35], Li et al. [14], Perera et al. [49], and Gurgun and Koc [42].

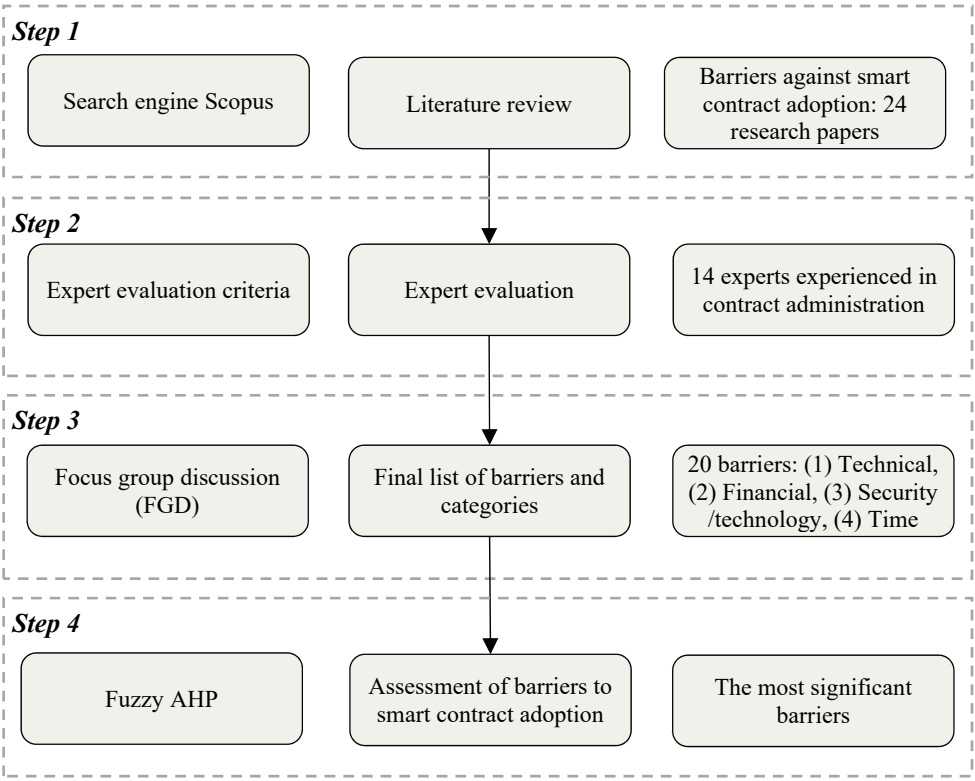

Figure 1 - Research flow.

3.2. Expert Evaluation

This study adopted two consecutive steps to analyze the identified operational barriers. In the first step, a focus group discussion (FGD) was employed with industry professionals to finalize the decision framework. It was organized before the data analysis since including expert opinions to construct decision framework is an effective approach [50], [51]. This step was followed by a fuzzy AHP analysis to prioritize the operational barriers. Both steps (FGD and fuzzy AHP) are based on expert knowledge, thus evaluating the eligibility of experts becomes a critical concern of this study. First, the required sample size for FGD and fuzzy AHP was identified through a literature survey. Accordingly, 5 and 9 experts were

determined to be adequate sample size for FGD [47], [52], [53] and fuzzy AHP [42], [54]–[56] analyses, respectively. The major reasons to perform FGD sessions with 5 experts can be summarized as follows: too many focus group participants may cause the session complexity (e.g., between 10 and 20) [57], and few participants might hinder sharing critical and creative opinions (e.g. <5) [50], [58]. Similar to FGD sessions, more efficient data collection can be realized and reliable results can be generated in AHP or fuzzy AHP applications with small sample sizes [50]. The method may even result in unassured criteria weights owing to the tendency of "cold-called" participants to provide random preferences as the sample size is increased [59]. Hence, data quality is signified in AHP applications compared to data quantity [60]. Furthermore, the AHP method is usually preferred by researchers due to its suitability for dealing with sample size limitations [59].

All the participants attended to this study were carefully examined based on the following criteria: (i) having at least 5-year experience in contract administration in the construction industry, (ii) having at least BSc degree in civil engineering or architecture programs, (iii) having a managerial experience in at least 2 construction projects. After contacting 14 experts, 9 and 5 of them showed their willingness to participate in this study in fuzzy AHP and FGD steps, respectively. Participants had diverse backgrounds (Table 1) and are currently working in Turkey. Table 1 shows the contribution of the participants, their positions in the organizations, organization type, and experience in the construction industry.

Table 1 - Profile of participants.

Expert ID	Contribution	Position in the organization	Organization type	Experience
Expert 1	Fuzzy AHP	Tendering engineer	Private client	11
Expert 2	Fuzzy AHP	Site chief	Private contractor	16
Expert 3	Fuzzy AHP	Cofounder	Private contractor	34
Expert 4	Fuzzy AHP	Technical office engineer	Private consultant to client	8
Expert 5	Fuzzy AHP	Design manager	Private consultant to client	14
Expert 6	Fuzzy AHP	Senior executive director	Public client	41
Expert 7	Fuzzy AHP	Procurement manager	Private contractor	12
Expert 8	Fuzzy AHP	Contract manager	Public client	18
Expert 9	Fuzzy AHP	Cost control manager	Public client	29
Expert 10	FGD	Design architect	Private contractor	9
Expert 11	FGD	Planning and cost control manager	Public client	17
Expert 12	FGD	Owner	Private sub-contractor	33
Expert 13	FGD	Interim payment engineer	Private contractor	12
Expert 14	FGD	Director	Private consultant to client	24

3.3. Focus Group Discussion (FGD)

FGD is an exploratory discussion technique that has been extensively used in research studies to collect expert opinions [47], [61] and is particularly convenient for exploring the diverse perspectives of participants with similar backgrounds, opinions, or experiences on a research

topic [62], [63]. Gold and Vassell [61] highlighted the advantages of focus groups such as time-effective and cost-effective. They can also generate satisfactory output with the involvement of 5 to 10 participants [62]. Yu and Leung [64] addressed that 4 to 6 participants constituted mini focus groups and 7 to 10 participants constituted small focus groups. The reason to adopt the FGD technique in this research was to obtain the expert opinions that have the required level of experience in contract management and administration to identify the operational barriers against the adoption of smart contracts and develop a framework that would facilitate their adoption in construction projects. Based on the results of FGDs with 5 experts, the selected operational barriers are illustrated in Table 2.

Table 2 - Operational barriers to smart contract adoption.

Barrier category	Barrier ID	Barrier	Reference
Technical (Tc)	Tc1	Lack of experienced personnel	Etemadi et al. [65]
	Tc2	Complexity in draft development	Etemadi et al. [65]
	Tc3	Irrevocable nature of smart contracts	Li et al. [14]
	Tc4	Updating issues after changes	Yamashita et al. [66]
	Tc5	Inaccurate recorded information	Li et al. [14]
	Tc6	Incorrect coding and interoperability issues	Wong et al. [67]
Financial (Fn)	Fn1	Expensive and clunky drafting and registration process	Gurgun and Koc [42]
	Fn2	Cost of upskilling	Mason and Escott [35]
	Fn3	Cost of updates required frequently	Li et al. [14]
	Fn4	Cost of adequate human resource	Meier and Sannajust [8]
Security/ Technological (St)	St1	Bug probability leading to permanent failure	Mason and Escott [35]
	St2	Privacy issues in terms of information security	Deebak and AL-Turjman [68]
	St3	Possible cyber-attacks/security risks	Zhao et al. [69]
	St4	Lack of technological advancements in the company	Wong et al. [67]
	St5	Error prone nature of transactions in smart contracts	Wong et al. [67]
Time (Tm)	Tm1	Requirement of excessive time for approval procedures in construction	Perera et al. [49]
	Tm2	Difficulty in setting deadlines and original time scales	Mason [48]
	Tm3	Time constraints (such as insurance arrangements etc.)	Mason [48]
	Tm4	Time consuming process of developing the contract draft	Li et al. [14]
	Tm5	Long lasting negotiation process in construction	Mason and Escott [35]

3.4. Fuzzy Analytical Hierarchy Process

The AHP method is one of the most widely used multi-criteria decision making (MCDM) methods in the literature [70]–[72], mostly due to its simplicity regarding hierarchical representation and the understanding of mathematical calculations. However, uncertainty about expressing the decision maker's decisions with exact numbers is a critical concern in most of the MCDM methods. To overcome this difficulty, the fuzzy AHP method was developed to address the fuzziness of decision makers [70]. In this method, fuzzy set theory proposed by Zadeh [73] was incorporated into AHP method by Chang [74], which is called extent analysis. Since then, it has widely been used in the literature and adopted in this study. There are four steps in the employment of the fuzzy AHP analysis:

Step 1. Data collection: Linguistic variables were used by experts to indicate the importance of barriers by means of pairwise comparisons. Triangular fuzzy scale for linguistic variables that are adopted in the current study is given in Table 3 [70], [75].

Table 3 - Triangular fuzzy scales.

	AHP		Fuzzy AHP	
Linguistic variables	Importance	Value for reciprocals	Triangular fuzzy numbers (l_{ij}, m_{ij}, u_{ij})	Triangular fuzzy reciprocals $(1/u_{ij}, 1/m_{ij}, 1/l_{ij})$
Equally important	1	(1/1)	(1, 1, 1)	(1, 1, 1)
Intermediate value	2	(1/2)	(1, 2, 3)	(1/3, 1/2, 1)
Moderately important	3	(1/3)	(2, 3, 4)	(1/4, 1/3, 1/2)
Intermediate value	4	(1/4)	(3, 4, 5)	(1/5, 1/4, 1/3)
Important	5	(1/5)	(4, 5, 6)	(1/6, 1/5, 1/4)
Intermediate value	6	(1/6)	(5, 6, 7)	(1/7, 1/6, 1/5)
Very important	7	(1/7)	(6, 7, 8)	(1/8, 1/7, 1/6)
Intermediate value	8	(1/8)	(7, 8, 9)	(1/9, 1/8, 1/7)
Extremely important	9	(1/9)	(9, 9, 9)	(1/9, 1/9, 1/9)

Step 2: Consistency check: The consistency ratio of each expert need to be determined to ensure the reliability of the survey outcomes [76], [77]. The consistency ratio (CR) values given by the experts are regarded as acceptable if it is calculated as lower than 0.10 (or 10%). Otherwise, the experts are regarded as inconsistent, and revised pairwise comparisons are requested from the corresponding expert [76], [78]. Calculation procedures to check the consistency can be found at [42].

Step 3: Attaining group decisions: The linguistic variables that were taken from each expert individually were converted into the corresponding triangular fuzzy scales for each pairwise comparison matrix. Then, group decision is augmented by taking the geometric mean values of the fuzzy scales [77], [79]:

$$l_{ij} = \left(\prod_{k=1}^{K} l_{ijk}\right)^{1/K},\ m_{ij} = \left(\prod_{k=1}^{K} m_{ijk}\right)^{1/K},\ u_{ij} = \left(\prod_{k=1}^{K} u_{ijk}\right)^{1/K} \quad (1)$$

where *K* is the total number of respondents.

Step 4: Application of Chang's extent analysis: Chang's [74] extent analysis was utilized to identify weights of barriers to smart contract adoption. The steps of Chang's fuzzy extent analysis can be found at [74].

4. RESULTS

In the fuzzy AHP implementation, consistency ratios of each expert were checked. In case of an inconsistency, the corresponding evaluations were revised, and the data collection step was finalized after all the matrices were found consistent. In addition, assessment of experts' consistency proves that the AHP method can be an effective tool in selection and/or prioritization problems, addressed in the literature [59]. The results of consistency analysis are shown in Table 4. Findings show that all experts were consistent with their judgments in each cluster (barrier category, financial, technical, security/technological, and time). Therefore, further analysis of fuzzy AHP was applied.

Table 4 - Consistency ratios of experts.

Expert ID	Category (%)	Financial (%)	Technical (%)	Security/ Technological (%)	Time (%)
Expert 1	4.31	0.71	8.89	2.34	9.42
Expert 2	4.31	7.45	9.62	1.64	7.64
Expert 3	6.95	4.19	8.73	9.14	8.27
Expert 4	2.64	2.43	9.45	7.63	9.42
Expert 5	8.37	6.33	7.42	8.13	9.16
Expert 6	5.33	2.65	9.89	9.50	8.19
Expert 7	4.50	8.15	8.29	7.87	6.42
Expert 8	0.00	0.00	8.60	7.86	8.93
Expert 9	5.16	1.90	4.64	3.01	6.39

Fuzzy AHP analysis results of barrier categories are presented in Table 5. It was found that the financial and technical aspects were the most significant operational barrier groups with a weight of 0.4165 and 0.2379, respectively. Time (weight: 0.1634) and security / technological (weight: 0.1822) barrier categories were determined less significant.

Table 5 - Weights and ranks of barrier categories.

Barrier category	ID	Weight	Rank
Financial	Fn	0.4165	1
Technical	Tc	0.2379	2
Security/Technological	St	0.1822	3
Time	Tm	0.1634	4

The findings related to individual barriers under each barrier category are shown in Table 6. Among the evaluated barriers, the experts highlighted the significance of Tc3 (*Irrevocable nature of smart contracts*) and Tc6 (*Incorrect coding and interoperability issues*) compared to other barriers in technical category. Tc3 and Tc6 were assessed with weight values of 0.2201 and 0.1964, and Tc1 (*Lack of experienced personnel*) was found the least significant barrier. Among the financial barriers, Fn1 (*Expensive and clunky drafting and registration process*) was the most significant financial barrier with a weight of 0.3915, and the rest of the barriers in this category were all determined with weights of less than 0.25.

In terms of security/technology category, the respondents emphasized their concerns related to the security of the confidential data used in smart contracts. In line, the findings illustrated that St2 (*Privacy issues in terms of information security*) and St3 (*Possible cyber-attacks/security risks*) were the most critical barriers (0.2488 and 0.2483), while experts considered St5 (*Error prone nature of transactions in smart contracts*) as the least challenging barrier. Regarding time category, respondents highlighted the features particular to construction projects and addressed that Tm1 (*Requirement of excessive time for approval procedures in construction*) and Tm2 (*Difficulty in setting deadlines and original time scales*) were the most critical barriers limiting the use of smart contracts with importance scores of 0.2635 and 0.2196, respectively. On the other hand, Tm5 (*Long lasting negotiation process in construction*) and Tm4 (*Time consuming process of developing the contract draft*) were the least significant time-related barriers.

The ranking of the barriers might be sensitive to the degree of fuzziness in the opinions of experts. Therefore, sensitivity analysis was employed to ensure the stability of the proposed approach under different degrees of fuzziness [71], [80]. Accordingly, the degree of fuzziness ranged between 1 and 2 with a step of 0.2 to explore whether the ranking of barrier categories and barriers change. Figure 2 and Figure 3 show the results of sensitivity analysis regarding barrier category and barriers in each category, respectively. The results show that the developed decision framework and rankings attained were stable under diverging degree of fuzziness.

Table 7 and Table 8 show the ranking difference based on the roles, organization types, and sectors of the experts, in terms of main categories and barriers, respectively. Findings show that all the participant types assessed “financial” category at the top. While experts involved in the managerial team considered “security/technological” as the second most significant category, other groups regarded as the third or fourth category in the rank (Table 7). Regarding barriers, it is especially worth mentioning that Fn4 (*Human resource cost*) is of paramount significance for the majority of expert groups, apart from public and client groups.

Interestingly, even though Tc2 (*Complexity in draft development*) was among the top five barriers when judgments of the experts from client are considered, other groups had opposite views (Table 8).

Table 6 - Weights and ranks of barriers.

Barrier category	Barrier ID	Weight	Rank	Overall weight	Overall rank
Technical	Tc1	0.1192	6	0.0284	18
	Tc2	0.1441	4	0.0343	13
	Tc3	0.2201	1	0.0524	5
	Tc4	0.1344	5	0.0320	14
	Tc5	0.1857	3	0.0442	9
	Tc6	0.1964	2	0.0467	6
Financial	Fn1	0.3915	1	0.1631	1
	Fn2	0.2112	2	0.0880	2
	Fn3	0.2016	3	0.0840	3
	Fn4	0.1957	4	0.0815	4
Security/ Technological	St1	0.2098	3	0.0382	11
	St2	0.2488	1	0.0453	7
	St3	0.2483	2	0.0452	8
	St4	0.1637	4	0.0298	17
	St5	0.1294	5	0.0236	19
Time	Tm1	0.2635	1	0.0431	10
	Tm2	0.2196	2	0.0359	12
	Tm3	0.1947	3	0.0318	15
	Tm4	0.1918	4	0.0313	16
	Tm5	0.1304	5	0.0213	20

Table 7 - Ranks of barrier categories based on expert profile.

Categories	Overall	Public	Private	Managerial	Engineer/architect	Client	Contractor	Consultant
Financial	1	1	1	1	1	1	1	1
Technical	2	2	2	4	2	2	2	4
Security/Technological	3	3	4	2	4	3	3	3
Time	4	4	3	3	3	4	4	2

Table 8 - Ranks of barriers based on expert profile.

Barriers	Overall	Public	Private	Managerial	Engineer/architect	Client	Contractor	Consultant
Tc1	18	14	17	19	10	8	18	17
Tc2	13	7	15	17	8	4	14	16
Tc3	5	5	5	15	2	3	8	12
Tc4	14	15	16	18	9	10	15	15
Tc5	9	16	7	13	7	11	6	14
Tc6	6	10	6	14	6	5	12	13
Fn1	1	1	1	1	1	1	1	2
Fn2	2	2	4	2	5	2	5	3
Fn3	3	8	2	3	3	6	2	8
Fn4	4	11	3	4	4	15	7	1
St1	11	4	14	9	16	7	19	11
St2	7	6	9	5	16	13	3	5
St3	8	3	10	6	16	9	4	10
St4	17	13	18	10	16	12	11	17
St5	19	17	20	16	16	14	20	17
Tm1	10	12	8	7	11	16	9	4
Tm2	12	9	11	8	14	18	10	6
Tm3	15	18	12	11	13	19	13	7
Tm4	16	19	13	12	12	17	16	9
Tm5	20	20	19	20	15	20	17	17

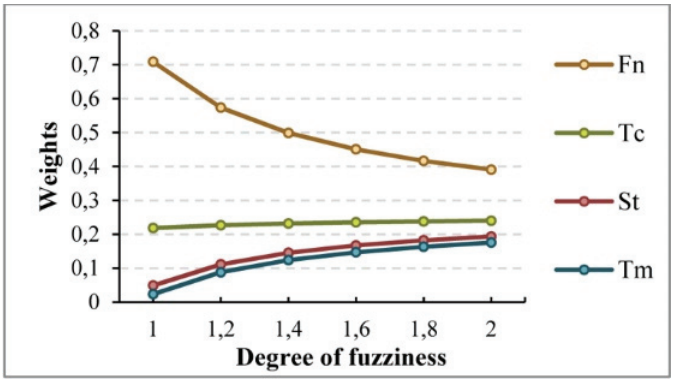

Figure 2 - Sensitivity analysis of main barrier categories.

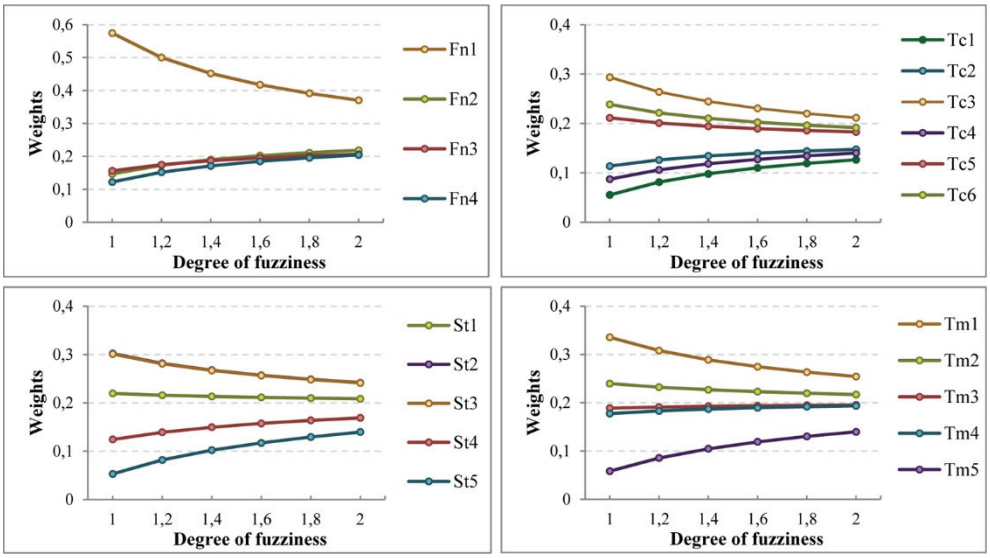

Figure 3 - Sensitivity analysis of categories a. Financial, b. Technical, c. Security/technological, d. Time.

5. DISCUSSION

Digital transformation in many industries including the construction industry is developing with the contribution of blockchain technology and smart contracts [37], yet the projects still suffer from budget constraints. Most of the companies act slowly in adopting recent technologies due to limited investment budgets. According to Yang et al. [81] cost is a key concern in adopting blockchain systems. Costs associated with smart contracts include initial drafting and registration cost (Fn1), upskilling cost (Fn2), updating cost (Fn3), and human resource cost (Fn4). In line with the results of this study, Mason and Escott [35] also highlighted the concerns of stakeholders about several types of costs associated with smart contracts such as time and cost required to educate human resource, system installation, and having qualified employees. Omar and Nehdi [82] emphasized that when applying any information technology in the construction sector, the update costs of the hardware, the needs for technical support personnel in the organizations, and the training of the employees become critical concerns. Similarly, Li et al. [14] underlined that the shortage of suitably upskilled, sufficiently trained, and talented personnel can be significant barriers for a construction company during digital capacity improvement processes. Recruitment and training the qualified employees can be costly [83], however, they are the prerequisites of successful transitions. Sonmez et al. [84] revealed that technical staff in construction projects do not feel confident about using newly developed systems if they are not familiar with implementing and supporting these advances. Therefore, gaining control over the information management system and contract management with qualified employees, the contribution of smart contracts may become more significant for the organizations.

Smart contracts can be characterized by immutability and inflexibility, yet changes and updates are common in construction contracts. Therefore, additional manual efforts and computational overheads related to use of smart contracts can also incur significant costs during the transition period from conventional to smart contracts. Security testing can help the prevention of vulnerabilities in terms of information security that may require a huge number of updates [85]. Hence, updates are technically applicable when the contract has repairable vulnerabilities [86]. Another important barrier is the privacy issues of smart contracts (St2) in the projects, which reflects the findings of Wang et al. [86] addressing privacy issues related to "contract data" and "personal data". In line with the results regarding financial category, Li et al. [87] and Agapiou [88] also addressed the possible financial losses in sustaining smart contracts due to security vulnerabilities. Automated vulnerability detection can be a solution to overcome this concern [85]. Contractual clauses, specific and/or general conditions, and risk mitigation instruments are critical in contract management. In this context, robust solution mechanisms and clear procedures are required to ensure the security of smart contracts throughout their life cycle [89].

Another type of problem was related to the "*irrevocable nature of smart contracts* (Tc3)". This result emerged from the analysis corroborates the earlier findings of some scholars [39], [90], who considered Tc3 as one of the risks in the implementation of smart contracts. Once smart contracts are initiated, the outcomes cannot be stopped as the procedures are coded by rule-based operators [48], [91]. This feature may be catastrophic if contract codes are incorrect [22]. To overcome this barrier, critical information should be shared, read, and approved by all members using the blockchain network with respect to the consensus between client and contractor, while not being changed or removed by any members [8], [22].

The results showed that the "*requirement of excessive time for approval procedures in construction* (Tm1)" was the most critical time-related concerns of construction professionals. In line with this finding, late approvals are acknowledged to be the major source of project delays in construction projects [92]. This outcome contradicts with one of the major objectives of smart contracts, which is to facilitate and accelerate the approval procedures during the initial drafting and information management processes throughout project execution [93]. However, as Perera et al. [49] addressed, the construction industry involves many approval processes since it includes numerous organizations in supply networks. Therefore, diligent organization of approval management systems is essential during the smart contract drafting stage. As stated by Das et al. [89], smart contracts can be adopted to ensure both the information approval workflow and document management systems.

As provided in Table 7 and Table 8, the experts from different roles and organization types have stated some similar as well as some opposite views about barriers. For instance, "financial" category was quite important for all expert types regardless of stakeholder profile. The experts from managerial team considered the "security/technological" category as more significant than others (Table 7). The most reasonable reason behind this logic is that handling unwanted transactions and security are huge challenges for management-level personnel [94]. Besides, the "*privacy issues in terms of information security* (St2)" was among the top three barriers in terms of the assessment of the experts from contractor firms

(Table 8). This can be supported with the results of Ahmadisheykhsarmast and Sonmez [43], who highlighted significant concerns of contractors about privacy issues.

On the other hand, other than operational barriers, several studies have critically addressed administrative [42] and legal issues [88] in the adoption of smart contracts in the construction industry. Although operational barriers were focused in this study, legal barriers and awareness/consciousness of project stakeholders towards smart contracts should be considered to manifest the successful implementations. For example, Agapiou [88] highlighted that enforceability, data protection and privacy, intellectual property rights, and dispute resolution were crucial barriers to designing smart contracts in the context of legal and regulation policies. These issues are of greater concern in raising legal uncertainty as a result of rapid changes in technology. Hence, new technological solutions requires updating existing legislation and developing new policies for better contract administration [95].

There are different legislative systems, and smart contract development can change accordingly. Law developments in Anglo-Saxon legislative system (also known as common law, followed in UK, USA, Canada, Australia, etc.) is largely based on past court decisions, which serve as an authority for future decisions. On the other hand, Continental European system (the most commonly followed legal system, e.g., Germany, France, Italy, and Turkey) relies on extensive codes that highlight the rules and procedures. In Anglo-Saxon system, a contract is regarded as a "promise" for a "counter-provision", while it is considered as an "agreement" in the Continental European system [95]. Kasatkina [95] stated that the identification of the contractual inception of a smart contract varies between approaches in the continental legal system family and Anglo-Saxon law. The researcher addressed that legislative experience of smart contracts is different in the EU and the USA, for example, and there is no legislation for the implementation of smart contracts in most countries. Thus, technological barriers can be minimized, and costs can be achieved with the help of standardization and common procedures at legislative level.

Furthermore, it is also worth mentioning that the use of smart contract is related to the awareness of senior management in construction firms [96]. Ameyaw et al. [41] stated that awareness of stakeholders is critical to aiding its adoption process. This is further confirmed by Elbashbishy et al. [97], in which the researchers emphasized that increasing the awareness and capabilities of staff is one of the important factors to the widespread adoption of blockchain technology, which integrates smart contracts in construction contracts.

6. IMPLICATIONS FOR PRACTITIONERS

This study proposes a smart contract implementation framework based on life cycle of contract management (drafting, review/approval, implementation, and closure/renewals processes) (Figure 4). To develop a practical structure, responsibilities of all contracting parties need to be clarified and included. With the integration of contractual claims, potential disputes among the parties related to contract clauses, progresses, and payment issues can be mitigated or prevented. Unforeseen conditions, discrete requirements of the projects, and change orders should also be included in the smart contract drafting process to perform effective contract administration [42]. Rendering contract documents in their digital forms and automated legal review of contract clauses can also help minimize uncertainties and incompleteness, while enabling a better control of contract requirements. Blockchain

network can be used in the review and approval process of smart contracts to monitor workflows, automate approvals, and perform updating without human interference [93]. During the implementation process, automated control and monitoring systems, artificial intelligence, optimization algorithms [8], and dynamic operations (security analysis, automatic updates and self-destruction etc.) [86] can be useful for effective administration. Once a setback is observed or predicted, IT team members can be informed earlier to minimize failure in contract administration along with the regular maintenance [8]. In the closure phase, all data should be collected via project database and contract can be closured by reporting errors/failures to help improve smart contract drafts in future projects.

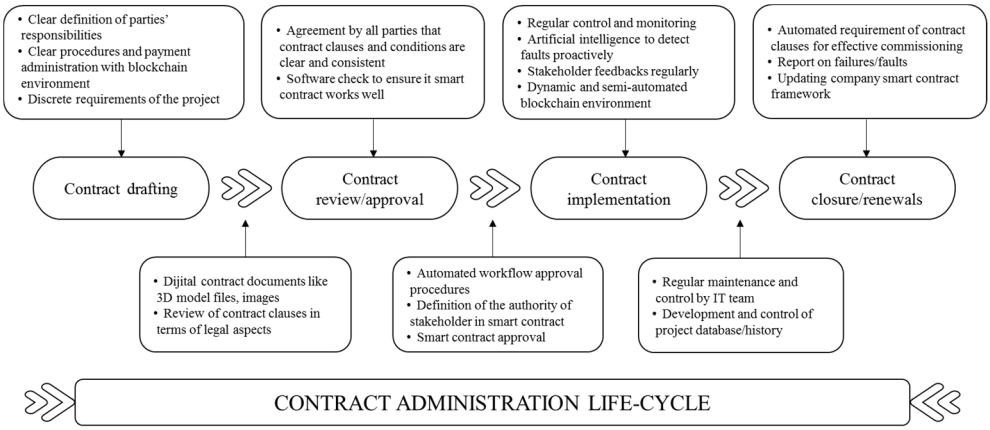

Figure 4 - Proposed smart-contract adoption framework.

Construction managers are the major authorities in construction projects that are responsible to facilitate effective communication management methods and establish sustainable working environments through useful means for engineers/designers/site supervisors. They need to look for applicable decision strategies and integrate appropriate technological solutions into their organizations to add value. With the continuously evolving technology, construction managers realized how crucial technological knowledge and capabilities are for organizational development [98]. Hence, they need to work with advanced technological tools to enhance project management techniques and their competitive advantage in the construction sector. Contract administration based on "smart contract" technology has great potential to improve the efficiency of construction projects. The adoption of smart contracts with digital documents and automated approval systems enables implementation of different control strategies for more robust contract administration processes and fosters stronger relationships among project parties. However, it is essential for the construction managers to handle the critical barriers such as "expensive and clunky drafting and registration process", and "cost of upskilling" in the process of using smart contracts. Therefore, the framework promoting robust contract management can be useful for improved project performance.

7. CONCLUSION

Digital management of contracts is expected to have significant impacts on the occurrence of conflicts, claims, and eventually disputes in construction projects. Smart contracts, which have the potential to change contract implementation process in construction projects, are one of the most frequently exploited technological improvements in recent years. However, construction managers may hesitate adopting smart contracts due to many operational barriers in the life cycle of the projects. To minimize the concerns of project teams and stakeholders, this study aims to explore the operational barriers against the adoption of smart contracts and to develop a model in the adoption process for construction projects.

In the present research, the operational barriers were defined under four categories: technical, financial, security/technological, and time, by conducting FGD with construction professionals. This step was followed by the fuzzy AHP analysis to identify the weights of the barrier categories and twenty individual barriers that were listed under these categories. Based on results of the fuzzy AHP analysis, expensive and sluggish drafting and registration process, cost of upskilling, cost of updates required frequently, cost of adequate human resource, and irrevocable nature of smart contracts were found to be the most significant barriers. The stability and robustness of the proposed approach and the research findings under different degrees of fuzziness were checked through sensitivity analysis. Furthermore, this study presents a smart contract implementation model for the construction projects that is expected to contribute to both directly and indirectly the performance and effectiveness in construction companies. Moreover, engineers and/or managers who have a significant role in construction management could facilitate evolution of contract administration practices into the digital platform by adopting this model.

Even though this study presents an insight into the barriers that may be faced in the implementation of smart contracts, it still poses some limitations. For instance, this study adopted several research techniques that rely on subjective evaluations of the experts in both fuzzy AHP and FGD method applications. Therefore, validation of the results with real-life observations can be a useful research direction to observe which operational barriers result in which hardships and to what extent. Additionally, the opinions of a limited number of experts from the Turkish construction industry were incorporated into this study. Hence, the number of experts can be increased in future studies by including the judgments of experts from different countries and industries. On the other hand, this study examined only the operational barriers to smart contract adoption. However, legal barriers, another important concern of stakeholders for implementing smart contracts, were not considered within the scope of this study. Therefore, significant barriers to smart contracts based on Turkey's legal structure can be investigated as a future research direction. Overall, the smart contract adoption framework proposed in this study is expected to help practitioners reduce the concerns of project stakeholders that hinder the adoption of smart contracts. The findings of this study can be used by both construction managers and technical engineers to upgrade the conventional contract forms and exchange them with more robust and automated contract forms.

References

[1] Zhang, Y., Wang, T., and Yuen, K. V., Construction Site Information Decentralized Management Using Blockchain and Smart Contracts, *Computer-Aided Civil and Infrastructure Engineering* 37, 1450–1467 2022.

[2] Ahn, S., Shokri, S., Lee, S., Haas, C. T., and Haas, R. C. G., Exploratory Study on the Effectiveness of Interface-Management Practices in Dealing with Project Complexity in Large-Scale Engineering and Construction Projects, *Journal of Management in Engineering* 33, 1–12 2017.

[3] Arcadis, Global Construction Disputes Report 2022, 2022. [Online]. Available: https://www.arcadis.com/en/knowledge-hub/perspectives/global/global-construction-disputes-report.

[4] Demirkesen, S. and Ozorhon, B., Measuring Project Management Performance: Case of Construction Industry, *EMJ - Engineering Management Journal* 29, 258–277 2017.

[5] Liu, L., Comparative Analysis of the Mechanism of Engineering Project Management Standardization, in *IOP Conference Series: Earth and Environmental Science*, 2020, 526, 012218.

[6] Wu, Q., Sheng, W., Wei, F., Liu, H., and Wen, H., Identification of Smart Construction Features and Impacts on Engineering Project Performance, in *Conference Proceedings of the 10th International Symposium on Project Management*, 2022, 837–842.

[7] Tang, L., Xiahou, X., Li, K., Li, Q., and Hu, X., Research on the Relationship Between Flexible Contract Term Setting Method and Setting Effect of Environmental Protection PPP Project, *EMJ - Engineering Management Journal* 00, 1–13 2022.

[8] Meier, O. and Sannajust, A., The Smart Contract Revolution: A Solution for the Holdup Problem?, *Small Business Economics* 57, 1073–1088 2021.

[9] Mahmudnia, D., Arashpour, M., and Yang, R., Blockchain in Construction Management: Applications, Advantages and Limitations, *Automation in Construction* 140, 104379 2022.

[10] Mutikanga, H. E., Abdul Nabi, M., Ali, G. G., El-adaway, I. H., and Caldwell, A., Postaward Construction and Contract Management of Engineering, Procurement, and Construction Hydropower Projects: Two Case Studies from Uganda, *Journal of Management in Engineering* 38, 05022012 2022.

[11] Mckinsey Global Insititute, Reinventing Construction: A Route to Higher Productivity, 2017.

[12] Sinha, A. K. and Jha, K. N., Critical Analysis of Contract Clauses in Road Sector: Case Study, *Journal of Legal Affairs and Dispute Resolution in Engineering and Construction* 12, 05020005 2020.

[13] Winanri, R. P., Susanti, B., and Juliantina, I., Comparison Analysis Between Traditional and Long Segment Contracts on National Road Preservation Activities in Indonesia, *Engineering, Technology & Applied Science Research* 9, 4230–4234 2019.

[14] Li, J., Greenwood, D., and Kassem, M., Blockchain in the Built Environment and Construction Industry: A Systematic Review, Conceptual Models and Practical Use Cases, *Automation in Construction* 102, 288–307 2019.

[15] Xu, Y., Chong, H. Y., and Chi, M., A Review of Smart Contracts Applications in Various Industries: A Procurement Perspective, *Advances in Civil Engineering* 2021, 2021.

[16] Negi, D., Sah, A., Rawat, S., Choudhury, T., and Khanna, A., Block Chain Platforms and Smart Contracts, in *EAI/Springer Innovations in Communication and Computing*, In Blockchain Applications in IoT Ecosystem. EAI/Springer Innovations in Communication and Computing. Springer, Cham., 2021, 65–76.

[17] Salmerón-Manzano, E. and Manzano-Agugliaro, F., The Role of Smart Contracts in Sustainability: Worldwide Research Trends, *Sustainability (Switzerland)* 11, 2019.

[18] Ge, X., Smart Payment Contract Mechanism Based on Blockchain Smart Contract Mechanism, *Scientific Programming* 2021, 2021.

[19] Milani, F., Garcia-Banuelos, L., Filipova, S., and Markovska, M., Modelling Blockchain-Based Business Processes: A Comparative Analysis of BPMN vs CMMN, *Business Process Management Journal* 27, 638–657 2021.

[20] Gurgun, A. P., Genc, M. I., Koc, K., and Arditi, D., Exploring the Barriers against Using Cryptocurrencies in Managing Construction Supply Chain Processes, *Buildings* 12, 357 2022.

[21] Sigalov, K. *et al.*, Automated Payment and Contract Management in the Construction Industry by Integrating Building Information Modeling and Blockchain-Based Smart Contracts, *Applied Sciences* 11, 7653 2021.

[22] Bolhassan, D. N., Changsaar, C., Khoso, A. R., Siawchuing, L., Bamgbade, J. A., and Hing, W. N., Towards Adoption of Smart Contract in Construction Industry in Malaysia, *Pertanika Journal of Science and Technology* 30, 141–160 2022.

[23] Feng, T., Yu, X., Chai, Y., and Liu, Y., Smart Contract Model for Complex Reality Transaction, *International Journal of Crowd Science* 3, 184–197 2019.

[24] McNamara, A. J. and Sepasgozar, S. M. E., Intelligent Contract Adoption in the Construction Industry: Concept Development, *Automation in Construction* 122, 103452 2021.

[25] Szabo, N., Smart Contracts, 1994. https://www.fon.hum.uva.nl/rob/Courses/InformationInSpeech/CDROM/Literature/LOTwinterschool2006/szabo.best.vwh.net/smart.contracts.html.

[26] Szabo, N., Formalizing and Securing Relationships on Public Networks, *First Monday* 2, 1997 [Online]. Available: Szabo, N.

[27] Norton Rose Fulbright, Smart Contracts: Coding the Fine Print | Global Law Firm | Norton Rose Fulbright, 2016. .

[28] Hamledari, H. and Fischer, M., Role of Blockchain-Enabled Smart Contracts in Automating Construction Progress Payments, *Journal of Legal Affairs and Dispute Resolution in Engineering and Construction* 13, 04520038 2021.

[29] Karamanlıoğlu, A., Concept of Smart Contracts – A Legal Perspective, *Kocaeli Üniversitesi Sosyal Bilimler Dergisi* 35, 29–42 2018.

[30] Fernandez-Vazquez, S., Rosillo, R., de la Fuente, D., and Puente, J., Blockchain in Sustainable Supply Chain Management: An Application of the Analytical Hierarchical Process (AHP) Methodology, *Business Process Management Journal* 28, 1277–1300 2022.

[31] Salmon, B., How Do Smart Contracts Work? An Introduction to Smart Contracts, 2017. .

[32] Ravishankar, B., Kulkarni, P., and Vishnudas, M. V., Blockchain-based Database to Ensure Data Integrity in Cloud Computing Environments, *2020 International Conference on Mainstreaming Block Chain Implementation, ICOMBI 2020* 2020.

[33] Hamledari, H. and Fischer, M., Measuring the Impact of Blockchain and Smart Contracts on Construction Supply Chain Visibility, *Advanced Engineering Informatics* 50, 101444 2021.

[34] Chong, H. Y. and Diamantopoulos, A., Integrating Advanced Technologies to Uphold Security of Payment: Data Flow Diagram, *Automation in Construction* 114, 2020.

[35] Mason, J. and Escott, H., Smart Contracts in Construction: Views and Perceptions of Stakeholders, *Proceedings of FIG Conference* 1–27 2018.

[36] Nanayakkara, S., Perera, S., and Sepani, S., Stakeholders' Perspective on Blockchain and Smart Contracts Solutions for Construction Supply Chains, *The CIB World Building Congress 2019* 2019.

[37] Li, J. and Kassem, M., Applications of Distributed Ledger Technology (DLT) and Blockchain-Enabled Smart Contracts in Construction, *Automation in Construction* 132, 2021.

[38] Li, J., Kassem, M., Ciribini, A. L. C., and Bolpagni, M., A Proposed Approach Integrating DLT, BIM, IOT and Smart Contracts: Demonstration Using A Simulated Installation Task, *International Conference on Smart Infrastructure and Construction 2019, ICSIC 2019: Driving Data-Informed Decision-Making* 2019, 275–282 2019.

[39] Rathnayake, I., Wedawatta, G., and Tezel, A., Smart Contracts in the Construction Industry: A Systematic Review, *Buildings* 12, 2082 2022.

[40] Shang, G., Pheng, L. S., and Zhong Xia, R. L., Adoption of smart contracts in the construction industry: an institutional analysis of drivers and barriers, *Construction Innovation* 2023.

[41] Ameyaw, E. E., Edwards, D. J., Kumar, B., Thurairajah, N., Owusu-Manu, D.-G., and Oppong, G. D., Critical Factors Influencing Adoption of Blockchain-Enabled Smart Contracts in Construction Projects, *Journal of Construction Engineering and Management* 149, 1–16 2023.

[42] Gurgun, A. P. and Koc, K., Administrative risks challenging the adoption of smart contracts in construction projects, *Engineering, Construction and Architectural Management* 29, 989–1015 2022.

[43] Ahmadisheykhsarmast, S. and Sonmez, R., A Smart Contract System for Security of Payment of Construction Contracts, *Automation in Construction* 120, 103401 2020.

[44] Luo, H., Das, M., Wang, J., and Cheng, J. C. P., Construction Payment Automation through Smart Contract-Based Blockchain Framework, *Proceedings of the 36th International Symposium on Automation and Robotics in Construction, ISARC 2019* 1254–1260 2019.

[45] Yu, Y., Chan, A. P. C., Chen, C., and Darko, A., Critical Risk Factors of Transnational Public-Private Partnership Projects: Literature Review, *Journal of Infrastructure Systems* 24, 04017042 2018.

[46] Hong, Y. and Chan, D. W. M., Research Trend of Joint Ventures in Construction: A Two-Decade Taxonomic Review, *Journal of Facilities Management* 12, 118–141 2014.

[47] Koc, K. and Gurgun, A. P., Stakeholder-Associated Life Cycle Risks in Construction Supply Chain, *Journal of Management in Engineering* 37, 04020107 2021.

[48] Mason, J., Intelligent Contracts and the Construction Industry, *Journal of Legal Affairs and Dispute Resolution in Engineering and Construction* 9, 04517012 2017.

[49] Perera, S., Nanayakkara, S., Rodrigo, M. N. N., Senaratne, S., and Weinand, R., Blockchain Technology: Is It Hype or Real in the Construction Industry?, *Journal of Industrial Information Integration* 17, 100125 2020.

[50] Durdyev, S., Koc, K., Karaca, F., and Gurgun, A. P., Strategies for implementation of green roofs in developing countries, *Engineering, Construction and Architectural Management* 2022.

[51] Alves, T. da C. L., Liu, M., Scala, N. M., and Javanmardi, A., Schedules and Schedulers: A Study in the U.S. Construction Industry, *EMJ - Engineering Management Journal* 32, 166–185 2020.

[52] Ajayi, S. O. and Oyedele, L. O., Policy Imperatives for Diverting Construction Waste from Landfill: Experts ' Recommendations for UK Policy Expansion, *Journal of Cleaner Production* 147, 57–65 2017.

[53] Chen, L., Lu, Q., and Zhao, X., Rethinking the Construction Schedule Risk of Infrastructure Projects Based on Dialectical Systems and Network Theory, *Journal of Management in Engineering* 36, 04020066 2020.

[54] Koulinas, G. K., Marhavilas, P. K., Demesouka, O. E., Vavatsikos, A. P., and Koulouriotis, D. E., Risk Analysis and Assessment in the Worksites Using the Fuzzy-Analytical Hierarchy Process and A Quantitative Technique – A Case Study for the Greek Construction Sector, *Safety Science* 112, 96–104 2019.

[55] Beltrão, L. M. P. and Carvalho, M. T. M., Prioritizing Construction Risks Using Fuzzy AHP in Brazilian Public Enterprises, *Journal of Construction Engineering and Management* 145, 05018018 2019.

[56] Yadav, G. and Desai, T. N., A Fuzzy AHP Approach to Prioritize the Barriers of Integrated Lean Six Sigma, *International Journal of Quality and Reliability Management* 34, 1167–1185 2017.

[57] Budayan, C., Okudan, O., and Dikmen, I., Identification and prioritization of stage-level KPIs for BOT projects – evidence from Turkey, *International Journal of Managing Projects in Business* 13, 1311–1337 2020.

[58] Ekmekcioğlu, Ö., Koc, K., Dabanli, I., and Deniz, A., Prioritizing urban water scarcity mitigation strategies based on hybrid multi-criteria decision approach under fuzzy environment, *Sustainable Cities and Society* 87, 104195 2022.

[59] Darko, A., Chan, A. P. C., Ameyaw, E. E., Owusu, E. K., Pärn, E., and Edwards, D. J., Review of application of analytic hierarchy process (AHP) in construction, *International Journal of Construction Management* 19, 436–452 2019.

[60] Okudan, O. and Budayan, C., Assessment of project characteristics affecting risk occurences in construction projects using fuzzy AHP, *Sigma Journal of Engineering and Natural Sciences* 38, 1447–1462 2020.

[61] Gold, B. and Vassell, C., Using Risk Management to Balance Agile Methods: A Study of the Scrum Process, in *2015 2nd International Conference on Knowledge-Based Engineering and Innovation (KBEI)*, Nov. 2015, 49–54.

[62] Rajadurai, R. and Vilventhan, A., Integrating Road Information Modeling (RIM) and Geographic Information System (GIS) for Effective Utility Relocations in Infrastructure Projects, *Engineering, Construction and Architectural Management* 2021.

[63] Hasan, A., Elmualim, A., Rameezdeen, R., Baroudi, B., and Marshall, A., An Exploratory Study on the Impact of Mobile ICT on Productivity in Construction Projects, *Built Environment Project and Asset Management* 8, 320–332 2018.

[64] Yu, J. and Leung, M. yung, Exploring Factors of Preparing Public Engagement for Large-Scale Development Projects via A Focus Group Study, *International Journal of Project Management* 33, 1124–1135 2015.

[65] Etemadi, N., Van Gelder, P., and Strozzi, F., An ISM Modeling of Barriers for Blockchain/Distributed Ledger Technology Adoption in Supply Chains towards Cybersecurity, *Sustainability* 13, 4672 2021.

[66] Yamashita, K., Nomura, Y., Zhou, E., Pi, B., and Jun, S., Potential Risks of Hyperledger Fabric Smart Contracts, 2019.

[67] Wong, L.-W., Tan, G. W.-H., Lee, V.-H., Ooi, K.-B., and Sohal, A., Psychological and System-Related Barriers to Adopting Blockchain for Operations Management: An Artificial Neural Network Approach, *IEEE Transactions on Engineering Management* 1–15 2021.

[68] Deebak, B. D. and AL-Turjman, F., Privacy-Preserving in Smart Contracts Using Blockchain and Artificial Intelligence for Cyber Risk Measurements, *Journal of Information Security and Applications* 58, 102749 2021.

[69] Zhao, H., Zhang, M., Wang, S., Li, E., Guo, Z., and Sun, D., Security Risk and Response Analysis of Typical Application Architecture of Information and Communication Blockchain, *Neural Computing and Applications* 33, 7661–7671 2021.

[70] Vahidnia, M. H., Alesheikh, A. A., and Alimohammadi, A., Hospital Site Selection Using Fuzzy AHP and Its Derivatives, *Journal of Environmental Management* 90, 3048–3056 2009.

[71] Zyoud, S. H., Kaufmann, L. G., Shaheen, H., Samhan, S., and Fuchs-Hanusch, D., A Framework for Water Loss Management in Developing Countries under Fuzzy Environment: Integration of Fuzzy AHP with Fuzzy TOPSIS, *Expert Systems with Applications* 61, 86–105 2016.

[72] Nikolić, N., Nikolić, D., Marinkovic, S., and Mihajlovic, I., Application of FAHP–PROMETHEE Hybrid Model for Prioritizing SMEs Failure Factors, *EMJ - Engineering Management Journal* 33, 1–18 2020.

[73] Zadeh, L. A., Fuzzy Sets, *Information and Control* 8, 338–353 1965.

[74] Chang, D. Y., Applications of the Extent Analysis Method on Fuzzy AHP, *European Journal of Operational Research* 95, 649–655 1996.

[75] Papaioannou, G., Vasiliades, L., and Loukas, A., Multi-Criteria Analysis Framework for Potential Flood Prone Areas Mapping, *Water Resources Management* 29, 399–418 2015.

[76] Suganthi, L., Multi Expert and Multi Criteria Evaluation of Sectoral Investments for Sustainable Development: An Integrated Fuzzy AHP, VIKOR / DEA Methodology, *Sustainable Cities and Society* 43, 144–156 2018.

[77] Meixner, O., Fuzzy AHP Group Decision Analysis and its Application for the Evaluation of Energy Sources, Jul. 2009.

[78] Saaty, T. L., Decision making — The Analytic Hierarchy and Network Processes (AHP/ANP), *Journal of Systems Science and Systems Engineering* 13, 1–35 2004.

[79] Koc, K., Ekmekcioğlu, Ö., and Özger, M., An Integrated Framework for the Comprehensive Evaluation of Low Impact Development Strategies, *Journal of Environmental Management* 294, 2021.

[80] Ishizaka, A. and Labib, A., Review of the Main Developments in the Analytic Hierarchy Process, *Expert Systems with Applications* 38, 14336–14345 2011.

[81] Yang, R. *et al.*, Public and private blockchain in construction business process and information integration, *Automation in Construction* 118, 2020.

[82] Omar, T. and Nehdi, M. L., Data Acquisition Technologies for Construction Progress Tracking, *Automation in Construction* 70, 143–155 2016.

[83] Ho, P. H. K., Forecasting Construction Manpower Demand by Gray Model, *Journal of Construction Engineering and Management* 136, 1299–1305 2010.

[84] Sonmez, R., Ahmadisheykhsarmast, S., and Güngör, A. A., BIM Integrated Smart Contract for Construction Project Progress Payment Administration, *Automation in Construction* 139, 104294 2022.

[85] Shao, W., Wang, Z., Wang, X., Qiu, K., Jia, C., and Jiang, C., LSC: Online Auto-Update Smart Contracts for Fortifying Blockchain-Based Log Systems, *Information Sciences* 512, 506–517 2020.

[86] Wang, S., Ouyang, L., Yuan, Y., Ni, X., Han, X., and Wang, F. Y., Blockchain-Enabled Smart Contracts: Architecture, Applications, and Future Trends, *IEEE Transactions on Systems, Man, and Cybernetics: Systems* 49, 2266–2277 2019.

[87] Li, X., Jiang, P., Chen, T., Luo, X., and Wen, Q., A survey on the security of blockchain systems, *Future Generation Computer Systems* 107, 841–853 2020.

[88] Agapiou, A., Overcoming the Legal Barriers to the Implementation of Smart Contracts in the Construction Industry: The Emergence of a Practice and Research Agenda, *Buildings* 13, 594 2023.

[89] Das, M., Tao, X., Liu, Y., and Cheng, J. C. P., A Blockchain-Based Integrated Document Management Framework for Construction Applications, *Automation in Construction* 133, 104001 2022.

[90] Altay, H. and Motawa, I., An investigation on the applicability of smart contracts in the construction industry, *ARCOM Doctoral Workshop* 12–16 2020.

[91] Koc, K. and Gurgun, A. P., Drivers for Construction Stakeholders to Adopt Smart Contracts, *Journal of Construction Engineering, Management & Innovation* 3, 101–112 2020.

[92] Lam, P. T. I., Kumaraswamy, M. M., and Ng, S. T., The use of construction specifications in Singapore, *Construction Management and Economics* 22, 1067–1079 2004.

[93] Das, M., Tao, X., and Cheng, J. C. P., A Secure and Distributed Construction Document Management System Using Blockchain, *Lecture Notes in Civil Engineering* 98, 850–862 2021.

[94] Carvalho, A., Merhout, J. W., Kadiyala, Y., and Bentley II, J., When good blocks go bad: Managing unwanted blockchain data, *International Journal of Information Management* 57, 102263 2021.

[95] Kasatkina, M., The Interpretation of Smart Contracts in the EU and the USA, *International Comparative Jurisprudence* 7, 202–217 2021.

[96] Badi, S., Ochieng, E., Nasaj, M., and Papadaki, M., Technological, organisational and environmental determinants of smart contracts adoption: UK construction sector viewpoint, *Construction Management and Economics* 39, 36–54 2021.

[97] Elbashbishy, T. S., Ali, G. G., and El-adaway, I. H., Blockchain technology in the construction industry: mapping current research trends using social network analysis and clustering, *Construction Management and Economics* 40, 406–427 2022.

[98] Tieng, K., Jeenanunta, C., Chea, P., and Rittippant, N., Roles of Customers in Upgrading Manufacturing Firm Technological Capabilities Toward Industry 4.0, *EMJ - Engineering Management Journal* 34, 329–340 2022.

Turkish Journal of Civil Engineering, 2023 107-127, Yazı 748, ***Araştırma Makalesi***

Betonarme Perdelerin Kesme Güvenliğinin TBDY-2018'e Göre İncelenmesi

Aytuğ SEÇKİN[1]
Bilge DORAN[2]

ÖZ

Bu çalışmada, betonarme perdelerin tasarım kesme kuvvetinin yeterliliği Türkiye Bina Deprem Yönetmeliği 2018 (TBDY-2018) esaslarına göre araştırılmıştır. Bu amaç doğrultusunda, taşıyıcı sistemi süneklik düzeyi yüksek betonarme çerçevelerden ve perdelerden oluşan 20 katlı bir binada doğrusal ve doğrusal olmayan analizler yürütülmüştür. Çalışma kapsamında öncelikle 20 katlı bir binanın dayanıma göre tasarımı mod birleştirme yöntemi ile gerçekleştirilmiştir. Tasarlanmış binada, yatay elastik tasarım spektrumuna göre eşleştirilmiş 11 deprem kaydı etkisi altında zaman tanım alanında doğrusal olmayan analizler yapılmıştır. Doğrusal analizlerden elde edilen tasarım kesme kuvvetleri ve doğrusal olmayan analizlerden elde edilen kesme talepleri, incelenen dikdörtgen ve L-kesitli perdelerin yükseklikleri boyunca karşılaştırılmıştır. Çalışma sonucunda, L-kesitli perdede hesaplanan tasarım kesme kuvvetinin talep değerini karşılamada yetersiz kaldığı görülmüştür. Betonarme perdelerin kesme talepleri, modifiye edilmiş modal süperpozisyon yaklaşımı (MMS) ile de hesaplanmış ve bu yaklaşımın TBDY-2018'e uygulanabilirliği incelenen perdeler üzerinde test edilmiştir.

Anahtar Kelimeler: Betonarme perdeler, dinamik büyütme katsayısı, modifiye edilmiş modal süperpozisyon yaklaşımı, TBDY-2018, zaman tanım alanında doğrusal olmayan analiz.

ABSTRACT

Investigation of Shear Safety in Reinforced Concrete Walls According to TBEC-2018

This study investigates the adequacy of the design shear force in reinforced concrete walls according to the Turkish Building Earthquake Code 2018 (TBEC-2018). For this purpose, linear and nonlinear analyses are conducted in a 20-story building, of which lateral load

Not: Bu yazı
- Yayın Kurulu'na 16 Ocak 2023 günü ulaşmıştır. 4 Ağustos 2023 günü yayımlanmak üzere kabul edilmiştir.
- 30 Kasım 2023 gününe kadar tartışmaya açıktır.

- https://doi.org/10.18400/tjce.1235472

1 Kocaeli Üniversitesi, İnşaat Mühendisliği Bölümü, Kocaeli, Türkiye
aytug.seckin@kocaeli.edu.tr - https://orcid.org/0000-0003-2037-4758

2 Yıldız Teknik Üniversitesi, İnşaat Mühendisliği Bölümü, İstanbul, Türkiye
doran@yildiz.edu.tr - https://orcid.org/0000-0001-6703-7279

resisting system consists of reinforced concrete frames and shear walls with a high ductility level. First, the force-based design of the 20-story building is carried out using response spectrum analysis. Then, nonlinear time history analyses (NLTHA) are performed on the building under eleven ground motions matched to the elastic design spectrum. Lastly, design shear forces from linear analysis and shear demands from nonlinear analyses are compared along the heights of the walls with rectangular and L-shaped cross-sections. The study reveals that the design shear force of the L-shaped shear wall is insufficient to meet the demand value. The shear demands of reinforced concrete walls are also calculated by the modified modal superposition approach (MMS), and the applicability of this approach to TBEC-2018 is tested on the shear walls examined.

Keywords: Dynamic amplification factor, modified modal superposition approach, nonlinear time history analysis, reinforced concrete shear walls, TBEC-2018.

1. GİRİŞ

6 Şubat 2023 tarihinde ülkemizde meydana gelen Kahramanmaraş merkezli depremler neticesinde; 11 ili kapsayan bölgede çok sayıda bina yıkılmış, farklı derecelerde hasar almış ve can kayıpları yaşanmıştır. Kocaeli Üniversitesi tarafından hazırlanan saha inceleme raporunda [1]; "betonarme perde duvarlarda, çevrimsel davranış altında kesme, tek yönde görülen erken seviyede kesme, perde ucunda burkulma, perde alt ucunda eğilme ve sürtünme kesmesi hasarları ile karşılaşıldığı" belirtilmiştir. Raporda, Şekil 1'de verilen hasar örneklerinin yeni yapılmakta olan binalara ait olduğu ayrıca belirtilmiştir. Bursa Teknik Üniversitesi tarafından hazırlanan inceleme ve değerlendirme raporunda [2], perde duvarların kesme veya eğilme nedeniyle hasar aldığının gözlemlendiği belirtilmiştir. Perde duvarların ağır hasar almış olmasına rağmen diğer yapısal elemanlarda hasarları azaltarak sistemin toptan göçmesini engellediği sonucu raporda paylaşılmıştır. Deprem bölgesinde yapılan incelemeler, betonarme binaların sismik etkiler altında sergileyeceği performansı önemli ölçüde etkileyen perde duvarlarda tasarım kriterlerinin gözden geçirilmesinin gerektiğini göstermektedir.

Betonarme perde davranışı üzerine yürütülen başlıca çalışmalarda (Blakeley vd. [3], Eibl ve Keintzel [4], Paulay ve Priestley [5], Krawinkler [6]), yapının doğrusal olmayan davranışı esnasında perde elemanların kesme kapasitelerini aşarak gevrek göçmeye maruz kalabileceği vurgulanmıştır. Uluslararası tasarım yönetmelikleri (NZS 3101-1995 [7], Eurocode 8-2004 [8], CSA A23.3-2014 [9], ACI 318-19 [10]), sismik etkiler altında perde elemanlarda meydana gelebilecek olası bir gevrek kırılmayı önlemek için tasarım kesme kuvvetinin hesabında dinamik büyütme katsayısının kullanılmasını önermişlerdir.

Literatürde, betonarme perdelerde dinamik büyütme katsayısını dikkate alan farklı analitik ve deneysel çalışmalar yürütülmüştür. Dinamik büyütme katsayısına dikkati çeken ilk çalışmayı gerçekleştiren Blakeley vd. [3] tarafından önerilen katsayı, NZS 3101-1995'te [7] yer alan dinamik büyütme katsayısına; Eibl ve Keintzel [4] tarafından önerilen katsayı da Eurocode 8-2004'te [8] süneklik düzeyi yüksek perdelerin tasarımında yer verilen dinamik büyütme katsayısına öncülük etmiştir. Paulay ve Priestley [5], Krawinkler [6] perde tabanında plastik mafsal oluşumuyla birlikte yüksek modlara ait etkilerin yapısal davranışta baskın hale geleceğini ve 1. modun etkinliğinin azalacağını belirtmişlerdir. Etkin mod şeklinin değişmesiyle birlikte de perde tabanında moment oluşturan atalet kuvvetlerinin

merkezi tabana doğru kaymakta ve perde eleman moment kapasitesine daha büyük bir kesme kuvveti altında ulaşmaktadır.

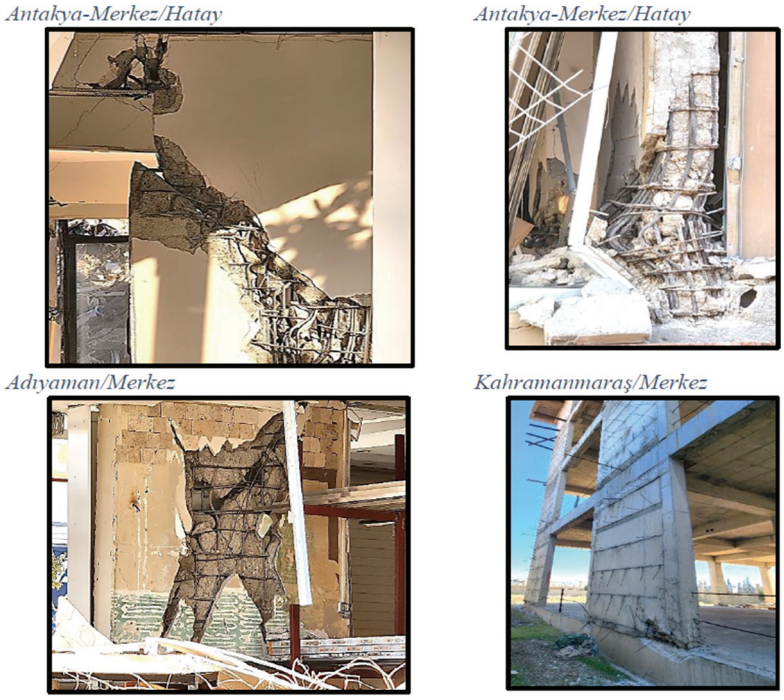

Şekil 1 - 2023 Kahramanmaraş merkezli depremlerde meydana gelen betonarme perde hasarları [1]

Dinamik büyütme katsayısının uluslararası deprem yönetmeliklerinde yer almasıyla birlikte yürütülen akademik çalışmaların sayısında da artış meydana gelmiştir. Priestley [11] konsol perdelerde dinamik büyütme etkisini NZS 4203-1992 [12] ve NZS 3101-1995 [7] esaslarına göre incelemiştir. Priestley [11] tarafından perdelerin kesme kuvveti talebinin hesabı için önerilen yaklaşım Denklem (1) ile verilmiştir. Modifiye edilmiş modal süperpozisyon (MMS) yaklaşımı, perde tabanında plastik mafsal oluştuktan sonra yüksek modlar sebebiyle kesme talebinde meydana gelecek artışın doğrudan dikkate alınması gerektiği varsayımına dayanarak geliştirilmiştir.

$$V_i = \left[V_1^2 + \mu^2 \left(V_2^2 + V_3^2 + ... \right) \right]^{0.5} \quad (1)$$

Denklem (1)'e göre; azaltılmış tasarım ivme spektrumu ile doğrusal analizden 1. mod için elde edilen kesme kuvveti (V_1), yüksek modlar için elde edilen kesme kuvvetlerinin süneklik katsayısı (μ) ile büyütülmüş değerleriyle birleştirilmektedir. Sullivan vd. [13], yapı kütlesini minimum %90 oranında hesaba katan titreşim modu sayısı ile MMS yaklaşımının uygulanmasını önermişlerdir.

Rutenberg ve Nsieri [14] süneklik düzeyi normal (DC-M) ve yüksek (DC-H) perde elemanlara ilişkin Eurocode-8 [8] esaslarının revizyona ihtiyaç duyduğunu belirtmişlerdir. Davranış katsayısı ile hâkim titreşim periyoduna bağlı olan dinamik büyütme katsayısı ve kesme kuvveti diyagramı önermişlerdir. Boivin ve Paultre [15] süneklik düzeyi yüksek konsol perdelerde, Luu vd. [16] süneklik düzeyi normal konsol perdelerde CSA A23.3-2014 [9] ve NBCC-2010 [17] esaslarına göre parametrik çalışma yürütmüşlerdir. Boivin ve Paultre [15] betonarme perdelerin tasarım kesme kuvvetinin hesabı için yeni bir yöntem ve kesme kuvveti diyagramı önermişlerdir. Luu vd. [16] incelediği yönetmeliklerin konsol perdelerde kesme talebini %15 ile %70 arasında daha az tahmin edilebileceğini ve perdelerin üst kısımlarında da plastik davranış olasılığının bulunduğunu belirtmişlerdir. Luu vd. [16], Rutenberg ve Nsieri [14] ile Boivin ve Paultre [15] tarafından önerilen kesme kuvveti diyagramlarını güncellemişlerdir. Luu vd. [16] tarafından önerilen kesme kuvveti diyagramı Şekil 2 (a)'da verilmiştir.

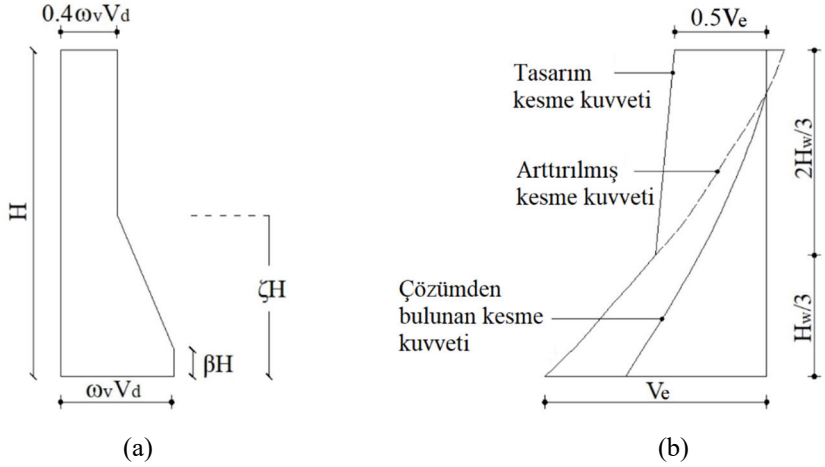

Şekil 2 - Kesme kuvveti diyagramları (a) Luu vd. [16] (b) TBDY-2018 [29]

Leng vd. [18], Najam ve Warnitchai [19], Khy vd. [20] çekirdek perdeli yüksek binalarda yürüttükleri çalışmalar sonucunda; zaman tanım alanında doğrusal olmayan analizlerden elde edilen kesme kuvvetlerinin, spektrum analizi ile elde edilen kesme kuvvetlerinden büyük olduğunu belirtmişlerdir. Khy vd. [20], ACI 318M-14 [21] esaslarına göre yürütülen spektrum analizi ile elde edilen perde kesme kuvvetlerinin tasarımda kullanılmaması gerektiğini vurgulamışlardır. Fatemi vd. [22] yüksek modların davranışa etkisini 8 katlı bir perde elemanda incelemek için hibrit testler gerçekleştirmiştir. Fatemi vd. [22] yürüttükleri deneysel çalışmada gözlemlenen kesme talebinin, CSA A23.3-2014'e [9] göre hesaplanan kesme kapasitesinden 2.27 kat daha büyük olduğunu belirtmişlerdir. Chaallal ve Gauthier [23], Fox vd. [24], Rivard vd. [25] bağ kirişli betonarme perdelerin kesme talebini araştırmışlardır. Rivard [25] dolu gövdeli perdelerde olduğu gibi bağ kirişli perdelerin kesme talebinde de yüksek modların etkisiyle artış meydana gelebileceğini ve bu durumun tasarım aşamasında dikkate alınması gerektiğini belirtmişlerdir.

Ülkemizde dinamik büyütme katsayısına ilk defa Deprem Bölgelerinde Yapılacak Binalar Hakkında Yönetmelik'te (DBYBHY-2007 [26]) yer verilmiş olup konuyla ilgili çalışmalar da ağırlıklı olarak bu yönetmelik esaslarına göre yürütülmüştür. Kazaz ve Gülkan [27] farklı perde oranına sahip temsili perde-çerçeve bina modellerinde dinamik büyütme katsayısını incelemişlerdir. Bina kat sayısının ve dayanım azaltma katsayısının fonksiyonu olarak önerilen dinamik büyütme katsayısının, 12 katlı ve periyodu 1.5 saniye kadar olan binalarda geçerli olduğunu belirtmişledir. Seçkin ve Doran [28], planda uzunluğu 1.5, 3 ve 4.5 metre, yüksekliği 30, 45 ve 60 metre olan dikdörtgen kesitli konsol perdelerde kesme güvenliğini, 2-boyutlu sonlu elemanlar yöntemiyle araştırmışlardır. Çalışmalarında, TBDY-2018 [29] esaslarına göre hesaplanan tasarım kesme kuvvetinin kesme talebini karşılamada yetersiz kaldığını belirtmişlerdir. Ayrıca, tasarım kesme kuvvetinin hesabında sadece dinamik büyütme katsayısının (β_v) yer aldığı denklemin (Denklem 3) dikkate alınmasıyla, perde elamanlarda kesme güvenliğinin sağlanacağı önerisini yapmışlardır.

2019 yılında yürürlüğe giren TBDY-2018'de [29] süneklik düzeyi yüksek perdelerin tasarım kesme kuvvetinin hesabında, dinamik büyütme katsayısı ile birlikte dayanım fazlalığı katsayısına da yer verilmiştir. TBDY-2018'e [29] göre, yüksekliğinin plandaki uzunluğuna oranı ikiden büyük ($H_w/l_w>2,0$) olan perdelerin enine donatı hesabında esas alınacak tasarım kesme kuvvetinin (V_e) belirlenmesi için iki ayrı hesap yapılması gerekmektedir. Süneklik düzeyi yüksek betonarme perdelerin tasarım kesme kuvveti, Denklem (2) ve Denklem (3) ile hesaplanan değerlerden küçük olanına eşit olmaktadır.

$$V_e = 1.2 D V_d \tag{2}$$

$$V_e = \beta_v \frac{(M_p)_t}{(M_d)_t} V_d \tag{3}$$

Denklemlerde yer alan simgelerden D, dayanım fazlalığı katsayısını; β_v, dinamik büyütme katsayısını; V_d ve $(M_d)_t$, sırasıyla düşey yükler ve deprem yüklerinin ortak etkisi altında hesaplanan kesme kuvvetini ve taban kesitindeki eğilme momentini; $(M_p)_t$, perdenin taban kesitinde hesaplanan plastik moment kapasitesini göstermektedir. Dinamik büyütme katsayısı, β_v sabit 1.5 değeriyle verilmiştir. $H_w/l_w>2,0$ koşulunu sağlayan perdeler için önerilen tasarım kesme kuvveti diyagramı Şekil 2 (b)'de verilmiştir. Perde kesitlerinin kesme dayanımı (V_r), Denklem (4) ile hesaplanmaktadır. Tasarım kesme kuvvetinin Denklem (5) ile verilen koşulları sağlaması gerekmektedir.

$$V_r = A_{ch}(0.65 f_{ctd} + \rho_{sh} f_{ywd}) \tag{4}$$

$$V_e \le V_r$$
$$V_e \le 0.85 A_{ch} \sqrt{f_{ck}} \tag{5}$$

Burada A_{ch}, perdenin brüt enkesit alanı; f_{ctd}, betonun tasarım çekme dayanımı; f_{ywd}, enine donatının tasarım akma dayanımı; f_{ck}, betonun karakteristik basınç dayanımı; p_{sh}, perdede yatay gövde donatılarının hacimsel oranıdır.

Bu çalışmada, örnek olarak seçilen 20 katlı betonarme perdeli-çerçeve sistemin dikdörtgen ve L-kesitli perde elemanlarında tasarım kesme kuvvetlerinin yeterliliği TBDY-2018 [29] esasları doğrultusunda araştırılmıştır. Literatürde yer alan çalışmalarda [24,30-32] değinilen eksikliği gidermek üzere, doğrusal/doğrusal olmayan sayısal analizler incelenen binanın 3-boyutlu sonlu eleman modelleri dikkate alınarak gerçekleştirilmiştir. Analizler neticesinde, L-kesitli perdede TBDY-2018'e [29] göre hesaplanan tasarım kesme kuvvetinin, mühendislik kabulleri ve tasarım varsayımları çerçevesinde kabul edilebilir bir oranla da olsa aşılmış olması, süneklik düzeyi yüksek betonarme perdelerde gevrek kırılma riskine işaret etmiştir. Bu sebeple, TBDY-2018'e [29] alternatif bir çözüm olarak, incelenen perdelerin kesme talepleri MMS yaklaşımı ile de araştırılmıştır. Sonuç olarak, literatürde kabul görmüş olan MMS yaklaşımının esas alınması durumunda ilgili perde elemanda kesme güvenliğinin sağlandığı görülmüştür.

2. ÇALIŞMADA İZLENEN YÖNTEM

TBDY-2018'de [29] deprem etkisi altındaki bina taşıyıcı sistemlerinin tasarımı için "Dayanıma Göre Tasarım" (DGT) ve "Şekil Değiştirmeye Göre Değerlendirme ve Tasarım" (ŞGDT) yaklaşımları önerilmiştir. Çalışmanın ilk aşamasında 20 katlı betonarme bir binanın tasarımı, DGT kapsamındaki doğrusal hesap yöntemlerinden biri olan mod birleştirme yöntemi ile gerçekleştirilmiştir. Tasarımı gerçekleştirilen binada zaman tanım alanında doğrusal olmayan analizler, Şekil Değiştirmeye Göre Değerlendirme ve Tasarım (ŞGDT) yaklaşımı kapsamında yürütülmüştür. TBDY-2018'de [29] deprem tasarım sınıfı (DTS) bir olan betonarme yapılarda DGT esaslarının uygulanabileceği sınır yükseklik 70 metre olarak verilmiştir. Betonarme perdelerde dinamik büyütme etkisinin bina yüksekliğine veya hâkim titreşim periyoduna bağlı olarak artacağını belirten çalışmalar da [3, 6, 11, 14, 27, 33] dikkate alınarak incelenen binanın yüksekliği, kat yüksekliğinin her katta 3 metre olduğu kabulü ile

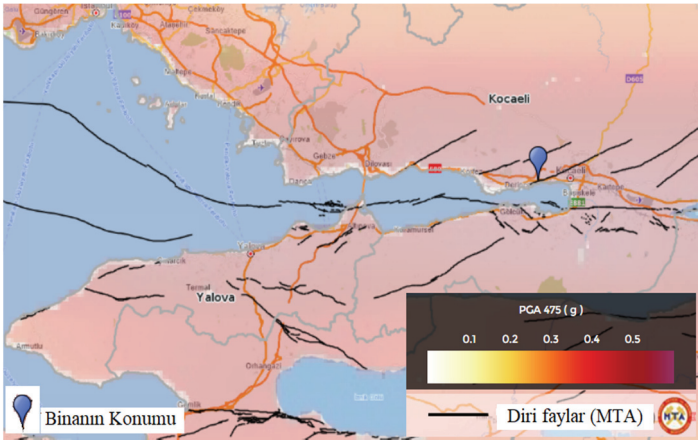

Şekil 3 - Binanın konumu [35]

60 metre olarak belirlenmiştir. Binanın coğrafi koordinatı, Kuzey Anadolu fay zonunun şiddetli deprem üretme potansiyeline sahip fay kolunun tehlikesi altında bulunan ve 1999 Marmara Depremi'nde büyük can ile mal kaybının yaşandığı Kocaeli ilinde seçilmiştir. Seçilen coğrafi koordinatın yerel zemin sınıfı, Ulusal Deprem Tehlikesini Azaltma Programı (NEHRP) [34] Kocaeli sınıflandırma haritasından faydalanılarak ZD olarak belirlenmiştir. Binanın konumu Şekil 3'te verilmiştir [35].

2.1. İncelenen Binanın Sayısal Modelleri

Kullanım amacı konut olarak düşünülen 20 katlı binanın taşıyıcı sistemi süneklik düzeyi yüksek betonarme çerçevelerden ve perdelerden oluşmaktadır. Binanın taşıyıcı sistemi

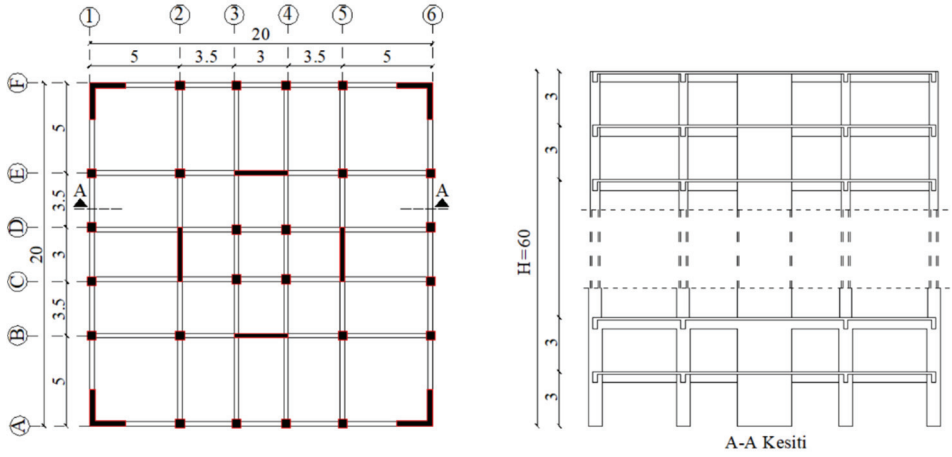

Şekil 4 - Kat planı ve kesit detayı (uzunluklar m birimindedir)

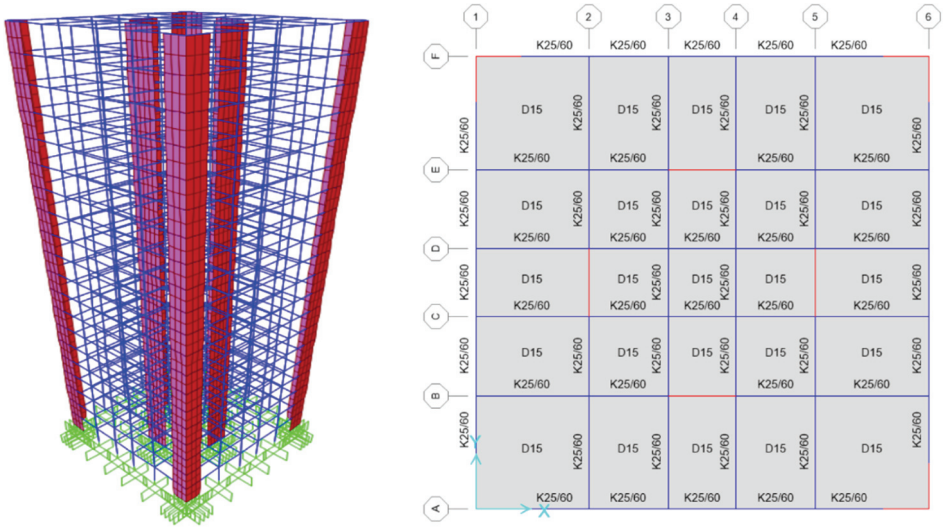

Şekil 5 - Binanın sayısal modeli

planda simetrik olarak düzenlenmiş olup, 20×20 metre uzunluklarındaki kat planı ve kesit detayı Şekil 4'te verilmiştir. İncelenen binanın dayanıma göre tasarımı mod birleştirme yöntemi kullanılarak yapılmıştır. Yapısal analizler, SAP2000 (versiyon 23) yazılımı [36] kullanılarak gerçekleştirilmiştir. Binanın sayısal modeli Şekil 5'te verilmiştir.

Kolon ve kirişler çubuk sonlu elemanlarla, perdeler kabuk sonlu elemanlarla, döşemeler de rijit diyafram kabulü ile modellenmiştir. Betonarme taşıyıcı sistem elemanlarının kesit özelliklerinin modellenmesinde TBDY-2018'de [29] verilen etkin kesit rijitliği çarpanları kullanılmıştır. Deprem etkilerinin süneklik düzeyi yüksek betonarme çerçeveler ve betonarme perdeler tarafından karşılanan binalar için taşıyıcı sistem davranış katsayısı (R) ve dayanım fazlalığı katsayısı (D) sırasıyla 7 ve 2.5 olmaktadır. Binanın kullanım amacına bağlı olan bina kullanım sınıfı (BKS) 3, tasarımda esas alınacak deprem tasarım sınıfı (DTS) 1 olarak belirlenmiştir. Binanın, DD-2 deprem yer hareketinin etkisi altında kontrollü hasar (KH) performans hedefini sağlaması gerekmektedir. Beton sınıfı C35, boyuna ve enine donatı için donatı çeliği sınıfı B420C seçilmiştir. Gerçekleştirilen tasarım neticesinde kolonların enkesit boyutları 1. ve 2. katlarda 0.75×0.75 m, 3. ve 6. katlar arasında 0.70×0.70 m, 7. ve 10. katlar arasında 0.6×0.6 m, 11. ve 20. katlar arasında 0.5×0.5 m olarak belirlenmiştir. Kirişlerin enkesit boyutu 0.25×0.60 m, döşeme kalınlığı da 0.15 m olarak seçilmiştir. İç akslarda yer alan dikdörtgen kesitli perdelerin plandaki uzunluğu 3 metre, gövde kalınlığı da yönetmelikte önerilen minimum değer olan 0.25 metredir. Dış akslarda yer alan L-kesitli perdelerin plandaki uzunluğu 2 metredir. TBDY-2018'de [29] süneklik düzeyi yüksek perdelerin minimum enkesit alanı için verilen koşulun kontrolü yapılmış ve L-kesitli perdelerin gövde kalınlığı 0.3 metre olarak hesaplanmıştır. Perdelerin plandaki uzunluğu belirlenirken; deprem yüklerinin etkisi altında perdelerin tabanında meydana gelen devrilme momentlerinin (M_{DEV}) toplamının, binanın tümü için tabanda meydana gelen toplam devrilme momentinin (M_o) %40'ından az ve %75'inden fazla olmayacaktır koşulu sağlanmıştır (Denklem 6).

$$0.40M_o < \Sigma M_{DEV} < 0.75M_o \tag{6}$$

Deprem yüklerinin etkisi altında, binanın tümü için tabanda meydana gelen toplam devrilme momenti 183697 kNm, perdelerin tabanında meydana gelen devrilme momentlerinin toplamı 89969 kNm olup, yönetmelikte verilen koşul Denklem (7) ile kontrol edilmiştir:

$$73479\ \text{kNm} < 89969\ \text{kNm} < 137773\ \text{kNm} \tag{7}$$

Perdelerin plandaki uzunluğu belirlenirken göreli kat ötelemesinin sınırlandırılması için verilen koşul da dikkate alınmıştır. Dolgu duvarların çerçeve elemanlarına, aralarında herhangi bir esnek derz veya bağlantı elemanı olmaksızın tamamen bitişik olması durumunda, binanın herhangi bir katında hesaplanan etkin göreli kat ötelemesi oranının Denklem (8) ile verilen koşulu sağlaması gerekmektedir. Burada κ katsayısı betonarme binalarda 1 olarak verilmiştir. λ katsayısı 0.423 olarak hesaplanmıştır. İncelenen binada en büyük göreli kat öteleme oranı 7. katta 0.006 olup izin verilen 0.008 değerinin altında kalmaktadır.

$$\lambda \frac{\delta_{i,max}^{(X)}}{h_i} < 0.008\kappa \quad (8)$$

Binanın toplam ağırlığı 108235 kN ve azaltılmış deprem yükü her iki doğrultu için 5450 kN'dur. Binanın, X-X ve Y-Y doğrultularındaki hâkim titreşim periyotları 2.12 saniyedir. Her iki deprem doğrultusu için %95 kütle katılım oranına 22. titreşim modunda ulaşılmıştır. Binanın ilk 10 titreşim moduna ait periyotlar ve kütle katılım oranları Tablo 1'de verilmiştir.

Tablo 1 - İlk 10 titreşim moduna ait periyotlar ve kütle katılım oranları

Titreşim Modu	Periyot (saniye)	Ux (%)	Uy (%)	Toplam Ux (%)	Toplam Uy (%)
1	2.12	0	0.733	0	0.733
2	2.12	0.733	0	0.733	0
3	1.54	0	0	0.733	0.733
4	0.69	0.124	0	0.857	0.733
5	0.69	0	0.124	0.857	0.857
6	0.50	0	0	0.857	0.857
7	0.37	0.045	0	0.902	0.857
8	0.37	0	0.045	0.902	0.902
9	0.26	0	0	0.902	0.902
10	0.24	0.004	0.023	0.906	0.925

TBDY-2018'de [29] süneklik düzeyi yüksek perdeler için verilen koşullar dikkate alınarak perdelerin boyutlandırılması ve donatı hesabı gerçekleştirilmiştir. Dikdörtgen kesitli perdenin kritik yüksekliği 6 metre, perde uç bölgesinin uzunluğu kritik perde yüksekliği boyunca 0.6 metredir. L-kesitli perdenin kritik yüksekliği 3 metre, perde uç bölgesinin uzunluğu kritik perde yüksekliği boyunca 0.6 metredir. Perdelere etkiyen iç kuvvetler dikkate alınarak oluşturulan taban enkesit detayları Şekil 6'da verilmiştir. Dikdörtgen kesitli perdenin uç bölgelerinde belirlenen 10ϕ14 boyuna donatı için hesaplanan alanın perde enkesit alanına oranı 0,0021'dir. Hesaplanan oran, kritik perde yüksekliğinde boyuna donatı için verilen minimum orandan (0,002) büyük olmaktadır. Perde gövdesinde belirlenen 16ϕ10 boyuna donatı için hesaplanan oran 0.0028 olup, minimum oran (0.0025) sağlanmaktadır. L-kesitli perdenin uç bölgesinde seçilen 16ϕ20 boyuna donatı için hesaplanan oran 0.0084 ve gövde bölgesinde seçilen 14ϕ20 boyuna donatı için hesaplanan oran 0.0183'tür. Yatay gövde donatısı dikdörtgen kesitli perde tabanında Φ10/130, L-kesitli perde tabanında Φ12/140 olarak belirlenmiştir. Yatay gövde donatılarının hacimsel oranları (p_{sh}), dikdörtgen kesitli perdede 0.0048 ve L-kesitli perdede 0.0054 olup, minimum oran olan 0.0025 sağlanmaktadır.

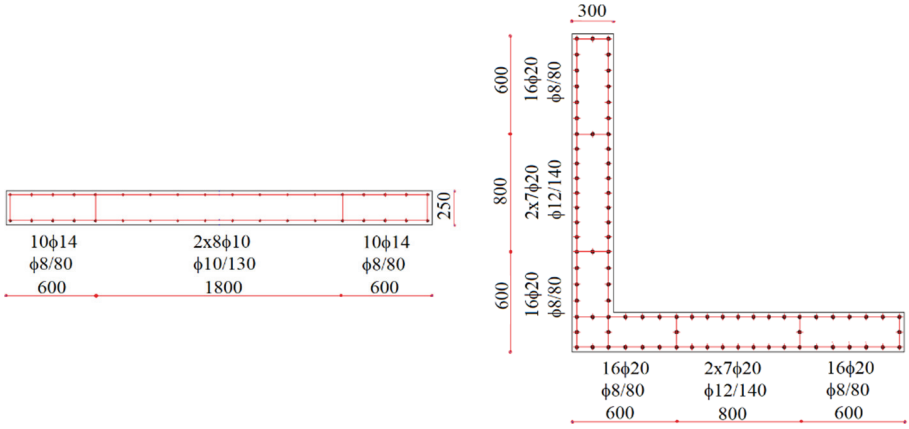

Şekil 6 - Perdelerin taban enkesit detayları

Tasarımı gerçekleştirilmiş binada zaman tanım alanında doğrusal olmayan analizler yapılmıştır. Çubuk sonlu elemanları olarak modellenen kolon ve kirişlerde doğrusal olmayan davranış, çubuk elemanların her iki ucuna atanan plastik mafsallar ile sağlanmıştır. Eksenel kuvvet ve eğilme momenti etkisinde bulunan kolon elemanlarda P-M2-M3 mafsal tanımı ile üç eksenli etkileşim diyagramı oluşturulmuş, kiriş elemanlarda eğilme davranışını temsil eden M3 mafsalı tanımlanmıştır. Perdelerin doğrusal olmayan davranışı için kompozit malzeme mekaniği prensiplerine dayanmakta olan çok katmanlı kabuk eleman modeli kullanılmıştır (Şekil 7). Çok katmanlı kabuk eleman modeli ile betonarme perdelerin doğrusal olmayan düzlem içi/düzlem dışı eğilme çifti ve düzlemsel eğilme-kesme çifti davranışları temsil edilebilmektedir. Kabuk eleman farklı kalınlığa sahip katmanlardan oluşabilmekte ve bu katmanlara farklı malzeme özellikleri tanımlanabilmektedir. Sonlu eleman yöntemi ile hesapta orta tabakanın eksenel birim şekil değiştirmesi ve eğriliği elde edilmektedir. Düzlem kesitin eğilmeden sonra düzlem kalacağı kabulüne göre diğer katmanlara ait birim şekil değiştirmeler ve eğrilikler hesaplanmaktadır. Bu değerlere karşı gelen gerilme, katmana tanımlanan malzemeye ait bünye denklemleri kullanılarak elde edilmektedir [37-39].

Sargılı ve sargısız beton davranışı için Mander modeli [40] kullanılmıştır. Perde elemanlarda çekme rijitleşmesi etkisi, Massicotte vd. [41] tarafından önerilmiş olan üç eğrili model ile dikkate alınmıştır. Donatı çeliğinin gerilme-şekil değiştirmesi eğrisi, TBDY-2018'de [29] verilen bağıntılar kullanılarak oluşturulmuştur. Doğrusal olmayan analizin başlangıç koşullarını belirlemek için öncelikle düşey yükler etkisi altındaki taşıyıcı sistemin artımsal statik hesabı yapılmıştır. Yatay deprem hesabı, dik doğrultulardaki deprem bileşenlerinin binaya eş zamanlı etkitilmesiyle gerçekleştirilmiştir. Analizlerde, Hilber-Hughes-Taylor integrasyon metodu ve Rayleigh sönüm modeli kullanılmıştır. Sönüm oranı, TBDY-2018'de [29] belirtildiği üzere %5 alınmıştır.

Perde elemanlarda doğrusal olmayan davranış için kullanılan modelleme yaklaşımının incelenmesi için Şekil 6'da detayı verilen 60 metre yüksekliğindeki dikdörtgen kesitli perdenin iki ayrı konsol modeli oluşturulmuştur. Çok katmanlı kabuk ile modellenen

betonarme perde, ayrıca çubuk eleman olarak modellenerek uçlarına fiber mafsal tanımlanmıştır. Kesit hücresi (fiber) modelinde; kesit içindeki beton yeteri kadar küçük hücrelerle ve çelik donatı çubukları tekil olarak modellenmekte olup, her bir hücrede doğrusal olmayan eksenel gerilme - birim şekil değiştirme bağıntıları çevrimsel olarak göz önüne alınabilmektedir. Oluşturulan iki ayrı modelde, perde elemana her kat seviyesinde $0.01f_{ck}A_{ch}$ değerinde eksenel kuvvet uygulanarak, doğrusal olmayan itme analizi gerçekleştirilmiştir. İtme analizleri sonucunda elde edilen taban kesme kuvveti - tepe yer değiştirmesi eğrileri Şekil 8'de verilmiştir. Şekil 8 incelendiğinde elde edilen eğrilerin, gerek taban kesme kuvvetleri gerekse de yer değiştirmeler bakımından uyumlu sonuç verdiği görülmüştür.

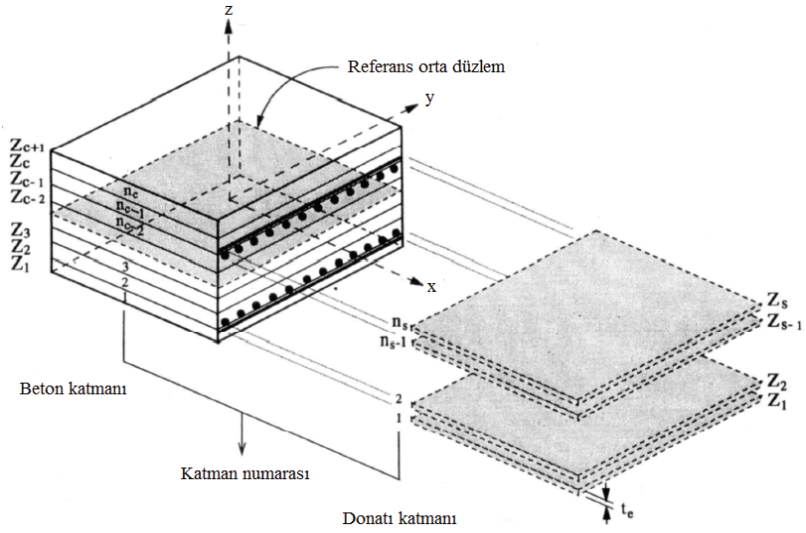

Şekil 7 - Çok katmanlı kabuk eleman modeli [39]

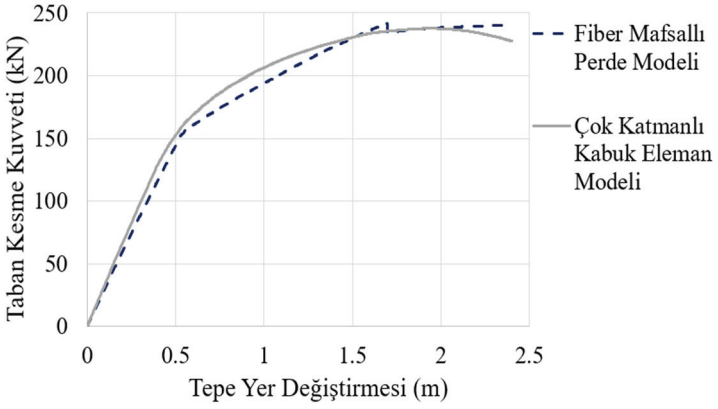

Şekil 8 - Konsol perdede elde edilen itme eğrileri

2.2. İvme Kayıtlarının Seçilmesi ve Ölçeklendirilmesi

TBDY-2018'e [29] göre zaman tanım alanında yapılacak hesaplarda gerçek ve benzeştirilmiş ivme kayıtları kullanılabilmektedir. Bu çalışmada doğrusal olmayan analizler benzeştirilmiş ivme kayıtları ile gerçekleştirilmiştir. İvme kayıtlarının seçiminde, moment büyüklüğü (M_w) 6.5'tan büyük olan ve kayıt yeri ile kaynak noktası arasındaki mesafesi (R_{jb}) 20 kilometreden küçük olan kayıtlar dikkate alınmıştır [42]. TBDY-2018'de [29] üst 30 metredeki ortalama kayma dalgası hızı $(V_s)_{30}$, ZD yerel zemin sınıfı için 180-360 m/s aralığında verilmiş olup seçilen ivme kayıtlarının $(V_s)_{30}$ değerleri bu aralıkta değişmektedir. Kuzey Anadolu fay hattının sağ yönlü doğrultu atımlı fay olması da ivme kayıtlarının fay tipinin seçiminde etken olmuştur. İvme kayıtları, Pasifik Deprem Mühendisliği Araştırma Merkezi (PEER) [43] tarafından oluşturulan veri tabanından elde edilmiştir. Bahsedilen kriterler dikkate alınarak seçilen ivme kayıtlarının özellikleri Tablo 2'de verilmiştir.

Tablo 2 - Seçilen ivme kayıtları (M_w: Moment büyüklüğü, R_{jb}: Joyner-Boore mesafesi, $(V_s)_{30}$: Üst 30 metredeki ortalama kayma dalgası hızı, D.A: Doğrultu atımlı fay)

Deprem	İstasyon	Bileşenler	M_w	R_{jb} (km)	$(V_s)_{30}$ (m/s)	Fay tipi
Imperial Valley	Brawley Airport	225, 315	6.53	8.54	208.71	D.A
Imperial Valley	Calexico Fire S.	225, 315	6.53	10.45	231.23	D.A
Imperial Valley	EC County Center	2, 92	6.53	7.31	192.05	D.A
Kobe	Port Island	0, 90	6.90	3.31	198.00	D.A
Kobe	Shin-Osaka	0, 90	6.90	19.14	256.00	D.A
Kocaeli	Düzce	180, 270	7.51	13.60	281.86	D.A
Kocaeli	Yarımca	60, 150	7.51	1.38	297.00	D.A
Superstition Hills	Kornbloom Road	270, 360	6.54	18.48	266.01	D.A
Superstition Hills	Westmorland Fire S.	90, 180	6.54	13.03	193.67	D.A
Düzce	Düzce	180, 270	7.14	0.00	281.86	D.A
Erzincan	Erzincan	NS, EW	6.69	0.00	352.05	D.A

50 yılda aşılma olasılığı %10 olan standart deprem yer hareketi düzeyine (DD-2) karşı gelen yatay elastik tasarım spektrumu, Afet ve Acil Durum Yönetimi Başkanlığı (AFAD) [35] tarafından hazırlanan deprem tehlike haritası web uygulaması kullanılarak oluşturulmuştur. Seçilen ivme kayıtları, SeismoMatch yazılımı [44] ile yatay elastik tasarım spektrumuna eşleştirilirken; dönüştürülen kayıtlara ait bileşke spektrumların ortalamasının genlikleri, tüm

periyotlar için tasarım spektrumunun genliklerinden daha küçük olmayacaktır koşulu uygulanmıştır. İvme kayıtlarının ortalama spektrumu ile elastik tasarım ivme spektrumu Şekil 9'da verilmiştir.

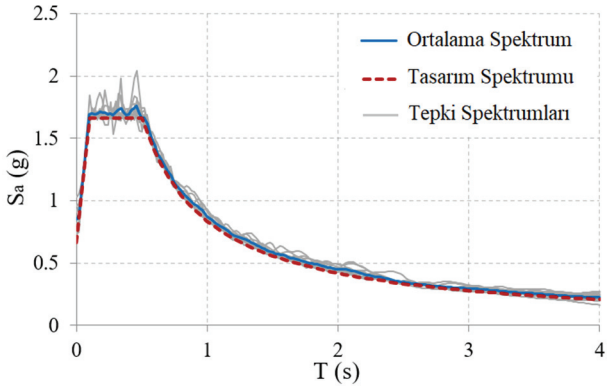

Şekil 9 - Seçilen ivme kayıtlarının ortalama spektrumu

3. ANALİZ SONUÇLARININ KARŞILAŞTIRILMASI

Bu bölümde; Denklem (2) ve Denklem (3) ile TBDY-2018'e [29] göre hesaplanan kesme kuvveti değerleri, Denklem (4) ile hesaplanan kesme kapasiteleri, 11 ivme kaydı ile yürütülen analizlerden elde edilen değerlerin ortalaması olan talep değerleri, modifiye edilmiş modal süperpozisyon (MMS) yaklaşımına göre Denklem (1) ile hesaplanan kesme kuvveti değerleri dikdörtgen ve L-kesitli perdelerin yükseklikleri boyunca birlikte verilmiştir (Şekil 10-11).

İncelenen dikdörtgen ve L-kesitli perdelerin tasarım kesme kuvvetleri, dayanım fazlalığı katsayısını (D) içeren Denklem (2) ile hesaplanan kesme kuvvetlerine eşittir. Dikdörtgen kesitli perdenin taban kesitinde Denklem (2) ile hesaplanan kesme kuvveti 1914 kN, Denklem (3) ile hesaplanan kesme kuvveti 2209 kN değerindedir. Dikdörtgen kesitli perdenin taban kesitinin tasarım kesme kuvveti, Denklem (2) ve Denklem (3) ile hesaplanan değerlerden küçük olanına karşı gelen 1914 kN olmaktadır. L-kesitli perdenin taban kesitinde Denklem (2) ile hesaplanan kesme kuvveti 1701 kN, Denklem (3) ile hesaplanan kesme kuvveti 2337 kN değerindedir. L-kesitli perdenin taban kesitinin tasarım kesme kuvveti 1701 kN olarak belirlenmiştir. Dikdörtgen ve L-kesitli perdelerin taban kesitindeki kesme talepleri sırasıyla 1633 kN ve 1825 kN değerindedir. Dikdörtgen kesitli perdenin taban kesitinde elde edilen kesme talebinin tasarım kesme kuvvetine oranı %85.3'tür. Dikdörtgen kesitli perdenin yüksekliği boyunca hesaplanan tasarım kesme kuvveti değerleri, kesme talebini karşılamada yeterli olmuştur. L-kesitli perdenin taban kesitinde hesaplanan tasarım kesme kuvveti, kesme talebini karşılamada yetersiz kalmıştır. L-kesitli perdenin taban kesitinde elde edilen kesme talebinin tasarım kesme kuvvetine oranı %107.3'tür. Şekil 11 incelendiğinde, L-kesitli perdede tasarım kesme kuvvetinin sadece taban kesitinde değil binanın 2. katında da aşıldığı görülmektedir. L-kesitli perde için binanın 2. katında elde edilen talep/tasarım kesme kuvveti oranı (%101), kesme kırılması riskine karşı önlemlerin perdenin üst kısımlarında da dikkate alınması gerektiğini göstermektedir. İncelenen perdelerde hesaplanan kesme kuvveti oranları binanın ilk 7 katı için Tablo 3'te verilmiştir.

Dikdörtgen kesitli perdenin taban kesitinin kesme kapasitesi 1996 kN, L-kesitli perdenin taban kesitinin kesme kapasitesi 1718 kN'dur. L-kesitli perdenin taban kesitinde hesaplanan kesme kapasitesi %6.2 oranında aşılmıştır. İncelenen perdelerde hesaplanan talep/kapasite oranları Tablo 3'te verilmiştir. Perdelerin kesme kapasiteleri, minimum enine donatı kullanılan kesitten itibaren sabit kalmıştır.

İncelenen perdelerin yükseklikleri boyunca Denklem (3) ile hesaplanan kesme kuvveti değerleri, kesme taleplerini güvenle karşılamaktadır. Kesme talebinin Denklem (3) ile hesaplanan kesme kuvvetine en büyük oranı, dikdörtgen kesitli perde için binanın 3. katında %80; L-kesitli perde için binanın 4. katında %87 değerindedir.

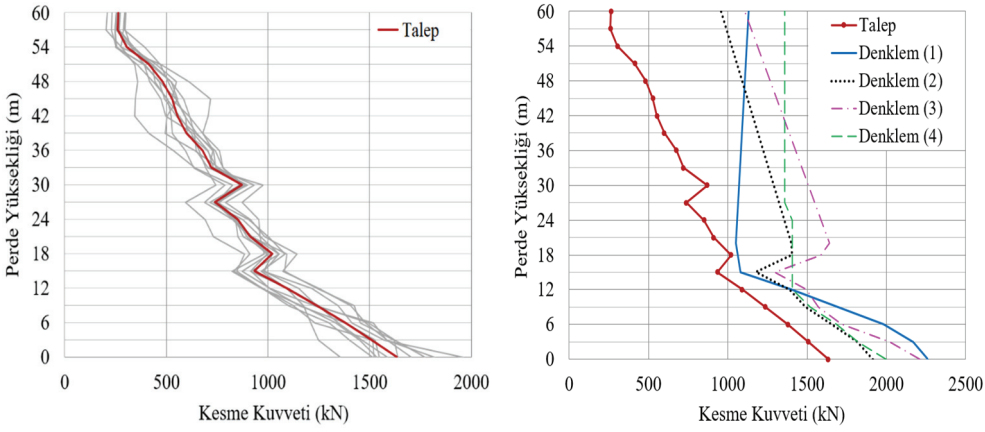

Şekil 10 - Dikdörtgen kesitli perdenin kesme kuvveti diyagramı (a) Ortalama dağılım (b) Denklem (1), (2), (3) ve (4) ile elde edilen kesme kuvveti dağılımları

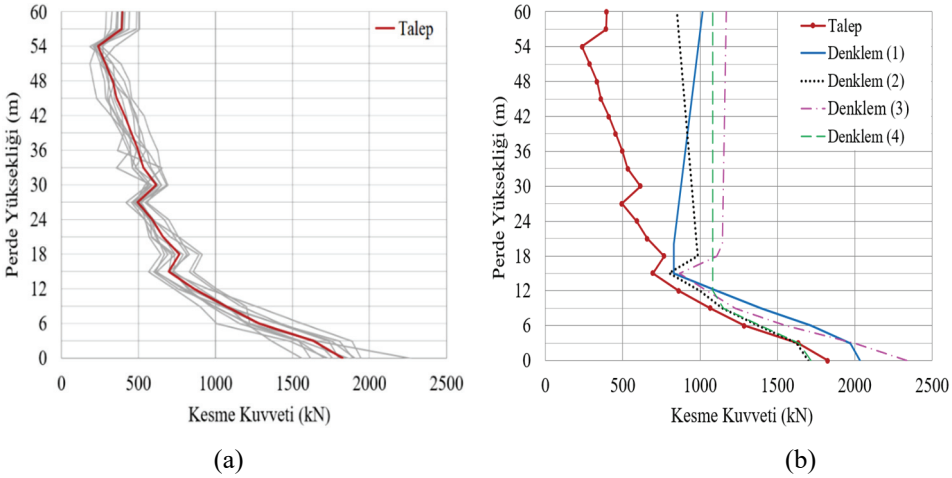

Şekil 11 - L-kesitli perdenin kesme kuvveti diyagramı (a) Ortalama dağılım (b) Denklem (1), (2), (3) ve (4) ile elde edilen kesme kuvveti dağılımları

Tablo 3 - İncelenen perdelerde hesaplanan kesme kuvveti oranları (D: Dikdörtgen kesitli perde, L: L-kesitli perde)

	Talep/Denklem (1)		Talep/Denklem (2)		Talep/Denklem (3)		Talep/ Denklem (4)	
KAT	D	L	D	L	D	L	D	L
1	0.72	0.90	0.85	1.07	0.74	0.78	0.82	1.06
2	0.69	0.83	0.83	1.01	0.75	0.82	0.83	1.00
3	0.70	0.75	0.83	0.93	0.80	0.83	0.82	0.93
4	0.73	0.76	0.83	0.94	0.79	0.87	0.81	0.93
5	0.78	0.78	0.78	0.86	0.73	0.83	0.77	0.80
6	0.86	0.84	0.79	0.87	0.72	0.80	0.66	0.64
7	0.95	0.92	0.73	0.78	0.64	0.69	0.73	0.71

İncelenen binada ilk sekiz titreşim moduna ait modal etkin kütlelerinin toplamı, toplam kütlenin %90'ına eşit olmaktadır. İlk sekiz titreşim moduna karşı gelen kesme kuvvetleri doğrusal analiz (R=7) ile belirlenmiş ve bu değerler Denklem (1)'e göre birleştirilmiştir. Kesme kuvvetleri Denklem (1)'e göre birleştirilirken her bir titreşim modu için hesaplanan deprem yükü azaltma katsayısı (R_a) kullanılmıştır. Deprem yükü azaltma katsayısı (R_a) hesaplanırken tasarım spektrumunun köşe periyodu (T_B) 0.503 saniye, bina önem katsayısı (I) "1", dayanım fazlalığı katsayısı (D) "2.5" olarak alınmıştır. Dikdörtgen ve L-kesitli perdelerde izlenen hesap adımları Tablo 4 ve 5'te verilmiştir. Titreşim modlarına ait kesme değerleri MMS yaklaşımına göre birleştirilirken, 1. moda karşı gelen azaltılmış kesme kuvveti doğrudan kullanıldığından, bu moda ait katsayı hesaplarda "1" alınmıştır.

Tablo 4 – Dikdörtgen kesitli perdede Denklem (1)'in uygulanması

Titreşim Modu	V (kN)	T (s)	R_a (T)	$R_a^2 \times V^2$
1	506.7	2.12	1	256741
2	0	2.12	7	0
3	0	1.54	7	0
4	53.8	0.69	7	141818
5	271.3	0.69	7	3607804
6	0	0.50	6.97	0
7	50.7	0.37	5.82	87028
8	172.8	0.37	5.82	1010878

Dikkate alınan titreşim modları için hesaplanan $R_a^2 \times V^2$ değerleri Denklem (9) ile birleştirilerek dikdörtgen kesitli perdenin taban kesme kuvveti hesaplanmıştır.

$$V_{taban} = \left[256741 + 141818 + 3607804 + 87028 + 1010878\right]^{0.5} = 2259\,\text{kN} \quad (9)$$

Tablo 5 – L-kesitli perdede Denklem (1)'in uygulanması

Titreşim Modu	V (kN)	T (s)	R_a (T)	$R_a^2 \times V^2$
1	438.4	2.12	1	192186
2	0	2.12	7	0
3	0	1.54	7	0
4	77.3	0.69	7	293100
5	234.4	0.69	7	2693055
6	0	0.50	6.97	0
7	57.5	0.37	5.82	111750
8	158.4	0.37	5.82	849069

Dikkate alınan titreşim modları için hesaplanan $R_a^2 \times V^2$ değerleri Denklem (10) ile birleştirilerek L-kesitli perdenin taban kesme kuvveti hesaplanmıştır.

$$V_{taban} = \left[192186 + 293100 + 2693055 + 111750 + 849069\right]^{0.5} = 2034\,\text{kN} \quad (10)$$

MMS yaklaşımı ile hesaplanan kesme kuvvetleri, TBDY-2018'de [29] perde yüksekliği boyunca verilen diyagrama göre birleştirilmiştir. Kesme taleplerinin, MMS yaklaşımı ile hesaplanan kesme kuvvetlerine oranı Tablo 3'te verilmiştir. Kesme talebinin Denklem (1) ile hesaplanan kesme kuvvetine oranı, dikdörtgen kesitli perdenin tabanında %72; L-kesitli perdenin tabanında %90 değerindedir. İncelenen oranın dikdörtgen ve L-kesitli perdelerdeki en büyük değerleri binanın 7. katında sırasıyla %95 ve %92 olarak elde edilmiştir. MMS yaklaşımı ile incelenen perdelerde hesaplanan kesme kuvvetleri, kesme taleplerini güvenli bir şekilde karşılamaktadır.

TBDY-2018'de [29] verilen tasarım kesme kuvveti diyagramına göre perde yüksekliğinin 1/3'ünde ($H_w/3$) hesaplanan kesme kuvveti, perdenin üst ucuna doğrusal olarak birleştirilmektedir. Perdenin en üst ucundaki değer, perde tabanında hesaplanan kesme kuvvetinin 0,5 katına eşit olmaktadır. İncelenen L-kesitli perdede yüksekliğin 1/3'ünde Denklem (3) ile hesaplanan kesme kuvveti değerinin (1143 kN), perde üst ucunda hesaplanan değerden (1169 kN) küçük olduğu görülmüştür. Benzer şekilde, Denklem (1) ile elde edilen dağılımlarda da kesme kuvveti değerleri yükseklikle birlikte artmaktadır. Luu vd. [16] tarafından önerilen kesme kuvveti diyagramına (Şekil 2-a) göre perdenin en üst ucundaki değer, perde tabanında hesaplanan kesme kuvvetinin 0,4 katına eşit olmaktadır. TBDY-

2018'de [29] verilen kesme kuvveti diyagramında, perdenin en üst ucundaki değerin perde tabanında hesaplanan kesme kuvvetinin 0,4 katına eşit alınmasıyla elde edilen dağılımlar ile üst katların kesme güvenliği, bahsedilen duruma imkân vermeden yine sağlanmaktadır (Şekil 12).

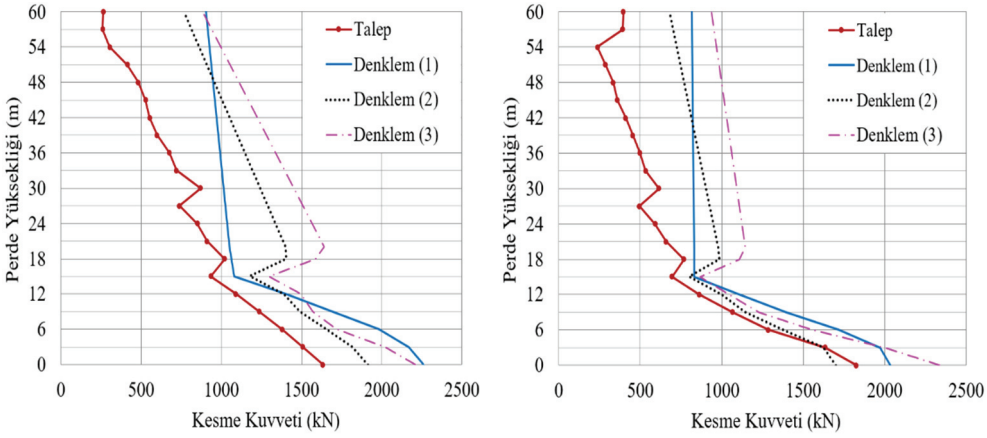

Şekil 12 - Güncellenen kesme kuvveti dağılımları (a) Dikdörtgen kesitli perde (b) L-kesitli perde

4. SONUÇLAR

Bu çalışmada, yüksek modların etkisiyle betonarme perdelerin kesme talebinde meydana gelecek artış TBDY-2018 esaslarına göre araştırılmıştır. Bu doğrultuda, taşıyıcı sistemi süneklik düzeyi yüksek betonarme çerçevelerden ve perdelerden oluşan 20 katlı betonarme bir binanın tasarımı Dayanıma Göre Tasarım (DGT) yaklaşımı ile gerçekleştirilmiş ve tasarlanan binada zaman tanım alanında doğrusal olmayan analizler gerçekleştirilmiştir. Doğrusal analizlerden elde edilen kesme kuvveti değerleri ve doğrusal olmayan analizlerden elde edilen kesme talepleri dikdörtgen ve L-kesitli perdelerin yüksekliği boyunca karşılaştırılmış ve elde edilen bulgular özetlenmiştir:

1. TBDY-2018 esaslarına göre süneklik düzeyi yüksek dikdörtgen kesitli perdede hesaplanan tasarım kesme kuvveti kesme talebini güvenle karşılarken, L-kesitli perdenin tasarım kesme kuvveti %7.3 oranında aşılmıştır. İncelenen bina özelinde L-kesitli perdede elde edilen oran, mühendislik kabulleri ve tasarım varsayımları çerçevesinde kabul edilebilir bir seviyede olmakla birlikte, süneklik düzeyi yüksek betonarme perdelerde gevrek kırılma riskine işaret edebilecek olup konuyla ilgili çalışmalara olan ihtiyacı vurgulamaktadır.

2. L-kesitli perdede tasarım kesme kuvveti sadece taban kesitinde değil, binanın 2. katında da aşılmıştır. Bu durum, perde tabanı ile birlikte perde yüksekliği boyunca da kesme kırılmasına karşı önlem alınması gerektiğini göstermektedir.

3. Tasarım kesme kuvvetinin hesabında sadece dinamik büyütme katsayısının (β_v) yer aldığı denklemin dikkate alınmasıyla kesme güvenliğinin sağlanacağı önerisi [28], incelenen perdeler için kesme talebini güvenle karşılayan sonuçlar vermiştir.

4. Analiz sonuçları, modifiye edilmiş modal süperpozisyon (MMS) yaklaşımı ile perde elemanlarda kesme güvenliğini sağlayan bir tasarımın gerçekleştirilebileceğini işaret etmektedir.

Bu çalışmada elde edilen sonuçlar, incelenen taşıyıcı sistem ve seçilen ivme kayıtları kapsamında değerlendirilmelidir. Ayrıca, benzer bir çalışmanın betonarme boşluklu perdeli binalar için de yapılması önerilir.

Semboller

A_{ch}	Boşluksuz perdenin brüt enkesit alanı
D	Dayanım fazlalığı katsayısı
f_{ck}	Betonun karakteristik basınç dayanımı
f_{ctd}	Betonun tasarım çekme dayanımı
f_{ywd}	Enine donatının tasarım akma dayanımı
H_w	Perde yüksekliği
l_w	Perdenin plandaki uzunluğu
$(M_d)_t$	Perdenin taban kesitinde yük katsayıları ile çarpılmış düşey yükler ve deprem yüklerinin ortak etkisi altında hesaplanan moment
$(M_p)_t$	Perdenin taban kesitinde f_{ck} , f_{yk} ve çeliğin dayanım artışı göz önüne alınarak hesaplanan moment kapasitesi
M_w	Moment büyüklüğü
R	Taşıyıcı sistem davranış katsayısı
R_a (T)	Deprem yükü azaltma katsayısı
R_{jb}	Joyner-Boore mesafesi
S_a (g)	Spektral ivme
T (s)	Doğal titreşim periyodu
V_d	Yük katsayıları ile çarpılmış düşey yükler ve deprem yüklerinin ortak etkisi altında hesaplanan kesme kuvveti
V_e	Perdede enine donatı hesabında esas alınan kesme kuvveti
V_i	Modifiye edilmiş modal süperpozisyon yaklaşımı ile perdede hesaplanan kesme kuvveti
V_r	Perde kesitinin kesme kuvveti dayanımı

$(V_s)_{30}$ Üst 30 metredeki ortalama kayma dalgası hızı

β_v Dinamik büyütme katsayısı

ρ_{sh} Perdede yatay gövde donatılarının hacimsel oranı

μ Süneklik katsayısı

ω_v Dinamik büyütme katsayısı

Kaynaklar

[1] Kocaeli Üniversitesi, 6 Şubat 2023 Kahramanmaraş Depremleri Saha İnceleme Raporu, KÜV Yayınları Nisan-2023, https://www.kocaeli.edu.tr/KOU_DEPREM_RAPORU1.pdf.

[2] Bursa Teknik Üniversitesi, Deprem Mühendisliği Uygulama ve Araştırma Merkezi, 6 Şubat 2023 Kahramanmaraş Depremleri İnceleme ve Değerlendirme Raporu, 2023/02, https://depo.btu.edu.tr/dosyalar/deprem/Dosyalar/BT%C3%9C%20DEPREM%20RAPORU_V18.pdf.

[3] Blakeley, R.W.G., Cooney, R.C., Megget, L.M., Seismic Shear Loading at Flexural Capacity in Cantilever Wall Structures, Bull. N. Z. Soc. Earth. Eng., 8(4), 278-290, 1975.

[4] Eibl, J., Keintzel, E., Seismic Shear Forces in RC Cantilever Shear Walls, Proceedings of Ninth World Conference on Earthquake Engineering, Kyoto, Japan, 1988.

[5] Paulay, T., Priestley, M.J.N., Seismic Design of Reinforced Concrete and Masonry Buildings, John Wiley & Sons, New York, 1992.

[6] Krawinkler, H., Importance of Good Nonlinear Analysis, Struct. Des. Tall Spec. Build., 15(5), 515-531, 2006.

[7] NZS 3101, The Design of Concrete Structures (Parts 1&2), New Zealand Standard, Wellington, 1995.

[8] Eurocode 8, Design of Structures for Earthquake Resistance - Part 1: General Rules, Seismic Actions and Rules for Buildings, European Committee for Standardization, Brussels, 2004.

[9] CSA A23.3, Design of Concrete Structures, Canadian Standards Association, Ontario, 2004.

[10] ACI 318M-19, Building Code Requirements for Structural Concrete and Commentary, American Concrete Institute, Farmington Hills, MI, 2019.

[11] Priestley, M.J.N., Does Capacity Design Do the Job? An Examination of Higher Mode Effects in Cantilever Walls, Bull. N. Z. Soc. Earth. Eng., 36(4), 276-292, 2003.

[12] NZS 4203, Code of Practice for the General Structural Design and Design Loadings for Buildings, New Zealand Standard, Wellington, 1992.

[13] Sullivan, T.J., Priestley, M.J.N, Calvi, G.M., Estimating the Higher-Mode Response of Ductile Structures, J. Earth. Eng., 12(3), 456-472, 2008.

[14] Rutenberg, A., Nsieri, E., The Seismic Shear Demand in Ductile Cantilever Wall Systems and the EC8 Provisions, Bull. Earth. Eng., 4, 1-21, 2006.

[15] Boivin, Y., Paultre, P., Seismic Force Demand on Ductile Reinforced Concrete Shear Walls Subjected to Western North American Ground Motions: Part 2 – New Capacity Design Methods, Can. J. Civ. Eng., 39(7), 738-750, 2012.

[16] Luu, H., Léger, P., Tremblay, R., Seismic Demand of Moderately Ductile Reinforced Concrete Shear Walls Subjected to High-Frequency Ground Motions, Can. J. Civ. Eng., 41(2), 125-135, 2014.

[17] NBCC-2010, National Building Code of Canada, National Research Council of Canada, Ottawa, 2010.

[18] Leng, K., Chintanapakdee, C., Hayashikawa, T., Seismic Shear Forces in Shear Walls of a Medium-Rise Building Designed by Response Spectrum Analysis, Eng. J., 18(4), 73-95, 2014.

[19] Najam, F.A., Warnitchai, P., A Modified Response Spectrum Analysis Procedure to Determine Nonlinear Seismic Demands of High-Rise Buildings with Shear Walls, Struct. Des. Tall Spec. Build., 27(1), 1-19, 2017.

[20] Khy, K., Chintanapakdee, C., Warnitchai, P., Wijeyewickrema, A.C., Eng. Struct., 180, 295-309, 2019.

[21] ACI 318M-14, Building Code Requirements for Structural Concrete and Commentary, American Concrete Institute, Farmington Hills, 2014.

[22] Fatemi, H., Paultre, P., Lamarche, C.P., Experimental Evaluation of Inelastic Higher-Mode Effects on the Seismic Behavior of RC Structural Walls, *J. Struct. Eng*., 146(4), 1-15, 2020.

[23] Chaallal, O., Gauthier, D., Seismic Shear Demand on Wall Segments of Ductile Coupled Shear Walls, Can. J. Civ. Eng., 27(3), 506-522, 2000.

[24] Fox, M.J., Sullivan, T.J., Beyer, K., Capacity Design of Coupled RC Walls, J. Earth. Eng., 18(5), 735-758, 2014.

[25] Rivard, G., Ambroise, S., Paultre, P., Inelastic seismic shear amplification due to higher mode effects in reinforced concrete coupled walls, Earthquake Spectra, 38(2), 1357-1381, 2021.

[26] DBYBHY-2007, Deprem Bölgelerinde Yapılacak Binalar Hakkında Yönetmelik, Bayındırlık ve İskân Bakanlığı, Ankara, 2007.

[27] Kazaz, İ, Gülkan, P., Dynamic Shear Force Amplification in Regular Frame–Wall Systems, Struct. Des. Tall Spec. Build., 25(2), 112–135, 2016.

[28] Seckin, A., Doran, B., A new approach for the computation of design shear force in reinforced concrete walls subjected to seismic loads, Struct. Des. Tall Spec. Build., 32(2), e1998, 2023.

[29] TBDY-2018, Türkiye Bina Deprem Yönetmeliği, Afet ve Acil Durum Yönetimi Başkanlığı, Ankara, 2018.

[30] Rad, B.R., Seismic Shear Demand in High-Rise Concrete Walls, Ph.D. Dissertation, The University of British Columbia, The Faculty of Graduate Studies (Civil Engineering), Vancouver, 2009.

[31] Kappos, A.J., Antoniadis, P.S., Evaluation and Suggestions for Improvement of Seismic Design Procedures for R/C Walls in Dual Systems, Earthq. Eng. Struct. Dyn., 40(1), 35-53, 2010.

[32] Dezhdar, E., Seismic Response of Cantilever Shear Wall Buildings, Ph.D. Dissertation, The University of British Columbia, The Faculty of Graduate Studies (Civil Engineering), Vancouver, 2012.

[33] Derecho, A., Corley, W., Design Requirements for Structural Walls in Multistory Buildings, Proceedings of the Eighth World Conference on Earthquake Engineering, San Francisco, California, 1984.

[34] NEHRP, Recommended Provisions for Seismic Regulations for New Buildings and Other Structures (FEMA 450), Building Seismic Safety Council, Washington, 2003.

[35] AFAD, Afet Acil Durum Yönetimi Başkanlığı, https://tdth.afad.gov.tr/TDTH/main.xhtml.

[36] SAP2000 v23, Structural and Earthquake Engineering Software, Computers & Structures, California.

[37] Loo, C.H., Guan, H., Cracking and Punching Shear Failure Analysis of RC Flat Plates, J. Struct. Eng., 123(10), 1321-1330, 1997.

[38] Miao, Z.W., Lu, X. Z., Jiang, J.J., Ye, L.P., Nonlinear FE Model for RC Shear Walls Based on Multi-Layer Shell Element and Micro-plane Constitutive Model, Computational Methods in Engineering & Science, Berlin, Heidelberg, Tsinghua University Press & Springer, 2006.

[39] Guan H., Loo C.H., Flexural and Shear Failure Analysis of Reinforced Concrete Slabs and Flat Plates, Adv. Struct. Eng., 1(1), 71-85, 1997.

[40] Mander, J.B., Priestley, M.J.N., Park R., Observed Stress Strain Behavior of Confined Concrete, J. Struct. Eng., 114(8), 1827-1849, 1988.

[41] Massicotte, B., Elwi, A.E., MacGregor, J.G., Tension stiffening model for planar reinforced concrete members, J. Struct. Eng., 116(11), 3039-3058, 1990.

[42] Somerville, P.G., Smith, N. F., Graves, R.W., Abrahamson N.A., Modification of Empirical Strong Ground Motion Attenuation Relations to Include the Amplitude and Duration Effects of Rupture Directivity, Seismol. Res. Lett. 68(1), 199-222, 1997.

[43] PEER, Pacific Earthquake Engineering Research Center, PEER Ground Motion Database, California, http://peer.berkeley.edu/smcat/.

[44] SeismoMatch version 2018 (Academic License), Earthquake Engineering Software Solutions, Seismosoft.

Turkish Journal of Civil Engineering (formerly Teknik Dergi)
Manuscript Drafting Rules

1. The whole manuscript (text, charts, equations, drawings etc.) should be arranged in Word and submitted in ready to print format. The article should be typed on A4 (210 x 297 mm) size paper using 10 pt (main title 15 pt) Times New Roman font, single spacing. Margins should be 40 mm on the left and right sides and 52.5 mm at the top and bottom of the page.
2. Including drawings and tables, articles should not exceed 25 pages, technical notes 10 pages.
3. Your contributed manuscript must be sent over the DergiPark system. (http://dergipark.gov.tr/tekderg)
4. The text must be written in a clear and understandable language, conform to the grammar rules. Third singular person and passive tense must be used, and no inverted sentences should be contained.
5. Title must be short (10 words maximum) and clear, and reflect the content of the paper.
6. Sections should be arranged as: (i) abstract and keywords, (ii) title, abstract and keywords in the other language, (iii) main text, (iv) symbols, (v) acknowledgements (if required) and (vi) references.
7. Both abstracts should briefly describe the object, scope, method and conclusions of the work and should not exceed 100 words. If necessary, abstracts may be re-written without consulting the author. At least three keywords must be given. Titles, abstracts and keywords must be fitted in the first page leaving ten line space at the bottom of the first page and the main text must start in the second page.
8. Section and sub-section titles must be numbered complying with the standard TS1212.
9. Symbols must conform to the international rules; each symbol must be defined where it appears first, additionally, a list of symbols must be given in alphabetic order (first Latin, then Greek alphabets) at the end of the text (before References).
10. Equations must be numbered and these numbers must be shown in brackets at the end of the line.
11. Tables, drawings and photographs must be placed inside the text, each one should have a number and title and titles should be written above the tables and below the drawings and photographs.
12. Only SI units must be used in the manuscripts.
13. Quotes must be given in inverted commas and the source must be indicated with a reference number.
14. Acknowledgement must be short and mention the people/ institutions contributed or assisted the study.
15. References must be numbered (in brackets) in the text referring to the reference list arranged in the order of appearance in the text. References must include the following information:

    If the reference is an article: Author's surname, his/her initials, other authors, full title of the article, name of the journal, volume, issue, starting and ending pages, year of publication.

    Example : Naghdi, P. M., Kalnins, A., On Vibrations of Elastic Spherical Shells. J. Appl. Mech., 29, 65-72, 1962.

    If the reference is a book: Author's surname, his/her initials, other authors, title of the book, volume number, editor if available, place of publication, year of publication.

    Example : Kraus. H., Thin Elastic Shells, New York. Wiley, 1967.

    If the reference is a conference paper: Author's surname, his/her initials, other authors, title of the paper, title of the conference, location and year.

    If the source is a thesis: Author's surname, his/her initials, thesis title, level, university, year.

    If the source is a report: Author's surname, his/her initials, other authors, title of the report, type, number, institution it is submitted to, publication place, year.
16. Discussions to an article published in Turkish Journal of Civil Engineering (formerly Teknik Dergi) should not exceed two pages, must briefly express the addressed points, must criticize the content, not the author and must be written in a polite language. Authors' closing remarks must also follow the above rules.
17. A separate note should accompany the manuscript. The note should include, (i) authors' names, business and home addresses and phone numbers, (ii) brief resumes of the authors and (iii) a statement "I declare in honesty that this article is the product of a genuinely original study and that a similar version of the article has not been previously published anywhere else" signed by all authors.
18. Copyright has to be transferred to UCTEA Turkish Chamber of Civil Engineers. The standard copyright form signed by the authorised author should therefore be submitted together with the manuscript.

UCTEA Turkish Chamber of Civil Engineers
TMMOB İnşaat Mühendisleri Odası
Necatibey St. No: 57, Kızılay, Ankara / Türkiye
Tel: +90.312.294 30 00 - Faks: 294 30 88
www.imo.org.tr